QCD corrections to $e^+e^- \to 4$ jets

Stefan Weinzierl

UNIVERSITE DE PARIS–SUD
U.F.R. SCIENTIFIQUE
D'ORSAY

THESE
présentée pour obtenir
Le GRADE de DOCTEUR EN
SCIENCES
DE L'UNIVERSITE PARIS XI ORSAY

par
Stefan Weinzierl

QCD Corrections to $e^+e^- \to$ 4 jets

Soutenue le 8 Septembre 1998 devant la Commission d'examen :

M. Patrik Aurenche	
M. Pierre Chiappetta	Rapporteur
M. Ulrich Ellwanger	Président
M. Michel Fontannaz	Rapporteur
M. Gregory Korchemsky	
M. David A. Kosower	Directeur de thèse

To Roberta

Acknowledgements

First of all I would like to thank my supervisor David A. Kosower. During the last three years I had the chance to learn a lot from him.

I would like to express my thanks to the members of the jury: Patrik Aurenche, Ulrich Ellwanger and Gregory Korchemsky. In particular I would like to thank Pierre Chiappetta and Michel Fontannaz, who have accepted to be the "rapporteurs" for my thesis.

It was a pleasure to work at the "Service de Physique Théorique". Thanks to all the people, who contributed to the good atmosphere, and special thanks to my office mates Kirone Mallick, Jean-François Mercier, Stéphane Munier and Laurent Charles.

The manuscript has been improved with the help of a lot of useful comments from David A. Kosower, Gregory Korchemsky, Roberta Marani and Karen Willbrand.

I am grateful for the financial support from the "Studienstiftung des deutschen Volkes" and from the "Commissariat à l'Energie Atomique".

Abstract

This thesis deals with perturbative QCD-corrections to four-jet production in electron-positron annihilation.
The one-loop corrections to the subprocess $e^+e^- \to q\bar{q}Q\bar{Q}$ are calculated, using modern techniques in order to calculate the one-loop amplitudes efficiently. These techniques include colour decomposition, the spinor helicity method and decompositions inspired by supersymmetry. The cut technique and the factorization in collinear limits are used to constrain the analytic form of the amplitudes. In a second step the virtual corrections from $e^+e^- \to q\bar{q}Q\bar{Q}$ and $e^+e^- \to qgg\bar{q}$ are implemented together with the corresponding real emission parts into a numerical program. The cancelation of the infrared singularities is based on the dipole formalism.
Numerical values are given for the total cross-section, the D-parameter and the jet broadening variable.

Résumé

Cette thèse a pour objet les corrections perturbatives de CDQ pour la production de quatre jets dans l'annihilation des électrons et positrons.
Les corrections à une boucle pour le sous-processus $e^+e^- \to q\bar{q}Q\bar{Q}$ sont calculées avec de nouvelles méthodes qui comprennent la décomposition de couleur, la méthode des spineur d'hélicité, et une décomposition inspirée par la supersymmétrie. Nous avons également profité des contraintes découlants de l'unitarité et des limites colinéaires pour restreindre la forme analytique des amplitudes.
Dans une deuxième phase, j'ai écrit un programme numérique qui combine des contributions dues aux corrections radiatives des sous-processus $e^+e^- \to q\bar{q}Q\bar{Q}$ et $e^+e^- \to qgg\bar{q}$ et dues aux corrections d'émission réelle. Le programme utilise le formalisme des dipoles pour annuler les divergences infra-rouge.
L'analyse numérique contient des résultats sur la section efficace totale, le paramètre D et la variable d'élargissement d'un jet.

Keywords

Perturbative QCD, spinor helicity method, cut technique, four-jet production in e^+e^--annihilation, phase space slicing, dipole formalism, global event shape variables and jet shape variables.

Contents

1 Introduction

The phenomenology of particle physics is the bridge between theory and experiment. On the theoretical side particle physics is described by the Standard Model, based on local gauge symmetries. The Standard Model describes strong, weak and electromagnetic interactions in terms of the gauge group

$$SU(3) \otimes SU(2)_L \otimes U(1)_Y. \tag{1}$$

The colour group $SU(3)$ is the symmetry group of the strong interactions. The theory of strong interactions is called Quantum Chromodynamics (QCD). The group $SU(2)_L \otimes U(1)_Y$ is the gauge group of the unified weak and electromagnetic interactions. The weak isospin group $SU(2)_L$ and the hypercharge group $U(1)_Y$ are at "low energies" (roughly below 250GeV) spontaneously broken down to the $U(1)_{em}$ gauge group of electromagnetism. The symmetry breaking mechanism is referred to as the Higgs mechanism and postulates the existence of an yet unobserved scalar particle, the Higgs boson. Gravity is not included in the Standard Model.

The particle content of the Standard Model is divided into three sectors: first there are the matter fields, quarks and leptons, carrying spin 1/2. The leptons, like the electron or the neutrino, do not carry any colour charges and therefore do not interact strongly.
Secondly the interactions are mediated by gauge bosons of spin 1. There are eight gauge bosons for the strong interaction, called gluons. After electroweak symmetry breaking the electroweak interactions are described by four gauge bosons, two of them carrying no charge (the photon and the Z-boson), and the two charged W-bosons W^+ and W^-. The photon is massless, whereas the W^+, W^- and the Z are massive.
The third part of the particle content of the Standard Model consists of the Higgs sector. In the Standard Model there is only one additional scalar particle, associated with the electroweak symmetry breaking and the generation of masses for the matter fields.

Experiments are mainly done at high-energy colliders like LEP (CERN), where electrons and positrons are accelarated and brought into collision. Other machines are, for example, the electron-proton collider HERA (DESY) or the proton-antiproton collider TEVATRON at Fermilab. Whereas the theoretical model of the strong interactions is formulated in terms of quarks and gluons, sometimes collectively called partons, experiments only observe leptons and hadrons. Hadrons are divided into mesons (like the pion or kaon) and baryons (like the proton or neutron). In this context two features of QCD are of relevance: confinement and asymptotic freedom. The non-observation of quarks and gluons is due to confinement: At low energies the effective strong coupling constant is large, and

colour-charged particles cannot be observed. Asymptotic freedom states that the effective coupling decreases with the energy scale. Thanks to asymptotic freedom one may calculate the hard subprocesses of high-energy scattering experiments in terms of quarks and gluons, using perturbation theory. On the other hand the formation of hadrons out of quarks and gluons is the domain of non-perturbative QCD. Quantities which are not sensitive to the details of hadronisation may therefore be calculated within perturbation theory.

This leads to the concept of jet physics. A jet is roughly speaking a bunch of hadrons in a small angular region. Viewed as pseudoparticles, it is assumed that jets correspond to the original partons in the hard scattering process and that hadronization corrections are small. Jet quantities are hadronic observables which are infrared safe. This means that their actual value does not vary if the final state changes by the addition of one more particle which is soft or collinear to another particle. Infrared safe quantities may be calculated within perturbation theory.

With the success of the Standard Model the ultimate goal of particle physics is no longer the verification of a well established model, but the search of new features beyond the Standard Model. One popular direction is the supersymmetric extension of the Standard Model.

The search for new physics beyond the Standard Model of particle physics relies on precise theoretical predictions of QCD background processes. Very often processes containing new physics will have the same signature in the detectors as standard QCD processes which might give the dominant contribution for a given final state. A precise understanding of the QCD background is therefore required. A leading-order (LO) calculation will give a rough estimate of the expected background, but suffers from an arbitrary choice of a renormalization scale. Furthermore, since in a leading-order calculation each jet is modelled by only one parton, the internal structure of a jet is overly simplified. In order to improve the calculation, one has to go to next-to-leading order (NLO). Here one explicitly takes into account the first logarithms, ultraviolet and infrared in nature, which are the source of the problems mentioned above.

One-loop amplitudes may have ultraviolet divergences. After renormalization, a logarithm depending on the arbitrary renormalization scale remains. In principle, if the calculation were done to all orders in perturbation theory, the dependence on the arbitrary renormalization scale would drop out. In practise, one is limited to the first few orders in perturbation theory and a residual renormalization scale dependence remains.

In an NLO calculation the cross section receives contributions not only from

the virtual corrections, but also from the real emission part (the $(n+1)$-parton tree-level matrix element integrated over the $(n+1)$-parton phase space). Both contributions are divergent, only their sum is finite. Since the two contributions are integrated over different phase spaces (the n-parton phase space for the virtual part and the $(n+1)$-parton phase space for the real part), the cancellation of these divergences is not a trivial matter. Since in an NLO-calculation the tree-level $(n+1)$-parton matrix element contributes to the n-jet cross section, one begins at NLO to reconstruct the internal structure of a jet, improving thus the simplifed model of "one parton = one jet" and taking into account the dependence of the observables on the jet defining parameters.

Needless to say, an NLO calculation is much more involved than an LO calculation. The two bottlenecks are the calculation of the one-loop amplitudes and the cancellation of infrared singularities needed in order to set up a numerical program.

In this work I consider the QCD corrections to $e^+e^- \to 4$ jets . This is the lowest-order proccess which contains the non-abelian three-gluon vertex at leading order and therefore allows a measurement of the colour charges (C_F, C_A, T_R) of QCD (for which the gauge group is of course supposed to be $SU(3)$). This measurement allows putting limits on additional light fermions or scalar particles (such as a light gluino in a supersymmetric extension of QCD).

The QCD-process $e^+e^- \to 4$ jets will also be a dominant background for the production of a pair of W-bosons at LEP 200, in the case where both W-bosons decay hadronically. Since the branching ratio is roughly 46% one does not want to ignore this channel.
Furthermore the QCD-process will be background to the process $e^+e^- \to Z^* \to ZH \to 4$ jets relevant for the Higgs search at LEP 200.

This thesis has two main parts :
The first part concerns the calculation of the one-loop amplitude for $e^+e^- \to q\bar{q}Q\bar{Q}$, which is one of the two subprocesses needed for the NLO-calculation.
Chapter 2 gives a short introduction to modern techniques, which were used in the calculation. This "toolbox" consists of colour decomposition, the spinor helicity method, the unitarity-based cut-technique, techniques using supersymmetry or inspired by string theory, as well as constructing ansätze from the known factorization in collinear limits. Various techniques for the reduction of tensor loop integrals are discussed as well.
Chapter 3 gives the decomposition of the one-loop amplitudes for $e^+e^- \to q\bar{q}gg$ and $e^+e^- \to q\bar{q}Q\bar{Q}$ into primitive amplitudes. The explicit results for the amplitudes $e^+e^- \to q\bar{q}Q\bar{Q}$ are also given here.

The second part of this work consists in setting up the numerical program "MERCUTIO", which allows the calculation of any infrared-safe observable up to four jets at NLO.
Chapter 4 is devoted to infrared singularities. Two general methods, phase space slicing and the dipole formalism, are discussed and compared. The numerical program uses the dipole formalism. The second part of this chapter reviews some technical details of various dimensional regularization schemes.
Since the integration over phase space has to be done numerically, I briefly review basic Monte Carlo integration techniques in chapter 5 and explain how the integration is performed in practise.
Chapter 6 is devoted to phenomenology. Through the comparision to event generators I show what a NLO-program does and what not. Several jet algorithms and event shape variables are introduced. Numerical results are given for the four-jet fraction, the D-parameter and the jet broadening variable for 3-jet events.
The appendix contains sections on Feynman rules, spinor algebra and renormalization. In a further section the tree- and loop-splitting amplitudes are collected. The last section contains various integral functions, used in the text, and shows how they are implemented numerically.

2 Tools and Techniques for the Calculation

Setting up a numerical NLO-program for jet quantities in e^+e^- collisions seems at first sight to be only a matter of work and good will, since for each step in the calculation there is a known solution. In principle one could follow the good old–fashioned approach:

- Draw all Feynman diagrams for the n-parton tree amplitude, the n-parton one-loop amplitude and the $(n+1)$-parton tree amplitude, which is relevant for the real emission part. If you are lucky, somebody has already calculated some of these processes (usually the tree-amplitudes). In any case you will realize that there are many diagrams, especially for the loop amplitude and the $(n+1)$-tree amplitudes.

- Do the calculation for each Feynman diagram. This may lead to a huge number of different structured terms. The non-abelian three gluon vertex, in particular, produces many different terms.

- Do the calculation with unspecified polarization vectors for external gluons. Sum over the polarizations only after squaring the amplitudes.

- Use a standard integral reduction algorithm for the loop integrals, like the Passarino-Veltman algorithm, in order to express tensor loop integrals in terms of standard scalar integrals. The good thing about these algorithms is, that they can be implemented into a symbolical computer program, the bad thing, that the result is often a rational function, where the numerator and the denominator are complicated expressions, and furthermore, the denominator contains spurious singularities, which cancel only after summation over different terms.

- To cancel the infrared singularities between the real and the virtual part, consider each corner of the $(n+1)$-parton phase space, in which singularities might occur, separately. Make extensive use of partial fraction decomposition, especially in the colour-subleading pieces of the real emission part.

Calculating the QCD corrections to $e^+e^- \to 4$ jets by this approach would involve a tremendous amount of work. Fortunately one can do better with the help of some modern techniques for the calculation of tree- and loop-amplitudes (and the cancelation of infrared singularities). This approach has sometimes been called "total quantum-number management" and is summarized in the following points:

- Keep track of quantum phases by computing analytically only the transition amplitude rather than the cross-section.

- Use the colour information to decompose the amplitude into simpler, gauge-invariant pieces, called partial amplitudes.

- Use the spinor helicity method to calculate the partial amplitudes in a helicity basis. This is easier than a calculation for arbitrary polarizations.
- In many cases the partial amplitudes may be built of still simpler objects, called primitive amplitudes.
- Exploit the "effective" supersymmetry of QCD at tree level, and use supersymmetry at loop-level to organize the particles, which are propagating around the loop, into super-multiplets.
- Square amplitudes to get probabilities, and sum over helicities and colours to obtain unpolarized cross-sections, only at the very end of the calculation. These steps should be done numerically.
- Cancel the infrared singularities by adding and subtracting a universal subtraction term. This subtraction term can be implemented into a separate subroutine in the numerical program, and there is no need to split up the matrix element for the $(n+1)$-parton configuration.

In the following I will give a short introduction to the tools and techniques, which simplify the calculation. The material is mainly based on reviews [1] - [5].

2.1 Colour Decomposition

Amplitudes in QCD may be decomposed into group-theoretical factors (carrying the colour structures) multiplied by kinematic functions called partial amplitudes [10] - [14]. These partial amplitudes do not contain any colour information and are gauge-invariant objects. The generators of the colour group $SU(N_c)$ in the fundamental representation are traceless $N_c \times N_c$ matrices T^a_{ij}. The conventional normalization of the colour matrices is $\mathrm{Tr} T^a T^b = \frac{1}{2}\delta^{ab}$. The commutation relation is then $[T^a, T^b] = i f^{abc} T^c$ and the field strength and the covariant derivative appearing in the Lagrange density are $F^a_{\mu\nu} = \partial_\mu A^a_\nu - \partial_\nu A^a_\mu + g f^{abc} A^b_\mu A^c_\nu$ and $D_\mu = \partial_\mu - igT^a A^a_\mu$. In the modern literature the normalization $\mathrm{Tr} T^a T^b = \delta^{ab}$ is often preferred. The commutation relation is then $[T^a, T^b] = i\sqrt{2} f^{abc} T^c$ and the field strenght and the covariant derivative are given by $F^a_{\mu\nu} = \partial_\mu A^a_\nu - \partial_\nu A^a_\mu + g f^{abc} A^b_\mu A^c_\nu$ and $D_\mu = \partial_\mu - \frac{ig}{\sqrt{2}} T^a A^a_\mu$. We choose here the normalization $\mathrm{Tr}\left(T^a T^b\right) = \delta^{ab}$. The colour decomposition is obtained by replacing the structure constants f^{abc} by

$$f^{abc} = -\frac{i}{\sqrt{2}} \left(\mathrm{Tr}\left(T^a T^b T^c\right) - \mathrm{Tr}\left(T^b T^a T^c\right) \right) \tag{2}$$

which follows from $\left[T^a, T^b\right] = i\sqrt{2} f^{abc} T^c$. The resulting traces and strings of colour matrices can be further simplified with the help of the Fierz identity :

$$T^a_{ij} T^a_{kl} = \delta_{il}\delta_{jk} - \frac{1}{N_c}\delta_{ij}\delta_{kl}. \tag{3}$$

The colour algebra can be carried out diagrammatically, resulting in colour flow lines. As an example we consider the exchange of a gluon between two quarks. Concentrating only on the colour part we can use the double line notation of 't Hooft [15] and write symbolically:

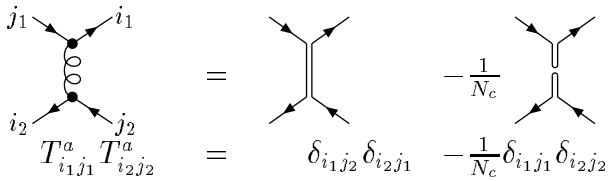

(4)

In the last line we have used the Fierz identity to contract out the generators of the $SU(3)$ algebra.
In the pure gluonic case tree level amplitudes with n external gluons may be written in the form

$$A_{\text{tree}} = g^{n-2} \sum_{\sigma \in S_n/Z_n} \text{Tr}\left(T^{a_{\sigma(1)}} ... T^{a_{\sigma(n)}}\right) A_n\left(\sigma(1), ..., \sigma(n)\right), \tag{5}$$

where the sum is over all non-cyclic permutations of the external gluon legs. The $A_n(\sigma(1), ..., \sigma(n))$, called the partial amplitudes, contain the kinematic information. They are colour-ordered, e.g. only diagrams with a particular cyclic ordering of the gluons contribute. Therefore they can only have singularities like poles and cuts in a limited set of momenta channels, those made out of sums of cyclically adjacent momenta.

The colour decomposition for a tree amplitude with a pair of quarks is

$$A_{tree}(q, 1, 2, ..., n, \bar{q}) = g^{n-2} \sum_{S_n} \left(T^{\sigma(1)} ... T^{\sigma(n)}\right)_{q\bar{q}} A_{n+2}(q, \sigma(1), \sigma(2), ..., \sigma(n), \bar{q}). \tag{6}$$

where the sum is over all permutations of the gluon legs. For the colour matrices I used a short-hand notation $(T^{\sigma(1)})_{q\bar{q}} = (T^{a_{\sigma(1)}})_{i_q j_{\bar{q}}}$. Similar decompositions may be obtained for amplitudes with more than one pair of quarks.

In the pure gluonic case the partial amplitudes A_n have the following properties :

1. A_n is gauge invariant. This follows from the orthogonality to leading order in $1/N$ of $\text{Tr}T^{a_1}...T^{a_n}$.

2. A_n is invariant under cyclic permutations (since $\text{Tr}T^{a_1}...T^{a_n}$ is invariant under cyclic permutations).

3. Reflective property :

$$A_n(n,...,1) = (-1)^n A_n(1,...,n). \tag{7}$$

4. The $U(1)$-decoupling identity (sometimes also called the dual Ward identity or subcyclic identity):

$$\sum_{\sigma \in Z_{n-1}} A_n\left(\sigma(1),...,\sigma(n-1),n\right) \;=\; 0. \tag{8}$$

This is most elegantly proven by enlarging the gauge group from $SU(N_c)$ to $U(N_c)$. The additional generator, sometimes called the $U(1)$-photon, is proportional to the unit matrix and commutes with all $SU(N_c)$ generators. Therefore $f^{abc} = 0$ if one index refers to the $U(1)$-photon and the photon does not couple directly to the gluons. Equation (8) is just the coefficient of $\mathrm{Tr}T^{a_1}...T^{a_{n-1}}$ which has to vanish if particle n corresponds to the $U(1)$-photon.

These properties reduce the number of independent amplitudes.
Example : For the tree-level process with four gluons ($n = 4$) there are only two independent partial amplitudes, e.g. $A_4(1,2,3,4)$ and $A_4(1,2,4,3)$.
Property (4) is just the identity

$$A_4(1,2,3,4) + A_4(1,2,4,3) + A_4(1,3,2,4) \;=\; 0. \tag{9}$$

The discrete symmetries of parity and charge-conjugation may be used to reduce further the number of independent partial amplitudes. Parity states that the partial amplitude with all helicities reversed is the complex conjugate of the original one:

$$A(1^{\lambda_1},2^{\lambda_2},...,n^{\lambda_n}) \;=\; A(1^{-\lambda_1},2^{-\lambda_2},...,n^{-\lambda_n})^* \tag{10}$$

where the particles $1...n$ may be either quarks or gluons. $\lambda_i = \pm$ denotes the helicity of particle i. Charge conjugation reverses the arrows of each fermion line. In addition there is a factor of (-1) for each external gauge boson:

$$\begin{aligned} &A(q_1^{\lambda_{q_1}},1^{\lambda_1},...,i^{\lambda_i},\bar{q}^{-\lambda_{q_1}};...;q_m^{\lambda_{qm}},(k+1)^{\lambda_{k+1}},...,n^{\lambda_n},\bar{q}^{-\lambda_{qm}}) = \\ &\quad (-1)^n A(\bar{q}_1^{-\lambda_{q_1}},i^{\lambda_i},...,1^{\lambda_1},q^{\lambda_{q_1}};...;\bar{q}_m^{-\lambda_{qm}},n^{\lambda_n},...,(k+1)^{\lambda_{k+1}},q^{\lambda_{qm}}). \end{aligned} \tag{11}$$

2.2 The Spinor Helicity Method

The spinor helicity method [16] -[19] allows one to obtain rather compact final expressions for tree and loop amplitudes in (massless) QCD. It also neatly captures the collinear behaviour of these amplitudes The basic idea is to work

with irreducible representations (of the universal covering group) of the Lorentz group $SL(2,C)$, namely two-component spinors of definite helicity, instead of the usual Lorentz four-vectors. The application to fermions is straightforward if one chooses the appropriate representation of the Dirac matrices (namely the Weyl representation):

$$\gamma^\mu = \begin{pmatrix} 0 & \sigma^\mu \\ \bar{\sigma}^\mu & 0 \end{pmatrix} \tag{12}$$

where $\sigma^\mu = (1, -\sigma_i)$, $\bar{\sigma}^\mu = (1, \sigma_i)$ and σ_i are the Pauli matrices. It is convenient to work with spinors of definite helicity :

$$\begin{aligned} u_\pm(p) &= \frac{1}{2}(1 \pm \gamma_5)\, u(p), \\ v_\pm(p) &= \frac{1}{2}(1 \mp \gamma_5)\, v(p). \end{aligned} \tag{13}$$

For the calculation of amplitudes with a large number of external momenta p_i it is useful to introduce the following short-hand notation for spinors :

$$\begin{aligned} |i\pm\rangle = |p_i\pm\rangle &= u_\pm(p_i) = v_\mp(p_i), \\ \langle i\pm| = \langle p_i\pm| &= \bar{u}_\pm(p_i) = \bar{v}_\mp(p_i). \end{aligned} \tag{14}$$

The spinor products are then defined as

$$\begin{aligned} \langle pq\rangle &= \langle p-|q+\rangle, \\ [pq] &\quad\ \langle p+|q-\rangle. \end{aligned} \tag{15}$$

A detailed explanation of the notation and useful properties of the spinor algebra are given in the appendix.
The application to massless vector bosons involves the introduction of an arbitrary null reference momentum q to express the polarization vectors :

$$\begin{aligned} \varepsilon^+_\mu(k,q) &= \frac{\langle q-|\gamma_\mu|k-\rangle}{\sqrt{2}\langle qk\rangle}, \\ \varepsilon^-_\mu(k,q) &= \frac{\langle q+|\gamma_\mu|k+\rangle}{\sqrt{2}\,[kq]}. \end{aligned} \tag{16}$$

The dependence on the arbitrary reference momentum q will drop out in gauge invariant quantities. Changing the reference momentum will give a term proportional to the momentum of the gluon:

$$\varepsilon^+_\mu(k,q_1) - \varepsilon^+_\mu(k,q_2) = -\frac{\sqrt{2}\langle q_1 q_2\rangle}{\langle q_1 k\rangle\langle q_2 k\rangle} k_\mu. \tag{17}$$

The polarization vectors are transverse to k and q,

$$\begin{aligned} \varepsilon^{\pm}(k,q)\cdot k &= 0, \\ \varepsilon^{\pm}(k,q)\cdot q &= 0, \end{aligned} \tag{18}$$

and normalized as

$$\begin{aligned} \varepsilon^{+}\cdot\left(\varepsilon^{+}\right)^{*} &= -1, \\ \varepsilon^{+}\cdot\left(\varepsilon^{-}\right)^{*} &= 0. \end{aligned} \tag{19}$$

Complex conjugation reverses the helicity:

$$\left(\varepsilon_{\mu}^{+}\right)^{*} = \varepsilon_{\mu}^{-}. \tag{20}$$

Further simplifying properties are:

$$\begin{aligned} &\varepsilon^{+}(k_1,q)\cdot\varepsilon^{+}(k_2,q) = \varepsilon^{-}(k_1,q)\cdot\varepsilon^{-}(k_2,q) = 0, \\ &\varepsilon^{+}(k_1,q)\cdot\varepsilon^{-}(k_2,k_1) = 0. \end{aligned} \tag{21}$$

The polarization sum is that of an light-like axial gauge:

$$\sum_{\lambda=\pm}\varepsilon_{\mu}^{\lambda}(k,q)\left(\varepsilon_{\nu}^{\lambda}(k,q)\right)^{*} = -g_{\mu\nu}+\frac{k_{\mu}q_{\nu}+k_{\nu}q_{\mu}}{k\cdot q}. \tag{22}$$

A separate reference momentum q may be chosen for each gluon. One should be careful not to change the reference momenta within the calculation of a gauge-invariant quantity, since the choice of a certain set of reference momenta corresponds to fixing a gauge. Of course for the calculation of different gauge-invariant quantities (like different partial amplitudes), one is free to change the reference momenta. A clever choice may reduce significantly the number of colour-ordered Feynman diagrams, which have to be evaluated. For example, it is useful to choose the reference momenta of like-helicity gluons to be identical and to equal the external momentum of one of the opposite-helicity set of gluons.

2.3 Recursive Relations

Recursive techniques [21] - [22] build tree amplitudes from smaller building blocks, usually called colour-ordered gluon currents or quark currents. These building blocks are neither gauge-invariant nor on-shell, but nevertheless quite useful. The colour-ordered gluon current J_{μ} is obtained through the following steps:

- One starts from a pure gluonic partial amplitude $A_{n+1}(1,...,n,n+1)$.
- One removes the polarization vector $\varepsilon^{\mu}(n+1)$ for the gluon $(n+1)$.

- One adds a propagator

$$\frac{-i}{k_{n+1}^2}\left(g^{\mu\nu}-(1-\xi)\frac{k_{n+1}^{\mu}\,k_{n+1}^{\nu}}{k_{n+1}^2}\right). \tag{23}$$

- The gluon $(n+1)$ may be off-shell, but momentum conservation is imposed

$$\sum_{i=1}^{n+1} k_i \;=\; 0. \tag{24}$$

The partial amplitude can be recovered from the gluonic current by multiplying by the inverse gluon propagator, contracting with a polarization vector and taking k_{n+1}^2 on mass-shell. It should be noted, that the gluon current J_μ is not a gauge invariant quantity. It depends on the choice of the reference momenta, on the choice of the gauge fixing parameter ξ and on the helicity configuration. The recursive relation states that a gluon couples to other gluons only via the three- or four-gluon vertices :

$$\begin{aligned} J^{\mu}(1,...,n) \;=\; &= \frac{-i}{P_{1,n}^2}\left[\sum_{i-1}^{n-1} V_3^{\mu\nu\rho}(P_{1,i},P_{i+1,n})J_\nu(1,...,i)J_\rho(i+1,...,n)\right. \\ &\left.\sum_{j=i+1}^{n-1}\sum_{i=1}^{n-2} V_4^{\mu\nu\rho\sigma}J_\nu(1,...,i)J_\rho(i+1,...,j)J_\sigma(j+1,...,n)\right] \end{aligned} \tag{25}$$

where

$$P_{i,j} \;=\; p_i + p_{i+1} + ... + p_j \tag{26}$$

and V_3 and V_4 are the colour-ordered three-gluon and four-gluon vertices

$$\begin{aligned} V_3^{\mu\nu\rho}(P,Q) \;&=\; \frac{i}{\sqrt{2}}\left(g^{\nu\rho}(P-Q)^{\mu}+2g^{\rho\mu}Q^{\nu}-2g^{\mu\nu}P^{\rho}\right), \\ V_4^{\mu\nu\rho\sigma} \;&=\; \frac{i}{2}\left(2g^{\mu\rho}g^{\nu\sigma}-g^{\mu\nu}g^{\rho\sigma}-g^{\mu\sigma}g^{\nu\rho}\right). \end{aligned} \tag{27}$$

The gluon current J_μ is conserved:

$$\left(\sum_{i=1}^{n} k_i^{\mu}\right) J_\mu \;=\; 0. \tag{28}$$

The gluon current further satisfies the photon decoupling relation

$$J^{\mu}(1,2,3,...,n)+J^{\mu}(2,1,3,...,n)+...+J^{\mu}(2,3,...,n,1) \;=\; 0 \tag{29}$$

and the reflection identity

$$J^{\mu}(1,2,3,...,n) \;=\; (-1)^{n+1}J^{\mu}(n,...,3,2,1). \tag{30}$$

In some cases the recurrence relations can be solved in closed form. If all the gluons have the same helicity one obtains [21]

$$J^{\mu}(1^+,2^+,...,n^+) \;=\; \frac{\langle q-|\gamma^{\mu}\not{P}_{1,n}|q+\rangle}{\sqrt{2}\langle q1\rangle\langle 12\rangle...\langle n-1,n\rangle\langle nq\rangle} \tag{31}$$

if a common reference momentum q is chosen for all gluons. The backslash notation stands for contraction with γ_{μ}, e.g.

$$\not{P}_{1,n} \;=\; \gamma_{\nu}\left(p_1^{\nu}+...+p_n^{\nu}\right). \tag{32}$$

If one gluon has opposite helicity, one obtains

$$J^{\mu}(1^-,2^+,...,n^+) \;=\; \frac{\langle 1-|\gamma^{\mu}\not{P}_{2,n}|1+\rangle}{\sqrt{2}\langle 12\rangle...\langle n1\rangle}\sum_{m=3}^{n}\frac{\langle 1-|\not{p}_m\not{P}_{1,m}|1+\rangle}{P_{1,m-1}^2P_{1,m}^2} \tag{33}$$

where the reference momentum choice is $q_1=p_2$, $q_2=...=q_n=p_1$.

By contracting with an appropriate polarization vector, it can be shown that pure gluonic amplitudes, where all gluons have equal helicities vanish, as well as gluon amplitudes where only one gluon has opposite helicity.
From the last equation one obtains the maximally helicity violating gluon amplitudes (where $(n-2)$ gluons have equal helicities and 2 gluons have opposite helicity):

$$A_n^{tree}(1^+,...,j^-,...,k^-,...,n^+) \;=\; i\frac{\langle jk\rangle^4}{\langle 12\rangle...\langle n1\rangle}. \tag{34}$$

This equation has been conjectured by S.J.Parke and T.R.Taylor [20] and proven by F.A.Berends and W.T.Giele [21] using recursive relations. A closed form for the amplitude with three opposite helicity gluons has been obtained by D.A. Kosower [22].

2.4 Use of Supersymmetry

After removing the colour factors, QCD at tree-level may be viewed as an effective supersymmetric theory, where the quarks and the gluons form a super-multiplet [23]. In an unbroken supersymmetric theory, the supercharge Q annihilates the vacuum, and therefore [24]

$$\langle 0\,|[Q,\Phi_1\Phi_2...\Phi_n]|\,0\rangle=\sum_{i=1}^{n}\langle 0\,|\Phi_1...\,[Q,\Phi_i]\,...\Phi_n|\,0\rangle=0 \tag{35}$$

where the field Φ_i denotes either a gauge boson g or a fermion Λ. It is convenient to multiply the supercharge Q by a Grassmann spinor $\bar{\eta}$, defining $Q(\eta)=\bar{\eta}^{\alpha}Q_{\alpha}$.

η is usually chosen to be a Grassmann number θ times a spinor for an arbitrary null-vector q. The commutators are then given by

$$\begin{aligned}\left[Q(q), g^{\pm}(k)\right] &= \mp\Gamma^{\pm}(k,q)\Lambda^{\pm}(k), \\ \left[Q(q), \Lambda^{\pm}(k)\right] &= \mp\Gamma^{\mp}(k,q)g^{\pm}(k),\end{aligned} \tag{36}$$

with

$$\Gamma^{+}(k,q) = \theta\langle q+|k-\rangle, \qquad \Gamma^{-}(k,q) = \theta\langle q-|k+\rangle. \tag{37}$$

Using the supersymmetric relation

$$\begin{aligned}0 &= \left\langle 0 \left| \left[Q, \Lambda^{+} g_1^{+} ... g_j^{-} ... g_n^{+} g_{n+1}^{-}\right] \right| 0 \right\rangle \\ &= -\Gamma^{-}(q,l) A(g^{+}, g_1^{+}, ..., g_j^{-}, ..., g_n^{+}, g_{n+1}^{-}) \\ &\quad +\Gamma^{-}(j,l) A(\Lambda^{+}, g_1^{+}, ..., \Lambda_j^{-}, ..., g_n^{+}, g_{n+1}^{-}) \\ &\quad +\Gamma^{-}(n+1,l) A(\Lambda^{+}, g_1^{+}, ..., g_j^{-}, ..., g_n^{+}, \Lambda_{n+1}^{-}),\end{aligned} \tag{38}$$

setting the reference momentum equal to $q_l = k_j$ and using the expression for the maximally helicity violating gluon amplitudes in equation (34) one obtains the expression for an amplitude with a pair of quarks:

$$A_n^{tree}(q^{+}, 1^{+}, ..., j^{-}, ..., n^{+}, \bar{q}^{-}) = i\frac{\langle jq\rangle\langle j\bar{q}\rangle^3}{\langle q1\rangle\langle 12\rangle ...\langle n\bar{q}\rangle\langle \bar{q}q\rangle}. \tag{39}$$

The effective supersymmetry of QCD at tree-level does not hold at loop-level. However it is still advantageous ([3], [5]) to rewrite the particles propagating in the loop in terms of supermultiplets plus remaining contributions of complex scalar particles. We have for a gluon and a fermion

$$\begin{aligned}g &= (g + 4f + 3s) - 4(f+s) + s = A^{N=4} - 4A^{N=1} + A^{scalar}, \\ f &= (f+s) - s = A^{N=1} - A^{scalar}.\end{aligned} \tag{40}$$

$A^{N=4}$ denotes a $N = 4$ super-Yang-Mills-multiplet, which contains a gluon g, four gluinos f and three complex scalars s, $A^{N=1}$ denotes an $N = 1$ chiral multiplet with one fermion and one complex scalar. The advantages of this decomposition are

- The supersymmetric terms are much simpler than the non-supersymmetric ones; not only do they obey the supersymmetric Ward identity, but one can also arrange of a diagram-by-diagram cancellation in a special gauge. Furthermore $N = 4$ amplitudes are known to satisfy a certain power counting criterion for cut-based calculations, explained in the next section, and can therefore be uniquely reconstructed from their cuts.

- The scalar loop, while more complicated than the supersymmetric components, is algebraically simpler then a gluon loop, because a scalar cannot propagate spin information around the loop.

2.5 Unitarity and the Cut Technique

The cut technique [26] is based on the unitarity of the S-matrix

$$S^\dagger S = 1. \tag{41}$$

With

$$S_{fi} = 1 + i(2\pi)^4 \delta^4 \left(\sum p_f - \sum p_i \right) T_{fi} \tag{42}$$

one derives

$$i \left(T_{fi} - T^*_{fi} \right) = \sum_n \sum_{hel} \int d\phi_n T^*_{fn} T_{ni} \tag{43}$$

where the sum is over all physical states crossing the cut. With the help of the Cutkosky rules [25] and by expanding the transition amplitude perturbatively we may rewrite this formula as

$$\text{Absorb} A^{loop} = \text{Absorb} \int \frac{d^4k}{(2\pi)^4} \frac{1}{k_1^2 + i\varepsilon} \frac{1}{k_2^2 + i\varepsilon} A_L^{tree} A_R^{tree}. \tag{44}$$

Therefore

$$A^{loop} = \int \frac{d^4k}{(2\pi)^4} \frac{1}{k_1^2 + i\varepsilon} \frac{1}{k_2^2 + i\varepsilon} A_L^{tree} A_R^{tree} + \text{ cut free pieces.} \tag{45}$$

One advantage of a cut-based calculation is that one starts with tree amplitudes on both sides of the cut, which are already sums of Feynman diagrams. Using the spinor helicity method simplifications can already performed at the level of the tree amplitudes.

Within the unitarity based approach one chooses first a basis of integral functions $I_i \in \mathcal{F}_n$. The loop amplitude A_n is written as a linear combination of these functions

$$A_n = \sum_i c_i I_i. \tag{46}$$

By evaluating the cuts, one determines the coefficients c_i.

Z.Bern, L.Dixon, D.C.Dunbar and D.A.Kosower have proven the following power counting criterion [26]: If a loop-amplitude has in some gauge a representation, in which all n-point loop integrals have at most $n-2$ powers of the loop momentum in the numerator (with the exception of two-point integrals, which are allowed to have one power of the loop momentum in the numerator), then the loop amplitude is uniquely determined by its cuts. This does not mean that the

amplitude has no cut-free pieces, but rather that all cut-free pieces are associated with some integral functions.
In particular $N = 4$ supersymmetric amplitudes satisfy the power-counting criterion above and are therefore cut-constructible.

If the amplitude does not satisfy the power-counting criterion, the cut calculation determines the amplitude up to an ambiguity, which is a rational function in the momentum invariants (scalar products and spinor products). One example for such an ambiguity would be

$$\int \frac{d^4k}{(2\pi)^4} \frac{k^\mu k^\nu - \frac{1}{3}q^\mu q^\nu + \frac{1}{12}g^{\mu\nu}q^2}{k^2(k-q)^2}. \tag{47}$$

This term does not have a cut and will therefore not be detected in a cut-based calculation. One way out is to do the calculation to order ε. At one-loop order an arbitrary scale $\mu^{2\varepsilon}$ is introduced in order to keep the coupling dimensionless. In a massless theory the factor $\mu^{2\varepsilon}$ is always accompanied by some kinematical invariant $s^{-\varepsilon}$ for dimensional reasons. If we write symbolically

$$A^{loop} = \frac{1}{\varepsilon^2}c_2\left(\frac{s_2}{\mu^2}\right)^{-\varepsilon} + \frac{1}{\varepsilon}c_1\left(\frac{s_1}{\mu^2}\right)^{-\varepsilon} + c_0\left(\frac{s_0}{\mu^2}\right)^{-\varepsilon}, \tag{48}$$

the cut-free pieces $c_0(s_0/\mu^2)^{-\varepsilon}$ can be detected at order ε:

$$c_0\left(\frac{s_0}{\mu^2}\right)^{-\varepsilon} = c_0 - \varepsilon c_0 \ln\left(\frac{s_0}{\mu^2}\right) + O(\varepsilon^2). \tag{49}$$

It is useful to split the loop momentum into a four-dimensional part and a (-2ε)-dimensional part

$$k^{(D)} = k^{(4)} + k^{(-2\varepsilon)}. \tag{50}$$

Setting $(k^{(-2\varepsilon)})^2 = -\lambda^2$ one replaces the propagator by

$$\frac{1}{\left(k^{(D)}+p\right)^2} \to \frac{1}{\left(k^{(4)}+p\right)^2 - \lambda^2} \tag{51}$$

and the integral by

$$\int \frac{d^{-2\varepsilon}\lambda}{(2\pi)^{-2\varepsilon}} \to -(4\pi)^\varepsilon \frac{\varepsilon}{\Gamma(1-\varepsilon)} \int_0^\infty d\lambda^2 \left(\lambda^2\right)^{-1-\varepsilon} \tag{52}$$

if the integrand is a function of λ^2 only. The net result is that one gets the cut-free pieces by using massive formulas on both sides of the cut.

2.6 Factorization and Constraints from Collinear Limits

The general form of an tree-level n-point partial amplitude in the limit that $P_{1,m}^2$ vanishes (where $P_{1,m} = p_1 + ... + p_m$) is

$$A_n^{tree}(1,...,n) \overset{P_{1,m}^2 \to 0}{\longrightarrow} \sum_{\lambda=\pm} A_{m+1}^{tree}(1,...,m,P^\lambda) \frac{i}{P_{1,m}^2} A_{n-m+1}^{tree}(m+1,...,n,P^{-\lambda}). \tag{53}$$

For two-particles channels ($m = 2$) three-point massless amplitudes are kinematically not possible. In the limit $P_{1,2}^2 \to 0$ the momenta p_1 and p_2 become collinear. The factorization property is then written in terms of "splitting amplitudes" as

$$A_n^{tree}(...,p_a^{\lambda_a},...,p_b^{\lambda_b},...) \overset{a||b}{\longrightarrow} \sum_{\lambda=\pm} \mathrm{Split}_{-\lambda}^{tree}(p_a^{\lambda_a},p_b^{\lambda_b}) A_{n-1}^{tree}(...,P^\lambda,...). \tag{54}$$

One-loop amplitudes factorize according to [28]

$$\begin{aligned} A_n^{loop}(1,...,n) \overset{P_{1,m}^2 \to 0}{\longrightarrow} \sum_{\lambda=\pm} \Big(& A_{m+1}^{loop}(1,...,m),P^\lambda) \frac{i}{P_{1,m}^2} A_{n-m+1}^{tree}(m+1,...,n,P^{-\lambda}) \\ & + A_{m+1}^{tree}(1,...,m),P^\lambda) \frac{i}{P_{1,m}^2} A_{n-m+1}^{loop}(m+1,...,n,P^{-\lambda}) \\ & + A_{m+1}^{tree}(1,...,m),P^\lambda) \frac{i\mathrm{Fact}_n(1,...,n)}{P_{1,m}^2} \\ & \cdot A_{n-m+1}^{tree}(m+1,...,n,P^{-\lambda}) \Big) \end{aligned} \tag{55}$$

where the one-loop factorization function Fact_n is independent of helicities and does not cancel the pole $P_{1,m}^2$. But Fact_n may contain logarithms of kinematic invariants built out of momenta from both side of the pole in $P_{1,m}^2$. The collinear limit of a one-loop amplitude is given by

$$\begin{aligned} A_n^{loop}(...,p_a^{\lambda_a},...,p_b^{\lambda_b},...) \overset{a||b}{\longrightarrow} \sum_{\lambda=\pm} \Big(& \mathrm{Split}_{-\lambda}^{tree}(p_a^{\lambda_a},p_b^{\lambda_b}) A_{n-1}^{loop}(...,P^\lambda,...) \\ & + \mathrm{Split}_{-\lambda}^{loop}(p_a^{\lambda_a},p_b^{\lambda_b}) A_{n-1}^{tree}(...,P^\lambda,...) \Big). \end{aligned} \tag{56}$$

The splitting amplitudes Split^{tree} and Split^{loop} are universal, they depend only on the two momenta becoming collinear, and not upon the specific amplitude under consideration. The splitting functions are collected in the appendix. One may use the above equation to constrain the analytic form of A_n^{loop}, since in any calculation of A_n^{loop} the amplitudes A_{n-1}^{loop} and A_{n-1}^{tree} are usually known. Especially the combination with the unitarity-based method allows one to place tight constraints on the possible analytic form of A_n^{loop}. There are not many terms, which

will vanish in any collinear limit and which do not contain any cut. One known exception for a five-point amplitude is the term

$$\frac{\varepsilon(1,2,3,4)}{\langle 12\rangle\langle 23\rangle\langle 34\rangle\langle 45\rangle\langle 51\rangle} \tag{57}$$

which vanishes in any collinear limit and which has no branch cuts.

2.7 Integral Reduction

Much tedious work is usually involved in the reduction of tensor loop integrals (e.g. integrals where the loop momentum appears in the numerator) to standard scalar integrals.

2.7.1 The Passarino–Veltman Algorithm

Consider the following three-point integral

$$I_3^{\mu\nu} = -(4\pi)^{2-\varepsilon} \int \frac{d^{4-2\varepsilon}k}{(2\pi)^{4-2\varepsilon}} \frac{k^\mu k^\nu}{k^2(k-p_1)^2(k-p_1-p_2)^2} \tag{58}$$

where p_1 and p_2 denotes the external momenta. The reduction technique according to Passarino and Veltman [43] consists in writing $I_3^{\mu\nu}$ in the most general form in terms of fourvectors times external momenta and/or the metric tensor. In our example above we would write

$$I_3^{\mu\nu} = p_1^\mu p_1^\nu C_{21} + p_2^\mu p_2^\nu C_{22} + \{p_1^\mu p_2^\nu\} C_{23} + g^{\mu\nu} C_{24} \tag{59}$$

where $\{p_1^\mu p_2^\nu\} = p_1^\mu p_2^\nu + p_2^\mu p_1^\nu$. One then solves for the form factors C_{21}, C_{22}, C_{23} and C_{24} by first contracting both sides with the external momenta $p_1^\mu p_1^\nu$, $p_2^\mu p_2^\nu$, $\{p_1^\mu p_2^\nu\}$ and the metric tensor $g^{\mu\nu}$. On the left-hand side the resulting scalar products between the loop momentum k^μ and the external momenta are rewritten in terms of the propagators, as for example

$$2p_1 \cdot k = k^2 - (k-p_1)^2 + p_1^2. \tag{60}$$

The first two terms of the right-hand side above cancel propagators, whereas the last term does not involve the loop momentum anymore. The remaining step is to solve for the formfactors C_{2i} by inverting the matrix which one obtains on the right-hand side of equation (59). Due to this step Gram determinants usually appear in the denominator of the final expression. In the example above we would encounter the Gram determinant of the triangle

$$\Delta_3 = 4 \begin{vmatrix} p_1^2 & p_1 \cdot p_2 \\ p_1 \cdot p_2 & p_2^2 \end{vmatrix}. \tag{61}$$

One drawback of this algorithm is closely related to these determinants : In a phase space region where p_1 becomes collinear to p_2, the Gram determinant will tend to zero, and the form factors will take large values, with possible large cancellations among them. This makes it difficult to set up a stable numerical program for automated evaluation of tensor loop integrals.

2.7.2 The Feynman Parameter Space Technique

This method is due to Z.Bern, L.Dixon and D.A.Kosower [48]. Within this approach one introduces Feynman parameters before reducing any tensor integral. After the usual shift of the loop momentum such that the denominator depends only on k^2 but not on k^μ any more, the momentum integration can be performed with the help of identities like

$$\begin{aligned} \int d^{4-2\varepsilon}k k^\mu f(k^2) &= 0, \\ \int d^{4-2\varepsilon}k k^\mu k^\nu f(k^2) &= \frac{1}{4-2\varepsilon} g^{\mu\nu} \int d^{4-2\varepsilon}k k^2 f(k^2). \end{aligned} \tag{62}$$

One is left with a Feynman parameter integral. Let $P(\{a_i\})$ be a polynomial in the Feynman parameter a_i and denote

$$I_n\left[P(\{a_i\})\right] = \Gamma(n-2+\varepsilon) \int da_i \delta(1-\sum a_i) \frac{P(\{a_i\})}{\left(\sum\limits_{i,j} S_{ij} a_i a_j - \varepsilon\right)^{n-2+\varepsilon}} \tag{63}$$

where $S_{ij} = -1/2(p_i + ... p_{j-1})^2$ if $i \neq j$ and $S_{ij} = 0$ otherwise. Here the indices i and j are understood to be mod n. Note that $I_n[1]$ is the scalar n-point integral

$$\begin{aligned} I_n[1] &= \Gamma(n-2+\varepsilon) \int da_i \delta(1-\sum_i a_i) \frac{1}{\left(\sum\limits_{i,j} S_{ij} a_i a_j - \varepsilon\right)^{n-2+\varepsilon}} \\ &= (-1)^n (4\pi)^{2-\varepsilon} \int \frac{d^{4-2\varepsilon}k}{(2\pi)^{4-2\varepsilon} i} \frac{1}{k^2 (k-p_1)^2 ... (k-p_1-...-p_{n-1})^2}. \end{aligned} \tag{64}$$

One changes then integration variables according to

$$\begin{aligned} a_i &= \frac{\alpha_i u_i}{\sum\limits_{j=1}^{n} \alpha_j u_j} \quad \text{(no sum on } i\text{)}, \\ a_n &= \frac{\alpha_n (1 - \sum\limits_{j=1}^{n-1} u_j)}{\sum\limits_{j=1}^{n} \alpha_j u_j} \end{aligned} \tag{65}$$

and defines a matrix ρ_{ij}

$$S_{ij} = \frac{\rho_{ij}}{\alpha_i \alpha_j} \text{ no summation implied,} \tag{66}$$

such that all dependence on the α_i-variables is scaled out of the denominator. It is convenient to introduce the reduced integrals

$$\hat{I}_n\left[P(\{a_i\})\right] = \left(\prod_{j=1}^{n} \alpha_j\right)^{-1} I_n\left[P(\{a_i/\alpha_i\})\right]. \tag{67}$$

If P_m is a homogenous polynomial of degree m, then the reduced integral

$$\hat{I}_n(P_m) = \Gamma(n-2+\varepsilon) \int du \delta(1-\sum_{i=1}^{n} u) \frac{\left(\sum\limits_{j=1}^{n} \alpha_j u_j\right) P\left(\{u_i\}\right)}{\left(\sum\limits_{i,j=1}^{n} \rho_{ij} u_i u_j\right)^{n-2+\varepsilon}} \tag{68}$$

can be obtained from the reduced scalar integral by differentiation :

$$\hat{I}_n\left[P(\{A_i\})\right] = \frac{\Gamma(n-3-m+2\varepsilon)}{\Gamma(n-3+2\varepsilon)} P_m\left(\left\{\frac{\partial}{\partial \alpha_i}\right\}\right) \hat{I}_n[1]. \tag{69}$$

Sometimes one wants to express a n-point integral in terms of lower point integrals plus a 6-dimensional n-point integral. In order to derive the equations, which relate these quantities, one defines the Gram determinant

$$\Delta_n = \det\left(2 p_i \cdot p_j\right). \tag{70}$$

(For an n-point function Δ_n is a $(n-1) \times (n-1)$ determinant, e.g. one of the external momenta has to be omitted. Note that the external momenta satisfy momentum conservation $\sum\limits_{i=1}^{n} p_i = 0$.) One further defines the rescaled Gram determinant

$$\hat{\Delta}_n = \left(\prod_{l=1}^{n} \alpha_l^2\right) \Delta_n = \sum_{i,j=1}^{n} \eta_{ij} \alpha_i \alpha_j \tag{71}$$

where the matrix η is proportional to the inverse of ρ:

$$\eta = N_n \rho^{-1} \tag{72}$$

where $N_n = 2^{n-1} \det\rho$. The variables γ_i are defined as

$$\gamma_i = \sum_{j=1}^{n} \eta_{ij} \alpha_j \tag{73}$$

and are in a sense conjugate to the α_j variables :

$$N_n \alpha_i = \sum_{j=1}^{n} \rho_{ij} \gamma_j . \tag{74}$$

The equations, which relate a n-point integral with up to two Feynman parameters in the numerator to a scalar 6-dimensional integral plus lower point integrals, are

$$\begin{aligned}
\hat{I}_n[1] &= \frac{1}{2N_n} \left(\sum_{i=1}^{n} \gamma_i \hat{I}_{n-1}^{(i)}[1] + (n-5+2\varepsilon)\, \hat{\Delta}_n \hat{I}_n^{D=6-2\varepsilon}[1] \right), \\
\hat{I}_n[a_i] &= \frac{1}{2N_n} \left(\sum_{j=1}^{n} \eta_{ij} \hat{I}_{n-1}^{(j)}[1] + (n-5+2\varepsilon)\, \gamma_i \hat{I}_n^{D=6-2\varepsilon}[1] \right), \\
\hat{I}_n[a_i a_j] &= \frac{\eta_{ij} \hat{\Delta}_n + (n-6+2\varepsilon)\gamma_i \gamma_j}{2N_n \hat{\Delta}_n} \hat{I}_n^{D=6-2\varepsilon}[1] \\
&\quad + \frac{n-6+2\varepsilon}{4N_n^2} \sum_{l=1}^{n} \left(\eta_{il}\gamma_j + \eta_{jl}\gamma_i - \frac{\eta_{il}\eta_{jl}\gamma_l}{\eta_{ll}} - \frac{\gamma_i \gamma_j \gamma_l}{\hat{\Delta}_n} \right) \hat{I}_{n-1}^{D=6-2\varepsilon\ (l)}[1] \\
&\quad + \frac{1}{4N_n^2} \sum_{l,p=1}^{n} \frac{\eta_{ip}\eta_{jl}\eta_{ll} - \eta_{il}\eta_{jl}\eta_{lp}}{\eta_{ll}} \hat{I}_{n-2}^{(l,p)}[1].
\end{aligned} \tag{75}$$

The above equations can be applied to reduce pentagon and hexagon integrals. For more than six external legs there are some complications, since in this case $\hat{\Delta}_n$ and N_n vanish and a careful limit has to be taken.
It has been shown in [48] that the six-dimensional pentagon integral always drops out of physical quantitites when applied to pentagon integrals.

2.7.3 Modified Integral Functions

One way to avoid Gram determinants in the denumerator is to enlarge the set of scalar integral functions. Apart from the scalar n-point functions in $D = 4 - 2\varepsilon$ one considers also scalar n-point functions in $(D + 2m)$ dimensions [51]. Of course, when relating these higher-dimensional integrals to the ordinary scalar loop integrals, the Gram determinant reappears. Campbell et al. [49] have set up a scheme which combines n-point scalar integrals with lower point scalar integrals to form a new set of integral functions :

$$L = I_n[1] + \sum B_l I_{n-1}^{(l)}. \tag{76}$$

These new integral functions are constructed in such a way that the ratio L/Δ_n is finite, when the Gram determinant Δ_n of the n-point system tends to zero.

2.7.4 Dual Vectors

In four dimensions an n-point integral ($n > 4$) can always be reduced to a combination of m_i-point functions, where all $m_i \leq 4$. This follows from the fact that there can be no more than 4 linear independent vectors in a 4 dimensional space. Vermaseren and van Neerven [46] have given an efficient method, which relates a scalar pentagon integral to scalar boxes. They introduce the (not necessarily orthogonal) dual vectors

$$\begin{aligned} v^1_\mu &= \varepsilon(\mu, q_1, q_2, q_3), \quad v^2_\mu = \varepsilon(q_1, \mu, q_3, q_4), \\ v^3_\mu &= \varepsilon(q_1, q_2, \mu, q_4), \quad v^4_\mu = \varepsilon(q_1, q_2, q_3, \mu) \end{aligned} \tag{77}$$

where the notation $\varepsilon(\mu, q_1, q_2, q_3) = 4i\varepsilon_{\mu\nu\rho\sigma} q_2^\nu q_3^\rho q_4^\sigma$ is used. They use the Schouten identity between the Levi-Civita tensor in order to express the loop momentum k_μ as a linear combination of the dual vectors v^i :

$$\begin{aligned} \varepsilon(q_1, q_2, q_3, q_4) k_\mu &= \varepsilon(\mu, q_2, q_3, q_4) k \cdot q_1 + \varepsilon(q_1, \mu, q_3, q_4) k \cdot q_2 \\ &\quad + \varepsilon(q_1, q_2, \mu, q_4) k \cdot q_3 + \varepsilon(q_1, q_2, q_3, \mu) k \cdot q_4. \end{aligned} \tag{78}$$

This equation is then contracted with k^μ and the scalar products written as $2kq_i = k_0^2 - k_i^2 + q_i^2$. After integration over d^4k the box integrals with one antisymmetric tensor in the numerator vanish for $i \geq 1$. The resulting expression is then multiplied by $\varepsilon(q_1, q_2, q_3, q_4)$ and the terms $\varepsilon(q_1, q_2, q_3, q_4) k \cdot v^i$ written in terms of $k \cdot q_i$ by contracting the Levi-Civita tensors. Finally one obtains a expression, which relates the five-point integral to 4-point integrals. This method works in four dimensions and can be used when the integral is finite. In the case where the integral is divergent one can rely on the Feynman parameter technique. The technique of dual vectors has been further developed by A.Signer [52].

2.7.5 Using the Spinor Algebra

Consider the integral

$$\int \frac{d^{4-2\varepsilon}k}{(2\pi)^{4-2\varepsilon} i} \frac{\not{k}\not{k}}{k^2 (k-p_1)^2 ... (k-p_1-...-p_4)^2}. \tag{79}$$

Calculating this integral using standard reduction techniques is quite tedious, but using

$$\not{k}\not{k} = k^2 \cdot 1, \tag{80}$$

immediately reduces the integral to a scalar box integral. Recently Pittau [50] has shown that, if at least two external momenta are massless, one can always permute Dirac-matrices inside traces such that

$$\mathrm{Tr}(\not{k}....\not{k}...) = \sum_j A_j \mathrm{Tr}^{(j)}(\not{k}...) + \sum_l B_l \mathrm{Tr}^{(l)}(...) \tag{81}$$

where $\mathrm{Tr}^{(j)}$ contain at most one power of the loop momentum, $\mathrm{Tr}^{(l)}$ does not contain the loop momentum, and the loop momentum dependence in the coefficients A_j and B_l can be rewritten in terms of propagators. Assume that p_1 and p_2 are the two massless legs. The algorithm consists in writing

$$\not{k} = \frac{1}{2p_1p_2}\left[(2kp_2)\not{p}_1 + (2kp_1)\not{p}_2 - \not{p}_1\not{k}\not{p}_2 - \not{p}_2\not{k}\not{p}_1\right]. \tag{82}$$

The first two term already cancel propagators, whereas a product of the last two terms can be rewritten as

$$\begin{aligned}
\langle 1-|\not{k}|2-\rangle\langle 2-|\not{k}|1-\rangle &= (2kp_1)\,(2kp_2) - (2p_1p_2)\,k^2, \\
\langle 1-|\not{k}|2-\rangle\langle 2+|\not{k}|1+\rangle &= \frac{1}{\langle 2-|3|1-\rangle}\left[(2p_1p_3)\,(2p_2k)\,\langle 1-|\not{k}|2-\rangle\right. \\
&\quad -(2p_1k)\,\langle 1-|\not{p}_2\not{k}\not{p}_3|2-\rangle \\
&\quad +(2p_3k)\,\langle 1-|\not{p}_2\not{k}\not{p}_1|2-\rangle \\
&\quad \left.+k^2\langle 1-|\not{p}_2\not{p}_3\not{p}_1|2-\rangle\right],
\end{aligned} \tag{83}$$

where p_3 is another (not necessarily massless) external leg.

2.7.6 The Trace Formula

Combining the basic ideas of reduction methods based on dual vectors and on the spinor algebra, I derive a formula, which allows an efficient reduction of higher point integrals.
The kinematics are

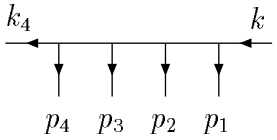

with

$$\begin{aligned}
q_i &= \sum_{j=1}^{i} p_i, \\
k_i &= k - q_i.
\end{aligned} \tag{84}$$

The p_i are supposed to be external momenta whereas k is taken as a loop momentum. It is convenient to set $k_0 = k$ and $p_5 = -q_4$. We have

$$\begin{aligned}
2k\cdot q_i &= k^2 - k_i^2 + q_i^2, \\
2k\cdot p_i &= k_{i-1}^2 - k_i^2 + p_i^2.
\end{aligned} \tag{85}$$

It is convenient to work in a scheme where the Dirac matrices are in four dimensions (like the four-dimensional helicity scheme). If the integral is finite we can take all vectors in four dimensions. The case of a divergent integral will be considered later on. As above I start from the dual vectors written as

$$v_\mu^a = \frac{1}{6}\varepsilon^{abcd} 4i\varepsilon_{\mu\nu\rho\sigma} q_b^\nu q_c^\rho q_d^\sigma, \tag{86}$$

and the Schouten identity

$$\varepsilon(q_1,q_2,q_3,q_4)k^2 = (k\cdot v^a)\,(k\cdot q_a)\,. \tag{87}$$

Now

$$\begin{aligned} k\cdot e^a &= \pm\frac{1}{6}\varepsilon^{abcd}\,(2\mathrm{Tr}_\pm \not{k}\not{q}_b\not{q}_c\not{q}_d - \mathrm{Tr}\not{k}\not{q}_b\not{q}_c\not{q}_d) \\ &= \pm\frac{1}{6}\varepsilon^{abcd} 2\mathrm{Tr}_\pm \not{k}\not{q}_b\not{q}_c\not{q}_d \end{aligned} \tag{88}$$

where $\mathrm{Tr}_\pm$ denotes a trace of Dirac matrices with the insertion of a projection operator $\frac{1}{2}(1\pm\gamma_5)$. Since

$$\mathrm{Tr}(\not{k}\not{q}_b\not{q}_c\not{q}_d) = (2kq_b)(2q_cq_d) - (2kq_c)(2q_bq_d) + (2kq_d)(2q_bq_c) \tag{89}$$

and each terms has one scalar product symmetric in two indices, these terms drop out.
Writing $2kq_a = k^2 - k_a^2 + q_a^2$, one sees that the first two terms cancel propagators, whereas the last term yields

$$\begin{aligned} \pm\frac{1}{6}\varepsilon^{abcd} q_a^2 \mathrm{Tr}_\pm \not{k}\not{q}_b\not{q}_c\not{q}_d &= \pm\Big(\mathrm{Tr}_\pm \not{k}\not{p}_1\not{p}_2\not{p}_3\not{p}_4\not{p}_5 + q_1^2q_3^2(k_0^2-k_4^2) \\ &\quad + q_1^2q_4^2(k_3^2-k_2^2) + q_2^2q_4^2(k_1^2-k_0^2)\Big)\,. \end{aligned} \tag{90}$$

This has been carefully arranged such that no constant term survives. One finally obtains

$$\begin{aligned} \mathrm{Tr}_\pm \not{k}_0\not{p}_1\not{p}_2\not{p}_3\not{p}_4\not{k}_4 &= -k_0^2\mathrm{Tr}_\pm \not{k}_1\not{p}_2\not{p}_3\not{p}_4 \\ &\quad + k_1^2\mathrm{Tr}_\pm \not{k}_0(\not{p}_1+\not{p}_2)\not{p}_3\not{p}_4 \\ &\quad - k_2^2\mathrm{Tr}_\pm \not{k}_0\not{p}_1(\not{p}_2+\not{p}_3)\not{p}_4 \\ &\quad + k_3^2\mathrm{Tr}_\pm \not{k}_0\not{p}_1\not{p}_2(\not{p}_3+\not{p}_4) \\ &\quad - k_4^2\mathrm{Tr}_\pm \not{k}_0\not{p}_1\not{p}_2\not{p}_3 \\ &\quad + \Big(\mathrm{Tr}_\pm \not{k}_0\not{k}_0\not{p}_1\not{p}_2\not{p}_3\not{p}_4 - k_0^2\mathrm{Tr}_\pm \not{p}_1\not{p}_2\not{p}_3\not{p}_4\Big)\,. \end{aligned} \tag{91}$$

This equation holds if the Dirac matrices and the external momenta are in four dimensions. The loop momentum k may be in D dimensions, allowing the application also to divergent integrals. (A careful inspection of the basic equation

(87) shows that the term $\varepsilon(q_1,q_2,q_3,q_4)k^2$ on the left-hand side has to be in four dimensions, whereas the manipulations on the right-hand side involved only scalarproducts $2kq_a = k^2 - k_a^2 + q_a^2$ which may be continued into D dimensions as long as the external momenta q_a stay in four dimensions.) If the integral is finite, k may be taken to be four dimensional and the last term vanishes. The equation above may be rewritten as :

$$\begin{aligned}
\mathrm{Tr}_\pm\left(\not{k}\not{p}_1\not{p}_2\not{p}_3\not{p}_4\not{p}_5\right) &= -\mathrm{Tr}_\mp\left(\not{p}_1\not{p}_2\not{p}_3\not{p}_4\right)\left(N_0+M_0^2\right) \\
&\quad -\frac{1}{2}\left(B_0 \pm \varepsilon(k-p_1,p_2,p_3,p_4)\right)\left(N_0+M_0^2\right) \\
&\quad +\frac{1}{2}\left(B_1 \pm \varepsilon(k,p_1+p_2,p_3,p_4)\right)\left(N_1+M_1^2\right) \\
&\quad -\frac{1}{2}\left(B_2 \pm \varepsilon(k,p_1,p_2+p_3,p_4)\right)\left(N_2+M_2^2\right) \\
&\quad +\frac{1}{2}\left(B_3 \pm \varepsilon(k,p_1,p_2,p_3+p_4)\right)\left(N_3+M_3^2\right) \\
&\quad -\frac{1}{2}\left(B_4 \pm \varepsilon(k,p_1,p_2,p_3)\right)\left(N_4+M_4^2\right) \\
&\quad +\mathrm{Tr}_\pm\left(\not{k}\not{k}\not{p}_1\not{p}_2\not{p}_3\not{p}_4\right) - \mathrm{Tr}_\pm\left(\not{p}_1\not{p}_2\not{p}_3\not{p}_4\right)\left(N_0+M_0^2\right)
\end{aligned} \tag{92}$$

where the internal propagators and masses are denoted by N_i and M_i, respectively. B_i depends only on the box integral under consideration and is given by

$$B_i = st - m_1^2 m_3^2 - m_2^2 m_4^2. \tag{93}$$

For a tensor box-integral one can use

$$\begin{aligned}
\mathrm{Tr}_\pm\left(\not{k}\not{p}_1\not{p}_2\not{p}_3\right) &= \frac{1}{2}\left(B \pm \varepsilon(k,p_1,p_2,p_3)\right) \\
&\quad -\frac{1}{2}C_0\left(N_0+M_0^2\right) \\
&\quad +\frac{1}{2}C_1\left(N_1+M_1^2\right) \\
&\quad -\frac{1}{2}C_2\left(N_2+M_2^2\right) \\
&\quad +\frac{1}{2}C_3\left(N_3+M_3^2\right)
\end{aligned} \tag{94}$$

with

$$C_i = m_1^2 + m_2^2 - m_3^2. \tag{95}$$

This equation is just obtained by expanding the trace. If there is only a single power of the loop momentum in the numerator, the terms with the antisymmetric

tensor will vanish after integration.

It remains to investigate under which condition the traces may be formed. In the next section I show that it is always possible to form a trace $\mathrm{Tr}_{\pm} k p_1 p_2 p_3 p_4 p_5$ with $p_5 = -p_1 - p_2 - p_3 - p_4$, if at least one external leg is massless.

2.7.7 Strings of Spinor Products

In practical calculations one often encounters strings of spinor products, so it is convenient to define some short-hand notation :
First of all, if q is a four-vector, it can be written as a sum of null-vectors :

$$q \;=\; \sum_i q^i. \tag{96}$$

A string of spinor products with one uncontracted spinor is denoted for even l by :

$$\langle\langle p - || = \sum_{i_2, i_3 \ldots i_l} [p_1 p_2^{i_2}] \langle p_2^{i_2} p_3^{i_3} \rangle \ldots [p_{l-1}^{i_{l-1}} p_l^{i_l}] \langle p_l^{i_l} - |, \tag{97}$$

whereas for odd l :

$$\langle\langle p - || = \sum_{i_2, i_3 \ldots i_l} \langle p_1 p_2^{i_2} \rangle [p_2^{i_2} p_3^{i_3}] \ldots [p_{l-1}^{i_{l-1}} p_l^{i_l}] \langle p_l^{i_l} - |. \tag{98}$$

All vectors $p_j^{i_j}$ are assumed to be null vectors. A similar definition applies for $\langle\langle p + ||$. The sign of the helicity corresponds to the sign of the helicity of the open spinor. Ket-spinors are defined analogously.
One example for the notation would be

$$\langle\langle p - || \;=\; \langle p_1 - | \, (\not{p}_2 + \not{p}_3) \, (\not{p}_4 + \not{p}_5 + \not{p}_6) \, . \tag{99}$$

In order to keep track of minus signs, it is also useful to define a "parity" of these objects.

$$P^p = 1 \text{ if } l \text{ is odd and}$$
$$P^p = -1 \text{ if } l \text{ is even.}$$

One can also define generalized spinor products :

$$\begin{aligned} \langle\langle pq \rangle\rangle &= \langle\langle p - || q + \rangle\rangle, \\ [[pq]] &= \langle\langle p + || q - \rangle\rangle. \end{aligned} \tag{100}$$

Then

$$\begin{aligned}
\langle\langle qp\rangle\rangle &= -P^p P^q \langle\langle pq\rangle\rangle, \\
[[qp]] &= -P^p P^q [[pq]], \\
\langle\langle pq\rangle\rangle\langle\langle kj\rangle\rangle &= \langle\langle pj\rangle\rangle\langle\langle kq\rangle\rangle + P^q P^k \langle\langle pk\rangle\rangle\langle\langle qj\rangle\rangle, \\
[[pq]]\,[[kj]] &= [[pj]][[kq]] + P^q P^k [[pk]][[qj]].
\end{aligned} \tag{101}$$

For $l = 1$ these definions give the usual spinor products.

Terms like $\langle\langle q - ||k||l-\rangle\rangle$, where k is the loop momentum, appear in the numerator of tensor integrals . Using the Schouten identity twice, one can write:

$$\begin{aligned}
[[ij]]\,\langle\langle ij\rangle\rangle\langle\langle q - ||k||l-\rangle\rangle &= -P^i P^j \langle\langle qj\rangle\rangle [[jl]] \langle\langle i - ||k||i-\rangle\rangle \\
&\quad -P^i P^j \langle\langle qi\rangle\rangle [[il]] \langle\langle j - ||k||j-\rangle\rangle \\
&\quad +\langle\langle qj\rangle\rangle [[il]] \langle\langle i - ||k||j-\rangle\rangle \\
&\quad +P^i P^j \langle\langle qi\rangle\rangle [[jl]] \langle\langle i + ||k||j+\rangle\rangle.
\end{aligned} \tag{102}$$

This will be the basic equation (together with suitable choices of i and j) for reducing tensor integrals. If a n-point integral ($n > 4$) has at least one massless external leg, say p_1, one can choose

$$\begin{aligned}
||i-\rangle\rangle &= |p_1-\rangle, \\
||j-\rangle\rangle &= \not{p}_5\not{p}_4\not{p}_3\not{p}_2|p_1-\rangle
\end{aligned} \tag{103}$$

where $p_5 = -p_4 - p_3 - p_2 - p_1$. Of course, if there are more massless legs, simpler choices are possible. This method is in some sense the completion of the algorithm given by Pittau. Pittau has shown how to reduce tensor integrals to scalar integrals plus integrals with a single power of the loop momentum in the numerator (rank 1 integrals). The trace method explained here allows an efficient reduction of the rank 1 integrals.

2.8 An Example

As an example I evaluate here explicitly the cut in the channel s_{12} for the one-loop amplitude $A(1_q^+, 2_{\bar{Q}}^+, 3_Q^-, 4_{\bar{q}}^-)$.

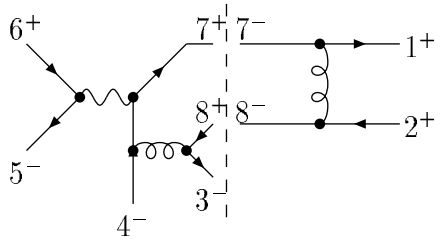

The notation for the cut evaluation. Only a representative diagram is drawn. Due to the convention to take all momenta outgoing the helicity assignment is reversed upon crossing a cut.

Momentum conservation reads as

$$\begin{aligned} p_1 + p_2 + p_3 + p_4 + p_5 + p_6 &= 0, \\ p_3 + p_4 + p_5 + p_6 + p_7 + p_8 &= 0. \end{aligned} \tag{104}$$

The amplitude on the left side of the cut (corresponding in this case to two Feynman diagrams) is given by

$$i\left(\frac{[78]\langle 54\rangle\langle 3-|7+8|6-\rangle}{s_{38}s_{56}s_{378}} + \frac{\langle 34\rangle[67]\langle 5-|3+4|8-\rangle}{s_{38}s_{56}s_{348}}\right). \tag{105}$$

The other diagram, where the positions of the electroweak vertex and the gluon vertex are exchanged is not shown here. The amplitude on the right side is simply

$$-i\frac{[12]\langle 87\rangle}{s_{17}}. \tag{106}$$

Here a factor of $(i)^2$ for two crossed spinors is included. Using the cut technique we may write

$$\begin{aligned} A^{loop}|_{cut} &= -\frac{1}{(56)}\int\frac{d^Dk_8}{(2\pi)^D}\left(\frac{s_{12}[12]\langle 54\rangle\langle 3-|1+2|6-\rangle}{s_{123}N_0N_1N_2N_3}\right. \\ &\quad \left. -\frac{\langle 34\rangle\langle 5-|(3+4)8(1+2)|6-\rangle[12]}{N_0N_1N_2N_3N_4}\right) \end{aligned} \tag{107}$$

where we have used momentum conservation and the notation $N_0 = k_7^2$, $N_1 = -s_{17}$, $N_2 = k_8^2$, $N_3 = s_{38}$ and $N_4 = s_{348}$ for the propagators. Note that the first line already corresponds to a scalar integral. To reduce the tensor integral in the second term, we first try to sandwich the loop momentum k_8 between its

neighbouring external legs by using twice the Schouten identity:

$$\begin{aligned}
&[23]\langle 23\rangle\langle 5-|(3+4)8(1+2)|6-\rangle = \\
&\quad = -\langle 6+|1+2|3+\rangle\langle 3+|3+4|5+\rangle\langle 2-|8|2-\rangle \\
&\qquad -\langle 6+|1+2|2+\rangle\langle 2+|3+4|5+\rangle\langle 3-|8|3-\rangle \\
&\qquad +\langle 6+|1+2|3+\rangle\langle 2+|3+4|5+\rangle\langle 2-|8|3-\rangle \\
&\qquad +\langle 6+|1+2|2+\rangle\langle 3+|3+4|5+\rangle\langle 3-|8|2-\rangle. \qquad (108)
\end{aligned}$$

The first two terms already cancel propagators, whereas the last two terms may be multiplied and divided by appropriate spinor products to form the traces $\mathrm{Tr}_\pm(\not{8}\not{2}\not{1}(\not{5}+\not{6})\not{4}\not{3})$. Using the trace formula from above and keeping only the terms which are relevant to the evaluation of this cut we may replace

$$\begin{aligned}
\mathrm{Tr}_\pm(\not{8}\not{2}\not{1}(\not{5}+\not{6})\not{4}\not{3}) \quad \to \quad & \frac{1}{2}s_{123}s_{34}N_1 + \frac{1}{2}s_{12}s_{234}N_3 \\
& -\frac{1}{2}s_{12}s_{34}N_4. \qquad (109)
\end{aligned}$$

(Since there are no other powers of the loop momentum in the numerator, the terms with an antisymmetric tensor vanish. Furthermore terms with N_0 or N_2 will give contributions which do not have a cut in the s_{12} channel and cannot be detected in this evaluation. We may therefore drop them. They will be fixed by evaluation in other channels.) This completes the evaluation of the cut. We collect the different pieces and obtain

$$\begin{aligned}
A^{loop}|_{cut_{12}} \quad = \quad & -\frac{s_{12}[12]\langle 54\rangle\langle 6+|1+2|3+\rangle}{s_{123}s_{56}}\mathrm{Box}_4 \\
& +\frac{s_{34}}{s_{56}s_{23}}[12]\langle 6+|1+2|3+\rangle\langle 45\rangle\mathrm{Box}_1 \\
& -\frac{s_{12}}{s_{56}s_{23}}\langle 34\rangle[61]\langle 2+|3+4|5+\rangle\mathrm{Box}_3 \\
& -\left(\frac{\langle 6+|1+2|3+\rangle\langle 2+|3+4|5+\rangle}{\langle 4+|5+6|1+\rangle} + \frac{[61][12]\langle 34\rangle\langle 45\rangle}{\langle 1+|5+6|4+\rangle}\right) \\
& \frac{1}{2}\left(\frac{s_{123}s_{34}}{s_{23}s_{56}}\mathrm{Box}_1 + \frac{s_{12}s_{234}}{s_{23}s_{56}}\mathrm{Box}_3 - \frac{s_{12}s_{34}}{s_{23}s_{56}}\mathrm{Box}_4\right) \qquad (110)
\end{aligned}$$

where Box_i denotes the four-dimensional box integral, where the propagator N_i has been removed, e.g.

$$\begin{aligned}
\mathrm{Box}_4 \quad &= \quad \int \frac{d^Dk}{(2\pi)^D}\frac{1}{N_0N_1N_2N_3} \\
&= \quad \frac{i}{(4\pi)^{2-\varepsilon}}I_4[1](s=s_{12},t=s_{23},m_4^2=s_{123}). \qquad (111)
\end{aligned}$$

Using the flip-symmetry we may obtain the coefficient of the scalar box integral Box_0 from the coefficient of Box_4 with the help of the flip-operation

$$1 \leftrightarrow 4, \quad 2 \leftrightarrow 3, \quad 5 \leftrightarrow 6, \quad \langle ab \rangle \leftrightarrow [ab]. \tag{112}$$

By the evaluation of a single cut we have obtained all coefficients of the scalar box integrals with the exception of Box_2, this integral demands the evaluation of the cut in the channel s_{23} or s_{56}. We also have shown that in the four-dimensional integral-function basis there are no triangles Tri_{13}, Tri_{14} or Tri_{34} nor a bubble integral Bubble_{134}. Again, making use of the flip-symmetry, it follows that the coefficients of Tri_{03}, Tri_{01} and Bubble_{013} vanish as well.

After some slight simplifications one obtains the result in the form published in [34].

3 Virtual Corrections to e^+e^- to Four Partons

The virtual corrections to e^+e^- to four partons require the one-loop amplitudes to $e^+e^- \to q\bar{q}gg$ and $e^+e^- \to q\bar{q}Q\bar{Q}$. These amplitudes have been calculated by two groups independently. One group, in which I participated, was able to obtain compact expressions by calculating helicity amplitudes using the cut-technique. The Durham group did a conventional calculation and furnished only computer code. The results can be found in [34] - [37] and they agree numerically. Here I collect the decomposition of the loop amplitudes into primitive amplitudes for both subprocesses $e^+e^- \to q\bar{q}gg$ and $e^+e^- \to q\bar{q}Q\bar{Q}$ and give the explicit results for the one-loop amplitude for the four quark process.

3.1 One-Loop Amplitude for $e^+e^- \to q\bar{q}gg$

By convention we take all momenta outgoing. A representative diagram for $e^+e^- \to q\bar{q}gg$ is depicted in figure 3.1 and explains the labelling of external legs.

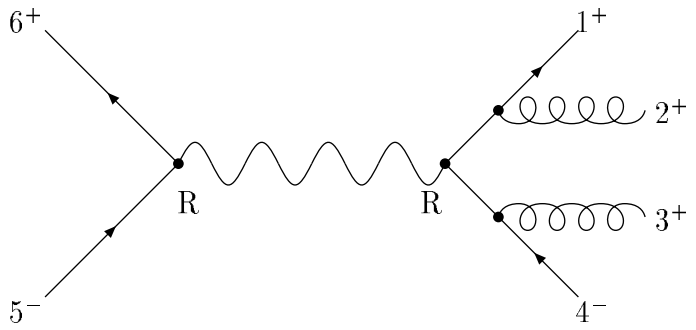

Figure 3.1: A tree-level Feynman diagram for $e^+e^- \to q\bar{q}gg$.

For this particular diagram we have for our convention at position 5 an outgoing positron with negative helicity and at position 6 an outgoing electron with positive helicity. Crossing the momenta at position 5 and 6 to incoming states, corresponding to the situation in e^+e^--annihilation, reverses the helicities and the particle – anti-particle assignment. Therefore the diagram above corresponds to an incoming electron with positive helicity at position 5 and an incoming positron with negative helicity at position 6. The letter R at the vertex denotes a right-handed coupling. If the arrow of the fermion line points from minus (e.g. from an outgoing particle with negative helicity) to plus (e.g to an outgoing particle with positive helicity) then we have a right-handed coupling, and conversely, if

the arrow points from plus to minus, we have a left-handed coupling. The colour decomposition for the tree amplitude is

$$\begin{aligned} A_{\text{tree}} &= 2e^2g^2c_0\left(\left(T^2T^3\right)_{14}A_{\text{tree}}(1,2,3,4)\right. \\ &\quad \left.+\left(T^3T^2\right)_{14}A_{\text{tree}}(1,3,2,4)\right) \end{aligned} \tag{113}$$

where the factor 2 results from the Fiertz identity for the electromagnetic current. The short-hand notation for the colour-matrices corresponds to $(T^2T^3)_{14} = (T^{a_2}T^{a_3})_{i_1j_4}$. c_0 denotes a factor from the electro-magnetic coupling:

$$\begin{aligned} c_0 &= -Q^q + v^e v^q \mathcal{P}_Z(s_{56}), \\ \mathcal{P}_Z(s) &= \frac{s}{s - M_Z^2 + i\Gamma_Z M_Z}. \end{aligned} \tag{114}$$

The electron – positron pair can either annihilate into a photon or a Z-boson. The first term in the expression for c_0 corresponds to an intermediate photon, whereas the last term corresponds to a Z-boson. The left- and right-handed couplings of the Z-boson to fermions are given by

$$v_L = \frac{I_3 - Q\sin^2\theta_W}{\sin\theta_W\cos\theta_W}, \qquad v_R = \frac{-Q\sin\theta_W}{\cos\theta_W} \tag{115}$$

where Q and I_3 are the charge and the third component of the weak isospin of the fermion. For an electron and up- or down-type quarks we have:

$$\begin{array}{ccc} & Q & I_3 \\ \left(\begin{array}{c} u \\ d \end{array}\right) & \left(\begin{array}{c} 2/3 \\ -1/3 \end{array}\right) & \left(\begin{array}{c} 1/2 \\ -1/2 \end{array}\right) \\ e^- & -1 & -1/2 \end{array}$$

The colour decomposition of the one-loop amplitude is

$$\begin{aligned} A_{\text{1-loop}} &= 2e^2g^4\Big\{c_0\Big[N_c\left((T^2T^3)_{14}A_1(1,2,3,4) + (T^3T^2)_{14}A_1(1,3,2,4)\right) \\ &\quad +\delta^{23}\delta_{14}A_3(1,4,2,3)\Big] \\ &\quad +c_1\left[(T^2T^3)_{14} + (T^3T^2)_{14} - \frac{2}{N_C}\delta^{23}\delta_{14}\right]A_4^v(1,4,2,3) \\ &\quad +c_2\left[\left((T^2T^3)_{14} - \frac{1}{N_C}\delta^{23}\delta_{14}\right)A_4^{ax}(1,4,2,3)\right. \\ &\quad +\left((T^3T^2)_{14} - \frac{1}{N_C}\delta^{23}\delta_{14}\right)A_4^{ax}(1,4,3,2) \\ &\quad \left.+\frac{1}{N_c}\delta^{23}\delta_{14}A_5^{ax}(1,4,2,3)\right]\Big\} \end{aligned} \tag{116}$$

where

$$
\begin{aligned}
c_1 &= \sum_{i=1}^{N_f} \left(-Q^i + \frac{1}{2} v^e_{L,R} (v^i_L + v^i_R) \mathcal{P}_Z(s_{56}) \right), \\
c_2 &= \frac{v^e_{L,R}}{\sin 2\theta_W} \mathcal{P}_Z(s_{56}).
\end{aligned} \tag{117}
$$

A_1 denotes the one-loop leading-colour partial amplitude, A_3 a subleading-colour contribution. The partial amplitudes A_4^v, A_4^{ax} and A_5^{ax} represent the contributions from a photon or Z coupling to a fermion loop through a vector or axial-vector coupling. For the squared amplitudes one obtains

$$
\begin{aligned}
&\sum_{\text{colours}} \left(A^*_{\text{tree}} A_{\text{tree}} \right) = \\
&= 4e^4 g^4 \frac{(N_C^2 - 1)}{N_C} |c_0|^2 \Big\{ (N_C^2 - 1) \left| A_{\text{tree}}(1,2,3,4) \right|^2 \\
&\quad - A^*_{\text{tree}}(1,2,3,4) A_{\text{tree}}(1,3,2,4) \Big\} \\
&\quad + \{2 \leftrightarrow 3\},
\end{aligned} \tag{118}
$$

$$
\begin{aligned}
&\sum_{\text{colours}} \left(A^*_{\text{tree}} A_{\text{1-loop}} + A^*_{\text{1-loop}} A_{\text{tree}} \right) = 2 \sum_{\text{colours}} \text{Re} \left(A^*_{\text{tree}} A_{\text{1-loop}} \right) \\
&= 8e^4 g^6 (N_C^2 - 1) \text{Re} \Big\{ c_0^* A^*_{\text{tree}}(1,2,3,4) \Big[c_0 \Big((N_C^2 - 1) A_1(1,2,3,4) \\
&\quad - A_1(1,3,2,4) + A_3(1,4,2,3) \Big) \\
&\quad + c_1 \left(N_c - \frac{4}{N_C} \right) A_4^v(1,4,2,3) \\
&\quad + c_2 \left(\left(N_c - \frac{2}{N_C} \right) A_4^{ax}(1,4,2,3) - \frac{2}{N_C} A_4^{ax}(1,4,3,2) + \frac{1}{N_C} A_5^{ax}(1,4,2,3) \right) \Big] \Big\} \\
&\quad + \{2 \leftrightarrow 3\}.
\end{aligned} \tag{119}
$$

The partial amplitudes A_1, A_3 and A_4^v may be further decomposed into primitive amplitudes. Primitive amplitudes are gauge-invariant objects from which one can build partial amplitudes. The main utility of primitive amplitudes as compared to partial amplitudes is that their analytic structures are generally simpler because

fewer orderings of external legs appear:

$$\begin{aligned}
A_1(1,2,3,4) &= A_{qgg\bar{q}}(1,2,3,4) - \frac{1}{N_C^2} A_{q\bar{q}gg}(1,4,3,2) \\
&\quad + \frac{N_s - N_f}{N_C} A^s(1,2,3,4) - \frac{N_f}{N_C} A^f(1,2,3,4) + \frac{1}{N_C} A^t(1,2,3,4), \\
A_3(1,4,2,3) &= A_{qgg\bar{q}}(1,2,3,4) + A_{qgg\bar{q}}(1,3,2,4) + A_{qg\bar{q}g}(1,2,4,3) \\
&\quad + A_{qg\bar{q}g}(1,3,4,2) + A_{q\bar{q}gg}(1,4,2,3) + A_{q\bar{q}gg}(1,4,3,2), \\
A_4^v(1,4,2,3) &= -A^{vs}(1,4,2,3) - A^{vf}(1,4,2,3).
\end{aligned} \tag{120}$$

The primitive amplitudes A^s and A^f correspond to diagrams where a scalar or a fermion is circulating in the loop and where only gluons are attached to the loop. A^t denotes the contribution from the top quark. The fermion loop in the vector coupling contribution A^v has been decomposed into a scalar loop piece A^{vs} and an additional piece A^{vf}. It is also useful to replace in the primitive amplitudes $A_{qgg\bar{q}}$, $A_{q\bar{q}gg}$ and $A_{qg\bar{q}g}$ the gluon in the loop by a scalar (labelled "sc") and the difference of a gluon and a scalar (labelled "cc"). For example $A_{qgg\bar{q}}$ is rewritten as

$$A_{qgg\bar{q}} = A^{cc}_{qgg\bar{q}} + A^{sc}_{qgg\bar{q}}. \tag{121}$$

It turns out that A^{cc} is cut-constructible. The primitive amplitudes are decomposed into a part containing the poles in ε and a finite part according to

$$A^{\text{one-loop}} = c_\Gamma \left(V A^{\text{tree}} + iF \right) \tag{122}$$

where

$$c_\Gamma = \frac{1}{(4\pi)^{2-\varepsilon}} \frac{\Gamma(1+\varepsilon)\Gamma^2(1-\varepsilon)}{\Gamma(1-2\varepsilon)}. \tag{123}$$

In order to add a term proportional to the tree contribution to the virtual contribution, one replaces

$$A_1 \to A_1 + \frac{\text{const}}{2g^2 N_C} A_{\text{tree}}. \tag{124}$$

For example this is needed to convert the one-loop amplitudes which have been calculated in the FDH-scheme from the FDH-scheme into the 't Hooft-Veltman scheme. The difference between the two schemes is proportional to the tree amplitude.

The explicit results for the primitive amplitudes can be found in ref. [35].

3.2 One-Loop Amplitude for $e^+e^- \to q\bar{Q}Q\bar{q}$

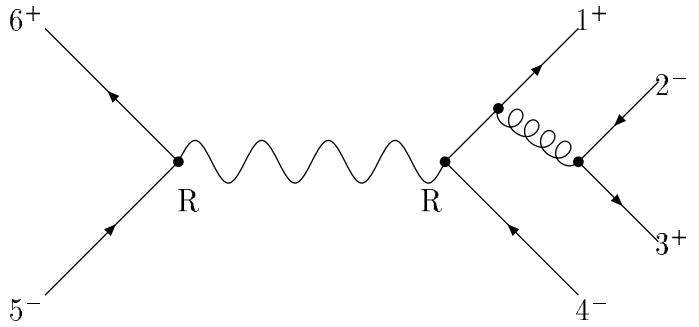

Figure 3.2: A tree-level Feynman diagram for $e^+e^- \to q\bar{Q}Q\bar{q}$.

The tree-level amplitude is decomposed as follows

$$\begin{aligned}
\hat{A}_{\text{tree}} &= A_{\text{tree}}(1,2,3,4) + A_{\text{tree}}(3,4,1,2) \\
&\quad -\delta_{flav} A_{\text{tree}}(1,4,3,2) - \delta_{flav} A_{\text{tree}}(3,2,1,4) \\
&= \chi_{\text{tree}}(1,2,3,4) - \delta_{flav}\chi_{\text{tree}}(1,4,3,2), \\
A_{\text{tree}}(1,2,3,4) &= 2e^2g^2\left(\delta_{12}\delta_{34} - \frac{1}{N_C}\delta_{14}\delta_{32}\right) c_0(1) A(1,2,3,4), \\
\chi_{\text{tree}}(1,2,3,4) &= 2e^2g^2\left(\delta_{12}\delta_{34} - \frac{1}{N_C}\delta_{14}\delta_{32}\right) (c_0(1)A(1,2,3,4) \\
&\quad + c_0(3)A(3,4,1,2)), \\
\chi(1,2,3,4) &= c_0(1)A(1,2,3,4) + c_0(3)A(3,4,1,2). \qquad (125)
\end{aligned}$$

Here $A_{\text{tree}}(1,2,3,4)$ denotes the contribution where the Z or the photon couples to the quark line $q_1\bar{q}_4$ and $c_0(1)$ denotes the corresponding electroweak coupling. The decomposition of the one-loop amplitude is

$$\begin{aligned}
\hat{A}_{\text{1-loop}} &= A_{\text{1-loop}}(1,2,3,4) + A_{\text{1-loop}}(3,4,1,2) \\
&\quad -\delta_{flav} A_{\text{1-loop}}(1,4,3,2) - \delta_{flav} A_{\text{1-loop}}(3,2,1,4) \\
&= \chi_{\text{1-loop}}(1,2,3,4) - \delta_{flav}\chi_{\text{1-loop}}(1,4,3,2), \\
A_{\text{1-loop}} &= 2e^2g^4\left(N_C\delta_{12}\delta_{34}c_0(1)A_1(1,2,3,4) + \delta_{14}\delta_{32}c_0(1)A_2(1,2,3,4)\right) \\
&\quad + \frac{1}{2}\left(\delta_{12}\delta_{34} - \frac{1}{N_C}\delta_{14}\delta_{32}\right) c_2 A_3(1,2,3,4),
\end{aligned}$$

$$
\begin{aligned}
\chi_{1\text{-loop}} &= 2e^2g^4\left(N_C\delta_{12}\delta_{34}\chi_1(1,2,3,4)+\delta_{14}\delta_{32}\chi_2(1,2,3,4)\right.\\
&\quad\left.+\left(\delta_{12}\delta_{34}-\frac{1}{N_C}\delta_{14}\delta_{32}\right)\chi_3(1,2,3,4)\right),\\
\chi_1(1,2,3,4) &= c_0(1)A_1(1,2,3,4)+c_0(3)A_1(3,4,1,2),\\
\chi_2(1,2,3,4) &= c_0(1)A_2(1,2,3,4)+c_0(3)A_2(3,4,1,2),\\
\chi_3(1,2,3,4) &= c_2A_3(1,2,3,4).
\end{aligned}
\tag{126}
$$

The function A_3 is symmetric in the simultaneous exchange $1\leftrightarrow 3$ and $2\leftrightarrow 4$ and arises from a fermion triangle graph with an axial coupling of the Z. For the squared amplitudes one obtains

$$
\begin{aligned}
&\sum_{\text{colours}}\left(A^*_{\text{tree}}A_{\text{tree}}\right)=\\
&\quad 4e^4g^4\frac{(N_C^2-1)}{N_C}\Big\{N_C\left(|\chi(1,2,3,4)|^2+\delta_{flav}|\chi(1,4,3,2)|^2\right)\\
&\quad+\delta_{flav}\left[\chi^*(1,2,3,4)\chi(1,4,3,2)+\chi^*(1,4,3,2)\chi(1,2,3,4)\right]\Big\},
\end{aligned}
\tag{127}
$$

$$
\begin{aligned}
&\sum_{\text{colours}}\left(A^*_{\text{tree}}A_{1\text{-loop}}+A^*_{1\text{-loop}}A_{\text{tree}}\right)=2\sum_{\text{colours}}\text{Re}\left(A^*_{\text{tree}}A_{1\text{-loop}}\right)\\
&\quad=8e^4g^6(N_C^2-1)\text{Re}\Big\{N_C\chi^*(1,2,3,4)\chi_1(1,2,3,4)\\
&\quad+\delta_{flav}N_C\chi^*(1,4,3,2)\chi_1(1,4,3,2)\\
&\quad+\chi^*(1,2,3,4)\chi_3(1,2,3,4)+\delta_{flav}\chi^*(1,4,3,2)\chi_3(1,4,3,2)\\
&\quad-\delta_{flav}\left[\chi^*(1,2,3,4)\chi_2(1,4,3,2)+\chi^*(1,4,3,2)\chi_2(1,2,3,4)\right]\\
&\quad+\delta_{flav}\frac{1}{N_C}\left[\chi^*(1,2,3,4)\chi_3(1,4,3,2)+\chi^*(1,4,3,2)\chi_3(1,2,3,4)\right]\Big\}.
\end{aligned}
\tag{128}
$$

To add a term proportional to the tree-amplitude one adds

$$
\begin{aligned}
\chi_1 &\rightarrow \chi_1+\frac{\text{const}}{2g^2N_C}\chi,\\
\chi_2 &\rightarrow \chi_2-\frac{\text{const}}{2g^2N_C}\chi.
\end{aligned}
\tag{129}
$$

The minus sign is due to our convention for the colour decomposition of $A_{1\text{-loop}}$.

The decomposition of the partial amplitudes A_1, A_2 and A_3 for the helicity con-

figuration $1^+2^+3^-4^-$ is

$$
\begin{aligned}
&A_1(1^+,2^+,3^-,4^-) = \\
&\quad = A^{++}(1,2,3,4) + \frac{N_s - N_f}{N_c} A^{s,++}(1,2,3,4) - \frac{N_f}{N_c} A^{f,++}(1,2,3,4) \\
&\qquad -\frac{2}{N_c^2}\Big(A^{++}(1,2,3,4) + A^{+-}(1,3,2,4)\Big) + \frac{1}{N_c^2} A^{sl}(2,3,1,4), \\
&A_2(1^+,2^+,3^-,4^-) = \\
&\quad = A^{+-}(1,3,2,4) - \frac{N_s - N_f}{N_c} A^{s,++}(1,2,3,4) + \frac{N_f}{N_c} A^{f,++}(1,2,3,4) \\
&\qquad +\frac{2}{N_c^2}\Big(A^{+-}(1,3,2,4) + A^{++}(1,2,3,4)\Big) - \frac{1}{N_c^2} A^{sl}(2,3,1,4), \\
&A_3(1^+,2^+,3^-,4^-) = A^{ax}(1,4,2,3)
\end{aligned}
\tag{130}
$$

where N_s is the number of scalars ($N_s = 0$ in QCD) and N_f is the number of Dirac fermions. The other independent helicity configuration is decomposed into primitive amplitudes as follows :

$$
\begin{aligned}
&A_1(1^+,2^-,3^+,4^-) = \\
&\quad = A^{+-}(1,2,3,4) + \frac{N_s - N_f}{N_c} A^{s,+-}(1,2,3,4) - \frac{N_f}{N_c} A^{f,+-}(1,2,3,4) \\
&\qquad -\frac{2}{N_c^2}\Big(A^{+-}(1,2,3,4) + A^{++}(1,3,2,4)\Big) - \frac{1}{N_c^2} A^{sl}(3,2,1,4), \\
&A_2(1^+,2^-,3^+,4^-) = \\
&\quad = A^{++}(1,3,2,4) - \frac{N_s - N_f}{N_c} A^{s,+-}(1,2,3,4) + \frac{N_f}{N_c} A^{f,+-}(1,2,3,4) \\
&\qquad +\frac{2}{N_c^2}\Big(A^{++}(1,3,2,4) + A^{+-}(1,2,3,4)\Big) + \frac{1}{N_c^2} A^{sl}(3,2,1,4), \\
&A_3(1^+,2^-,3^+,4^-) = -A^{ax}(1,4,3,2)
\end{aligned}
\tag{131}
$$

Note that A^{sl} and A^{ax} appear with a different permutation of the arguments, and the opposite sign, compared with the previous helicity structure. Although colour decompositions do not depend on the helicity choices, these sign differences appear because we have used the symmetries of the primitive amplitudes to reduce the number of independent ones required. The signs in the above expressions also depend on the relative phase conventions of the two helicity amplitudes; we have chosen a convention where

$$
A^{tree,+-}(1,3,2,4) \;\; = \;\; -A^{tree,++}(1,2,3,4). \tag{132}
$$

Of course, consistency in phase conventions between tree and loop amplitudes must be maintained.

The primitive amplitudes $A^{f,+\pm}$ and $A^{s,+\pm}$ are proportional to tree amplitudes and are given by

$$\begin{aligned} A^{s,+\pm} &= c_\Gamma A^{tree,+\pm}\left[-\frac{1}{3\varepsilon}\left(\frac{\mu^2}{-s_{23}}\right)^\varepsilon - \frac{8}{9}\right], \\ A^{f,+\pm} &= c_\Gamma A^{tree,+\pm}\left[\frac{1}{\varepsilon}\left(\frac{\mu^2}{-s_{23}}\right)^\varepsilon + 2\right] \end{aligned} \tag{133}$$

where $A^{tree,+\pm}$ is given below. The remaining primitive amplitudes are decomposed into divergent (V) and finite (F) pieces as

$$A^{\text{one-loop}} = c_\Gamma\left(VA^{\text{tree}} + iF\right). \tag{134}$$

In the formulae below the Lorentz products are denotes as $s_{ij} = (p_i + p_j)^2$ and $t_{ijk} = (p_i + p_j + p_k)^2$. It is convenient to appreviate the following combinations of kinematic invariants

$$\begin{aligned} \delta_{12} &= s_{12} - s_{34} - s_{56}, \\ \delta_{34} &= s_{34} - s_{56} - s_{12}, \\ \delta_{56} &= s_{56} - s_{12} - s_{34}, \\ \Delta_3 &= s_{12}^2 + s_{34}^2 + s_{56}^2 - 2s_{12}s_{34} - 2s_{34}s_{56} - 2s_{56}s_{12}. \end{aligned} \tag{135}$$

3.2.1 The Helicity Configuration $q^+\bar{Q}^+Q^-\bar{q}^-$

We first give the primitive amplitude $A_6^{++}(1,2,3,4)$ which contributes to the leading colour part of $A_{6;1}(1_q^+, 2_{\bar{Q}}^\pm, 3_Q^-, 4_{\bar{q}}^-; 5_{\bar{e}}^-, 6_e^+)$. This amplitude is odd under a 'flip symmetry', which is the combined operation of a permutation and spinor-product complex conjugation:

$$\begin{aligned} &\text{flip:} \qquad 1 \leftrightarrow 4\,, \quad 2 \leftrightarrow 3\,, \quad 5 \leftrightarrow 6\,, \\ &\langle a\,b\rangle \leftrightarrow [a\,b]\,, \quad \left\langle a^-\right|b\left|c^-\right\rangle \leftrightarrow \left\langle a^+\right|b\left|c^+\right\rangle\,. \end{aligned} \tag{136}$$

For example

$$\text{flip}\left(\langle 13\rangle \ln\left(\frac{-t_{123}}{-s_{56}}\right)\right) = [13]\ln\left(\frac{-t_{234}}{-s_{56}}\right). \tag{137}$$

The corresponding tree amplitude for this helicity configuration is

$$A_6^{\text{tree},++} = i\,\frac{[1\,2]\,\langle 5\,4\rangle\,\langle 3|(1+2)|6\rangle}{s_{23}s_{56}t_{123}} + i\,\frac{\langle 3\,4\rangle\,[6\,1]\,\langle 5|(3+4)|2\rangle}{s_{23}s_{56}t_{234}}\,. \tag{138}$$

We have

$$\begin{aligned} V^{++} &= -\frac{1}{\varepsilon^2}\left(\left(\frac{\mu^2}{-s_{12}}\right)^\varepsilon + \left(\frac{\mu^2}{-s_{34}}\right)^\varepsilon\right) + \frac{2}{3\varepsilon}\left(\frac{\mu^2}{-s_{23}}\right)^\varepsilon \\ &\quad -\frac{3}{2}\ln\left(\frac{-s_{23}}{-s_{56}}\right) + \frac{10}{9}, \end{aligned} \tag{139}$$

$$
\begin{aligned}
F^{++} = & \left(\frac{\langle 3|(1+2)|6\rangle^2}{\langle 2\,3\rangle\,[5\,6]\,t_{123}\langle 1|(2+3)|4\rangle} - \frac{[1\,2]^2\,\langle 4\,5\rangle^2}{[2\,3]\,\langle 5\,6\rangle\,t_{123}\langle 4|(2+3)|1\rangle} \right) \\
& \times \left[\mathrm{Ls}_{-1}\left(\frac{-s_{12}}{-t_{123}}, \frac{-s_{23}}{-t_{123}}\right) + \tilde{\mathrm{Ls}}^{2\mathrm{m}h}_{-1}(s_{34}, t_{123}; s_{12}, s_{56}) \right] \\
& - 2\,\frac{\langle 3|(1+2)|6\rangle}{[5\,6]\,\langle 1|(2+3)|4\rangle} \left[\frac{\langle 1|(2+3)|6\rangle\,[1\,2]}{t_{123}} \frac{\mathrm{L}_0\left(\frac{-s_{23}}{-t_{123}}\right)}{t_{123}} + \frac{\langle 3|4|6\rangle}{\langle 2\,3\rangle} \frac{\mathrm{L}_0\left(\frac{-s_{56}}{-t_{123}}\right)}{t_{123}} \right] \\
& - \frac{1}{2}\frac{1}{\langle 2\,3\rangle\,[5\,6]\,t_{123}\langle 1|(2+3)|4\rangle} \left[\Big(\langle 3|2|1\rangle\langle 1|(2+3)|6\rangle\Big)^2 \frac{\mathrm{L}_1\left(\frac{-t_{123}}{-s_{23}}\right)}{s_{23}^2} \right. \\
& \left. + \langle 3|4|6\rangle^2 t_{123}^2 \frac{\mathrm{L}_1\left(\frac{-s_{56}}{-t_{123}}\right)}{t_{123}^2} \right] \\
& - \mathrm{flip}\,,
\end{aligned}
\tag{140}
$$

where 'flip' is to be applied to all the preceding terms in F^{++}.

3.2.2 The Helicity Configuration $q^+\bar{Q}^-Q^+\bar{q}^-$

We now give the result for $A_6^{+-}(1,2,3,4)$, which contributes to the leading colour part of the partial amplitude $A_{6;1}(1_q^+, 2_{\bar{Q}}^-, 3_Q^+, 4_{\bar{q}}^-; 5_{\bar{e}}^-, 6_e^+)$. This amplitude is odd under the same flip symmetry as A_6^{++}. The tree amplitude is

$$
A_6^{\mathrm{tree},+-} = -i\,\frac{[1\,3]\,\langle 5\,4\rangle\,\langle 2|(1+3)|6\rangle}{s_{23}s_{56}t_{123}} - i\,\frac{\langle 2\,4\rangle\,[6\,1]\,\langle 5|(2+4)|3\rangle}{s_{23}s_{56}t_{234}}\,. \tag{141}
$$

For the one-loop contributions we have

$$
\begin{aligned}
V^{+-} \;=\; & -\frac{1}{\varepsilon^2}\left(\left(\frac{\mu^2}{-s_{12}}\right)^{\varepsilon} + \left(\frac{\mu^2}{-s_{34}}\right)^{\varepsilon}\right) + \frac{2}{3\varepsilon}\left(\frac{\mu^2}{-s_{23}}\right)^{\varepsilon} \\
& - \frac{3}{2}\ln\left(\frac{-s_{23}}{-s_{56}}\right) + \frac{10}{9},
\end{aligned}
\tag{142}
$$

$$
\begin{aligned}
F^{+-} = & \left(-\frac{[1\,3]^2\,\langle 4\,5\rangle^2}{[2\,3]\,\langle 5\,6\rangle\,t_{123}\langle 4|(2+3)|1\rangle} + \frac{\langle 1\,2\rangle^2\,\langle 3|(1+2)|6\rangle^2}{\langle 2\,3\rangle\,[5\,6]\,t_{123}\,\langle 1\,3\rangle^2\,\langle 1|(2+3)|4\rangle} \right) \\
& \times \mathrm{Ls}_{-1}\left(\frac{-s_{12}}{-t_{123}}, \frac{-s_{23}}{-t_{123}}\right) \\
& + \left(-\frac{[1\,3]^2\,\langle 4\,5\rangle^2}{[2\,3]\,\langle 5\,6\rangle\,t_{123}\langle 4|(2+3)|1\rangle} + \frac{\langle 3|(1+2)|6\rangle^2\langle 2|(1+3)|4\rangle^2}{\langle 2\,3\rangle\,[5\,6]\,t_{123}\langle 1|(2+3)|4\rangle\langle 3|(1+2)|4\rangle^2} \right) \\
& \times \tilde{\mathrm{Ls}}^{2\mathrm{m}h}_{-1}(s_{34}, t_{123}; s_{12}, s_{56})
\end{aligned}
$$

$$
\begin{aligned}
&+\Bigg[\frac{1}{2}\frac{(s_{12}-s_{34})\,\langle 5\,1\rangle\,\langle 5|(3+4)|2\rangle\langle 1|(2+4)|3\rangle}{\langle 5\,6\rangle\,\langle 1|(2+3)|4\rangle\langle 1|(3+4)|2\rangle^2}-\frac{1}{2}\frac{(s_{12}-s_{34})\,[2\,3]\,\langle 5\,1\rangle\,\langle 5\,2\rangle}{\langle 5\,6\rangle\,\langle 1|(2+3)|4\rangle\langle 1|(3+4)|2\rangle}\\
&-\frac{1}{2}\frac{(t_{134}-t_{234})\,[3\,4]\,\langle 5\,1\rangle\,\langle 5\,4\rangle}{\langle 5\,6\rangle\,\langle 1|(2+3)|4\rangle\langle 1|(3+4)|2\rangle}-\frac{[1\,2]\,\langle 5\,1\rangle\,\langle 5\,2\rangle\,\langle 1|(2+4)|3\rangle}{\langle 5\,6\rangle\,\langle 1|(2+3)|4\rangle\langle 1|(3+4)|2\rangle}\\
&+\frac{1}{2}\frac{\langle 5\,1\rangle\,[6\,2]\,\langle 1|(2+4)|3\rangle(t_{234}-2s_{34})}{\langle 1|(2+3)|4\rangle\langle 1|(3+4)|2\rangle^2}+\frac{1}{2}\frac{\langle 5|(1+2)|6\rangle\langle 1|(2+4)|3\rangle}{\langle 1|(2+3)|4\rangle\langle 1|(3+4)|2\rangle}\\
&-\frac{\langle 1|(2+4)|3\rangle\Big(s_{12}\delta_{12}(\langle 5|1|6\rangle-\langle 5|2|6\rangle)-\delta_{56}(\langle 5|1|2\rangle\langle 2|5|6\rangle-\langle 5|6|1\rangle\langle 1|2|6\rangle)\Big)}{\langle 1|(2+3)|4\rangle\langle 1|(3+4)|2\rangle\Delta_3}\\
&+\frac{1}{2}\frac{\langle 2|(1+4)|3\rangle\langle 5|(1+2)|6\rangle\delta_{56}}{\langle 1|(2+3)|4\rangle\Delta_3}\Bigg]I_3^{\rm 3m}(s_{12},s_{34},s_{56})\\
&+\frac{[1\,3]\,\langle 1\,2\rangle\,\langle 3|1+2|6\rangle^2}{[5\,6]\,t_{123}\,\langle 1\,3\rangle\,\langle 3|(1+2)|4\rangle}\frac{\mathrm{L}_0\left(\frac{-t_{123}}{-s_{12}}\right)}{s_{12}}-\frac{1}{2}\frac{[1\,3]^2\,\langle 2\,3\rangle\,\langle 1|(2+3)|6\rangle^2}{[5\,6]\,t_{123}\langle 1|(2+3)|4\rangle}\frac{\mathrm{L}_1\left(\frac{-t_{123}}{-s_{23}}\right)}{s_{23}^2}\\
&+\frac{[1\,3]\,\langle 1|(2+3)|6\rangle\langle 2|(1+3)|6\rangle}{[5\,6]\,t_{123}\langle 1|(2+3)|4\rangle}\frac{\mathrm{L}_0\left(\frac{-t_{123}}{-s_{23}}\right)}{s_{23}}\\
&+\frac{[1\,3]\,\langle 1\,2\rangle\,\langle 1|(2+3)|6\rangle\langle 3|(1+2)|6\rangle}{[5\,6]\,t_{123}\,\langle 1\,3\rangle\,\langle 1|(2+3)|4\rangle}\frac{\mathrm{L}_0\left(\frac{-t_{123}}{-s_{23}}\right)}{s_{23}}\\
&-\frac{1}{2}\frac{[6\,4]^2\,\langle 4\,2\rangle^2\,\langle 3|(1+2)|4\rangle\,t_{123}}{\langle 2\,3\rangle\,[5\,6]\,\langle 1|(2+3)|4\rangle\langle 3|(1+2)|4\rangle}\frac{\mathrm{L}_1\left(\frac{-s_{56}}{-t_{123}}\right)}{t_{123}^2}\\
&-\frac{[6\,4]^2\,\langle 4\,2\rangle\,t_{123}}{[5\,6]\,\langle 1|(2+3)|4\rangle\langle 3|(1+2)|4\rangle}\frac{\mathrm{L}_0\left(\frac{-t_{123}}{-s_{56}}\right)}{s_{56}}\\
&-2\,\frac{[6\,4]\,\langle 4\,2\rangle\,\langle 2|(1+3)|6\rangle}{\langle 2\,3\rangle\,[5\,6]\,\langle 1|(2+3)|4\rangle}\frac{\mathrm{L}_0\left(\frac{-t_{123}}{-s_{56}}\right)}{s_{56}}\\
&+\frac{1}{\langle 3|(1+2)|4\rangle\langle 1|(3+4)|2\rangle\Delta_3}\Bigg[(s_{12}-s_{34})\Bigg(\frac{\langle 1\,2\rangle\,[6\,1]\,[6\,2]\,t_{123}}{[5\,6]}\\
&+\frac{[1\,2]\,\langle 5\,1\rangle\,\langle 5\,2\rangle\,t_{124}}{\langle 5\,6\rangle}\Bigg)\\
&+(2s_{12}-\delta_{56})\,\langle 5\,2\rangle\,\langle 1|(3+4)|2\rangle\,[1\,6]\\
&+\Big((s_{13}+s_{23})(s_{23}+s_{24})-s_{12}(s_{12}+s_{23}-s_{14})\Big)\langle 5|1|6\rangle\\
&+\Big((s_{14}+s_{24})(s_{13}+s_{14})-s_{12}(s_{12}-s_{23}+s_{14})\Big)\langle 5|2|6\rangle\Bigg]\ln\left(\frac{-s_{12}}{-s_{56}}\right)\\
&-\text{flip}\,,
\end{aligned}
\tag{143}
$$

where 'flip' is to be applied to all the preceding terms in F^{+-}.

3.2.3 Subleading Colour Primitive Amplitude

Here we give the primitive amplitude $A_6^{\rm sl}(1,2,3,4)$, which contributes only at subleading order in N_c. The "tree amplitude" appearing in eq. 134 is

$$A_6^{\rm tree,sl} = i\,\frac{[1\,3]\,\langle 5\,4\rangle\,\langle 2|(1+3)|6\rangle}{s_{12}s_{56}t_{123}} - i\,\frac{\langle 2\,4\rangle\,[6\,3]\,\langle 5|(2+4)|1\rangle}{s_{12}s_{56}t_{124}}\,. \tag{144}$$

In this case it is convenient to introduce the 'exchange' operation where the $5,6$ fermion pair is exchanged with the $1,2$ fermion pair,

$$\text{exchange:} \qquad 1 \leftrightarrow 6\,, \qquad 2 \leftrightarrow 5\,. \tag{145}$$

Some of the terms also possess a symmetry 'flip_sl' (distinct from the leading-colour 'flip'),

$$\begin{aligned} &\text{flip\_sl:} \qquad 1 \leftrightarrow 5\,, \quad 2 \leftrightarrow 6\,, \quad 3 \leftrightarrow 4\,, \\ &\langle a\,b\rangle \leftrightarrow [a\,b]\,, \quad \left\langle a^-\right|b\left|c^-\right\rangle \leftrightarrow \left\langle a^+\right|b\left|c^+\right\rangle\,. \end{aligned} \tag{146}$$

The singular contribution is

$$\begin{aligned} V^{sl} \;=\; & \left[-\frac{1}{\varepsilon^2}\left(\frac{\mu^2}{-s_{34}}\right)^{\varepsilon} - \frac{2}{3\varepsilon}\left(\frac{\mu^2}{-s_{34}}\right)^{\varepsilon} - 4\right] \\ & + \left[-\frac{1}{\varepsilon^2}\left(\frac{\mu^2}{-s_{12}}\right)^{\varepsilon} - \frac{2}{3\varepsilon}\left(\frac{\mu^2}{-s_{12}}\right)^{\varepsilon} - \frac{7}{2}\right]. \end{aligned} \tag{147}$$

The finite contribution is

$$\begin{aligned} F^{\rm sl} = & \left[\frac{[1\,3]^2\,\langle 4\,5\rangle^2}{[1\,2]\,\langle 5\,6\rangle\,t_{123}\langle 4|(1+2)|3\rangle} - \frac{\langle 3|(1+2)|6\rangle^2\langle 2|(1+3)|4\rangle^2}{\langle 1\,2\rangle\,[5\,6]\,t_{123}\langle 3|(1+2)|4\rangle^3}\right] \\ & \times \tilde{\rm Ls}_{-1}^{\rm 2m}{}^{h}(s_{34},t_{123};s_{12},s_{56}) + T\,I_3^{\rm 3m}(s_{12},s_{34},s_{56}) \\ & + \left[\frac{1}{2}\frac{[6\,4]^2\,\langle 4\,2\rangle^2\,t_{123}}{\langle 1\,2\rangle\,[5\,6]\,\langle 3|(1+2)|4\rangle}\frac{{\rm L}_1\left(\frac{-s_{56}}{-t_{123}}\right)}{t_{123}^2} + 2\,\frac{[6\,4]\,\langle 4\,2\rangle\,\langle 2|(1+3)|6\rangle}{\langle 1\,2\rangle\,[5\,6]\,\langle 3|(1+2)|4\rangle}\frac{{\rm L}_0\left(\frac{-t_{123}}{-s_{56}}\right)}{s_{56}}\right. \\ & - \frac{\langle 2\,3\rangle\,\langle 2\,4\rangle\,[6\,4]^2\,t_{123}}{\langle 1\,2\rangle\,[5\,6]\,\langle 3|(1+2)|4\rangle^2}\frac{{\rm L}_0\left(\frac{-t_{123}}{-s_{56}}\right)}{s_{56}} - \frac{1}{2}\frac{\langle 2\,3\rangle\,[6\,4]\,\langle 2|(1+3)|6\rangle}{\langle 1\,2\rangle\,[5\,6]\,\langle 3|(1+2)|4\rangle^2}\ln\left(\frac{-t_{123}}{-s_{56}}\right) \\ & \left. - \frac{3}{4}\frac{\langle 2|(1+3)|6\rangle^2}{\langle 1\,2\rangle\,[5\,6]\,t_{123}\langle 3|(1+2)|4\rangle}\ln\left(\frac{-t_{123}}{-s_{56}}\right) - \text{flip\_sl}\right] \end{aligned}$$

$$
\begin{aligned}
&+\Bigg[\ln\Big(\frac{-s_{12}}{-s_{34}}\Big)\Bigg(\frac{3}{2}\frac{[1\,2]}{\langle 3|(1+2)|4\rangle\Delta_3^2}\Big([5\,6]\,\langle 2\,5\rangle^2\,\delta_{34}\delta_{56}-2\,\langle 1\,2\rangle^2\,\langle 5\,6\rangle\,[6\,1]^2\,\delta_{12}\\
&+4\,\langle 1\,2\rangle\,s_{56}\,\langle 5\,2\rangle\,[6\,1]\,\delta_{56}\Big)\\
&-\frac{1}{2}\frac{[1\,2]\,\langle 2\,5\rangle}{\langle 3|(1+2)|4\rangle\,\langle 5\,6\rangle\,\Delta_3}\Big(\langle 5\,2\rangle\,(s_{12}-s_{34})-2\,\langle 5\,6\rangle\,[6\,1]\,\langle 1\,2\rangle\Big)\\
&+\frac{3}{2}\frac{t_{123}}{\langle 3|(1+2)|4\rangle\Delta_3^2}\Big(\langle 5\,2\rangle\,[1\,6]\,(\delta_{34}\delta_{56}+2s_{12}\delta_{12})+2\,([1\,2]\,[5\,6]\,\langle 2\,5\rangle^2\\
&+\langle 1\,2\rangle\,\langle 5\,6\rangle\,[6\,1]^2)\,\delta_{56}\Big)\\
&-\frac{1}{2}\frac{t_{123}}{\langle 3|(1+2)|4\rangle\Delta_3}\Big(\langle 5\,2\rangle\,[1\,6]-\frac{[1\,2]\,\langle 2\,5\rangle^2}{\langle 5\,6\rangle}-\frac{\langle 1\,2\rangle\,[6\,1]^2}{[5\,6]}\Big)\\
&+\Big(-\frac{[1\,2]\,[6\,4]\,\langle 3\,2\rangle}{\langle 3|(1+2)|4\rangle^2\Delta_3}+\frac{\langle 5|(2+3)|1\rangle}{\langle 5\,6\rangle\,\langle 3|(1+2)|4\rangle\Delta_3}\Big)(\langle 5\,2\rangle\,\delta_{56}-2\,\langle 5|(3+4)|1\rangle\,\langle 1\,2\rangle)\\
&-\frac{[6\,4]\,\langle 3\,2\rangle\,t_{123}}{[5\,6]\,\langle 3|(1+2)|4\rangle^2\Delta_3}\Big([1\,6]\,\delta_{56}-2\,\langle 2|(3+4)|6\rangle\,[1\,2]\Big)\\
&+\frac{4}{\langle 3|(1+2)|4\rangle\Delta_3}\Big(\langle 5\,4\rangle\,[4\,1]\,\langle 2|(1+3)|6\rangle+[6\,3]\,\langle 2\,3\rangle\,\langle 5|(2+4)|1\rangle\Big)\\
&+2\,\frac{[6\,4]\,\langle 4\,2\rangle}{\langle 1\,2\rangle\,[5\,6]\,\langle 3|(1+2)|4\rangle\Delta_3}\Big(-2\,\langle 2|5|6\rangle\delta_{56}+\langle 2|(3+4)|6\rangle\delta_{34}\Big)\\
&-2\,\frac{\langle 5\,2\rangle}{\langle 1\,2\rangle\,\langle 5\,6\rangle\,\langle 3|(1+2)|4\rangle\Delta_3}\delta_{34}\,\Big(\langle 5\,3\rangle\,[3\,4]\,\langle 4\,2\rangle+\langle 5\,4\rangle\,[4\,1]\,\langle 1\,2\rangle\\
&-\langle 5|(1+2)|3\rangle\,\langle 3\,2\rangle\Big)\\
&-\frac{[6\,4]\,\langle 2|(1+3)|6\rangle\langle 2^-|(5+6)(1+2)|3^+\rangle}{\langle 1\,2\rangle\,[5\,6]\,t_{123}\langle 3|(1+2)|4\rangle^2}+\frac{1}{2}\frac{\langle 2\,3\rangle\,[4\,6]\,\langle 2|(1+3)|6\rangle}{\langle 1\,2\rangle\,[5\,6]\,\langle 3|(1+2)|4\rangle^2}\\
&-\frac{1}{4}\frac{\langle 2|(1+3)|6\rangle^2}{\langle 1\,2\rangle\,[5\,6]\,t_{123}\langle 3|(1+2)|4\rangle}+\frac{\langle 5\,2\rangle\,(\langle 4\,5\rangle\,\langle 2|(1+3)|4\rangle-\langle 2\,5\rangle\,t_{123})}{\langle 1\,2\rangle\,\langle 5\,6\rangle\,t_{123}\langle 3|(1+2)|4\rangle}\Bigg)\\
&-\text{flip\_sl}\Bigg]\\
&-\frac{1}{2}\frac{(t_{123}\delta_{34}+2s_{12}s_{56})}{\langle 3|(1+2)|4\rangle\Delta_3}\Big(\frac{[6\,1]^2}{[1\,2]\,[5\,6]}+\frac{\langle 5\,2\rangle^2}{\langle 1\,2\rangle\,\langle 5\,6\rangle}\Big)+(t_{123}-t_{124})\frac{[6\,1]\,\langle 5\,2\rangle}{\langle 3|(1+2)|4\rangle\Delta_3}\\
&+\text{exchange},
\end{aligned}
\tag{148}
$$

where 'exchange' is to be applied to all the preceding terms in $F^{\rm sl}$, but 'flip_sl' is to be applied only to the terms inside the brackets ([ ]) in which it appears. The

three-mass triangle coefficient T is given by

$$
\begin{aligned}
T = {} & 3s_{34}(t_{123}\delta_{34} + 2s_{12}s_{56})\frac{([1\,2]\,\langle 2\,5\rangle^2\,[5\,6] + \langle 5\,6\rangle\,[6\,1]^2\,\langle 1\,2\rangle)}{\langle 3|(1+2)|4\rangle\Delta_3^2} \\
& -6s_{12}s_{56}s_{34}\,\langle 5\,2\rangle\,[6\,1]\,\frac{(t_{123}-t_{124})}{\langle 3|(1+2)|4\rangle\Delta_3^2} \\
& -\frac{t_{123}}{\langle 3|(1+2)|4\rangle)\Delta_3}(\langle 5\,2\rangle\,[6\,1]\,(s_{56}+s_{12}+s_{34}) + [1\,2]\,\langle 2\,5\rangle^2\,[5\,6] \\
& + \langle 5\,6\rangle\,[6\,1]^2\,\langle 1\,2\rangle) \\
& -\frac{\langle 5|(2+3)|1\rangle}{\langle 3|(1+2)|4\rangle\Delta_3}([6\,5]\,\langle 5\,2\rangle\,\delta_{56} - [6\,1]\,\langle 1\,2\rangle\,\delta_{12}) - \frac{[1\,2]\,\langle 5\,6\rangle\,\langle 2|(3+4)|6\rangle^2}{\langle 3|(1+2)|4\rangle\Delta_3} \\
& -\frac{\langle 2\,3\rangle\,[6\,4]}{\langle 3|(1+2)|4\rangle^2\Delta_3}\Big(\langle 5\,6\rangle\,\delta_{56}\,([6\,1]\,t_{123} - [6\,5]\,\langle 5\,2\rangle\,[2\,1]) \\
& -[1\,2]\,\delta_{12}(\langle 2\,5\rangle\,t_{123} - \langle 2\,1\rangle\,[1\,6]\,\langle 6\,5\rangle)\Big) \\
& -\frac{\langle 2\,3\rangle\,[6\,4]\,\langle 5|(2+3)|1\rangle}{\langle 3|(1+2)|4\rangle^2} - \frac{1}{2}(t_{123}\delta_{34} + 2s_{12}s_{56})\frac{\langle 2\,3\rangle^2\,[6\,4]^2}{\langle 1\,2\rangle\,[5\,6]\,\langle 3|(1+2)|4\rangle^3} \\
& -2\Big([6\,5]\,\langle 5\,2\rangle\,\delta_{56} - [6\,1]\,\langle 1\,2\rangle\,\delta_{12}\Big)\frac{[6\,3]\,\langle 2\,4\rangle}{\langle 1\,2\rangle\,[5\,6]\,\Delta_3} \\
& +2\Big(-\langle 2|3|4\rangle\langle 4|5|6\rangle\delta_{56} + \langle 2|1|3\rangle\langle 3|4|6\rangle\delta_{12} + \langle 2|(1+3)|6\rangle s_{34}\delta_{34}\Big) \\
& \times\frac{\langle 2|(1+3)|6\rangle}{\langle 1\,2\rangle\,[5\,6]\,\langle 3|(1+2)|4\rangle\Delta_3} \\
& +4\,\frac{\langle 2|(1+3)|6\rangle\langle 5|(2+3)|1\rangle s_{34}}{\langle 3|(1+2)|4\rangle\Delta_3} - (t_{123}\delta_{34} + 2s_{12}s_{56})\frac{\langle 2|(1+3)|6\rangle\,[1\,4]\,\langle 3\,5\rangle}{s_{12}s_{56}\langle 3|(1+2)|4\rangle^2} \\
& +2\Big(-[1\,2]\,\langle 2\,3\rangle\,[3\,4]\,\langle 4\,5\rangle + \langle 5\,6\rangle\,[6\,4]\,\langle 4\,3\rangle\,[3\,1] + \langle 5|(2+3)|1\rangle s_{34}\Big) \\
& \times\frac{\langle 2|(1+3)|6\rangle}{s_{12}s_{56}\langle 3|(1+2)|4\rangle} \\
& -\frac{1}{2}(t_{123}\delta_{34} + 2s_{12}s_{56})\frac{[1\,6]\,\langle 2\,5\rangle}{s_{12}s_{56}\langle 3|(1+2)|4\rangle} \\
& -\frac{1}{2}\frac{(t_{123}-t_{124})}{s_{12}s_{56}\langle 3|(1+2)|4\rangle}\Big(2\,\langle 2|(1+3)|6\rangle(\langle 5|3|1\rangle - \langle 5|4|1\rangle) \\
& +(\langle 2|3|6\rangle - \langle 2|4|6\rangle)\langle 5|(2+4)|1\rangle + [6\,1]\,\langle 2\,5\rangle\,\delta_{34}\Big) \\
& +\left(-\langle 5|3|1\rangle + \langle 5|4|1\rangle + \frac{1}{2}(t_{123}-t_{124})\Big(\frac{[1\,4]\,\langle 3\,5\rangle}{\langle 3|(1+2)|4\rangle} + \frac{[1\,3]\,\langle 4\,5\rangle}{\langle 4|(1+2)|3\rangle}\Big)\right) \\
& \times\frac{[3\,6]\,\langle 2\,4\rangle}{s_{12}s_{56}} \\
& -\Big(4\,\langle 2|(1+3)|6\rangle - \langle 2|3|6\rangle + \langle 2|4|6\rangle\Big)\frac{[1\,3]\,\langle 4\,5\rangle}{s_{12}s_{56}}\,. \qquad (149)
\end{aligned}
$$

3.2.4 Axial Vector Contribution

The primitive amplitude $A_6^{\rm ax}(1,2,3,4)$ is unique in that neither of the external quark pairs couples directly to the vector boson; instead they couple through the fermion-loop triangle diagram. The contribution to the amplitude vanishes when the vector boson is a photon (by Furry's theorem, i.e. charge conjugation invariance) The Z contribution is proportional to the axial vector coupling of the Z to the quarks in the loop. Ignoring the u, d, s, c quark masses, only the t, b quark pair survives an isodoublet cancellation in the loop, due to its large mass splitting. We use the results of ref. [39] to obtain this contribution; they present the fully off-shell Zgg vertex, and we need only contract it with the three fermion currents. The infrared- and ultraviolet-finite result is :

$$\begin{aligned} A_6^{ax} &= -\frac{2i}{(4\pi)^2}\frac{f(m_t;s_{12},s_{34},s_{56}) - f(m_b;s_{12},s_{34},s_{56})}{s_{56}} \\ &\quad \cdot\left(\frac{[63]\langle 42\rangle\langle 25\rangle}{\langle 12\rangle} - \frac{[61][13]\langle 45\rangle}{[12]}\right) \\ &\quad + (1\leftrightarrow 3, 2\leftrightarrow 4)\,, \end{aligned} \tag{150}$$

where the integral $f(m)$ is defined in the appendix. We need only the large mass expansion (for $m = m_t$) and the $m = 0$ limit (for $m = m_b$) of this integral; these are presented in the appendix.

4 Cancellation of Infrared Divergences

Throughout this chapter the conventional normalization of the colour matrices is used: $\mathrm{Tr} T^a T^b = \frac{1}{2}\delta^{ab}$.

4.1 Infrared Divergences

The NLO cross section receives contributions from virtual corrections and from real emission. For $e^+e^- \to 4$ jets the virtual part consists of the interference terms between the tree amplitudes and the one-loop amplitudes for $e^+e^- \to qgg\bar{q}$ and $e^+e^- \to q\bar{q}Q\bar{Q}$ The real emission part consists of the squared tree-level amplitudes with one additional parton, e.g. $e^+e^- \to qggg\bar{q}$ and $e^+e^- \to q\bar{q}Q\bar{Q}g$. Both the virtual and the real emission contributions contain infrared divergences, arising when one particle becomes soft or two particles collinear. Only the sum of the virtual corrections and the real emission part is finite. Since the virtual part is integrated over n-particle phase-space, whereas the real emission part is integrated over the $(n+1)$-particle phase space, this gives rise to a numerical problem: Obviously it is not possible to integrate the divergent contributions numerically and to cancel the divergences after the (numerical) integration. The cancellation of infrared singularities has to be performed before any numerical integration is done. There are basically two approaches to overcome this obstacle: phase-space slicing [54] and the subtraction method. (Within the subtraction method there are two variants: the subtraction method by Frixione, Kunszt and Signer [56] and the dipole formalism of Catani and Seymour [57].) To illustrate the difference between the two approaches consider the following toy example due to Z. Kunszt [4]: consider integrals of the form

$$\langle F \rangle \quad = \quad \int_0^1 \frac{dx}{x^{1+\varepsilon}} F(x) + \frac{1}{\varepsilon} F(0), \tag{151}$$

where the first term on the right-hand side corresponds to real emission, whereas the second term corresponds to the virtual corrections. The function $F(x)$ represents a final-state observable that is infrared safe, i.e. with the requirement that $F(x)$ tends smoothly to $F(0)$ as x tends to 0.

4.1.1 Slicing the Integration Region

Within the phase-space slicing method, the $(n+1)$-particle phase-space is divided into a small part, containing all singular regions, and the remaining part, which is by definition free of divergences. In the latter one the integration can be performed numerically, whereas in the former the integrand is approximated by the eikonal or collinear approximation. This approximation is then integrated analytically over the one-particle subspace and then combined with the virtual

part. In the sum all divergences cancel and the integral over the remaining hard n-particle phase space can be performed. In the simple example above we would split the region of integration into $[0, s_{min}]$ and $[s_{min}, 1]$ and approximate $F(x)$ in the former by $F(0)$:

$$\begin{aligned}\langle F\rangle &= \int\limits_{s_{min}}^{1} \frac{dx}{x^{1+\varepsilon}} F(x) + \int\limits_{0}^{s_{min}} \frac{dx}{x^{1+\varepsilon}} F(0) + \frac{1}{\varepsilon} F(0) + O(s_{min} F'(0)) \\ &= \int\limits_{s_{min}}^{1} \frac{dx}{x^{1+\varepsilon}} + F(0) \ln s_{min} + O(s_{min} F'(0)) + O(\varepsilon). \end{aligned} \tag{152}$$

Note that this method introduces an error of $O(s_{min})$. In an actual calculation one has to show that it is possible to choose s_{min} small enough such that the systematical error of $O(s_{min})$ is smaller than the desired accuracy. It should also be noted that in general the resulting numerical values of the terms $\int dx/x^{1+\varepsilon}$ and $F(0) \ln s_{min}$ will be large in magnitude, whereas their sum may not. This forces us to calculate the integrals over the real emission and the virtual parts with high precision. Since this is usually done by Monte Carlo techniques, it is computer-time consuming.

4.1.2 Subtraction Method

The subtraction method consists in subtracting and adding again suitable chosen functions to the integrand. In the simple example above one would add and subtract $F(0)/x^{1+\varepsilon}$.

$$\begin{aligned}\langle F\rangle &= \int\limits_{0}^{1} \frac{dx}{x^{1+\varepsilon}} F(x) - \int\limits_{0}^{1} \frac{dx}{x^{1+\varepsilon}} F(0) + \int\limits_{0}^{1} \frac{dx}{x^{1+\varepsilon}} F(0) + \frac{1}{\varepsilon} F(0) \\ &= \int\limits_{0}^{1} \frac{dx}{x^{1+\varepsilon}} \left(F(x) - F(0)\right) + \left(-\frac{1}{\varepsilon} x^{-\varepsilon} F(0) \Big|_0^1 + \frac{1}{\varepsilon} F(0) \right) \\ &= \int\limits_{0}^{1} \frac{dx}{x^{1+\varepsilon}} \left(F(x) - F(0)\right). \end{aligned} \tag{153}$$

In this approach no approximation is involved. The modified real and virtual parts can be integrated without further problems. In this toy example the integrand had only one singularity at $x = 0$. In an actual calculation there are usually multiple singularities. Care has to be taken in overlapping regions of phase space, where the integrand has more than one singularity. If the subtraction term does not approximate the integrand in all singularities these singularities have to be disentangled and subtracted separately.
Depending on the precise shape of the function $F(x)$ the term $F(x) - F(0)$ might

oscillate such that there is a cancellation between different integration regions. Monte Carlo integration will yield the (small) result with large statistical errors. Again one is forced to use a high number of integrand evaluations.

4.2 Phase Space Slicing

Phase space slicing ([54], [55]) is the oldest general method on the cancellation of infrared divergences. In the next subsection I outline the main points of this method for the terms leading in the number of colours. Colour-subleading terms are dealt with in the subsequent section.

4.2.1 Cross Section

Within the phase space slicing method one introduces the auxiliary concept of a parton cross section. If two partons have an invariant mass smaller than s_{min} they are considered not to be resolved by a hypothetical parton detector. In this case they are considered as one parton and the integration over the soft or collinear phase space is performed analytically, using the appropriate approximation formulae. Denote the momenta of the incoming particles by p_1 and p_2, and their helicities by λ_1 and λ_2. Denote the mommenta of the outgoing partons by k_i and the helicities by μ_i. The parton cross section is defined as

$$d\sigma^{\text{parton}} = \frac{1}{8K(s)} \sum_{\substack{\lambda_1,\lambda_2 \\ \mu_1,...,\mu_n}} \sum_{\substack{\text{n partons} \\ \text{resolved}}} |A|^2 \, d\Phi_n^{\text{res}}(p_1+p_2,k_1,...,k_2) \tag{154}$$

where we have averaged over all initial particle helicities and summed over all outgoing parton helicities. The kinematical factor is given by

$$K(s) = \sqrt{\left(s-(m_1+m_2)^2\right)\left(s-(m_1-m_2)^2\right)}. \tag{155}$$

$|A|^2$ is the relevant matrix element for n resolved partons to a given order in α_s. The resolved n-parton phase space is given by (including identical particle factors):

$$\begin{aligned} & d\Phi_n^{\text{res}}(Q,1,..,n) = \\ & = \frac{1}{n_g! \prod n_q^{flav}! \prod n_{\bar{q}}^{flav}!} \prod_{i,j} \Theta(s_{ij}-s_{min}) d\Phi_n(Q,1,...,n). \end{aligned} \tag{156}$$

The jet cross-section is then obtained from the parton cross-section by applying the jet algorithm and/or the experimental cuts:

$$d\sigma^{\text{jet}} = \Theta(\text{experimental cuts}) d\sigma^{\text{parton}}. \tag{157}$$

This gives the following picture :

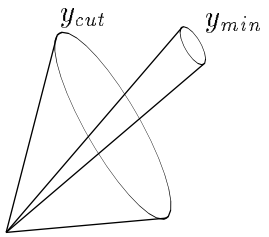

Inside the small cone of order $y_{min} = s_{min}/Q^2$ the $(n+1)$ parton matrix element is approximated by its soft and collinear limits and integrated analytically over the soft or collinear phase space. The result is combined with the virtual part. The sum is infrared finite and can be integrated over the remaining n-parton phase space. Outside the small cone, but inside the big cone of order y_{cut}, which represents the experimental cuts and the jet clustering algorithm, the $(n+1)$-parton matrix element is integrated numerically. (Depending on the details of the jet finding algorithm and the experimetal cuts, the big cone need not be "cone-shaped".) By construction this region does not contain any singularities and the integration can therefore be performed safely. The region outside the big cone corresponds to the $(n+1)$-jet region, and is therefore of no relevance for the n-jet cross-section.

The Lorentz-invariant phase space $d\Phi_n$ is given by

$$\begin{aligned} d\Phi_n(Q, k_1, .., k_n) &= (2\pi)^D \delta^D \left(Q - \sum_{i=1}^{n} k_i \right) \prod_{i=1}^{n} \frac{d^D k_i}{(2\pi)^{D-1}} \Theta(k_i^0) \delta(k_i^2) \\ &= (2\pi)^D \delta^D \left(Q - \sum_{i=1}^{n} k_i \right) \prod_{i=1}^{n} \frac{d^{D-1} k_i}{(2\pi)^{D-1} 2E_i}. \end{aligned} \tag{158}$$

The phase space volume is

$$\int d\Phi_n = (2\pi)^{4-3n} \left(\frac{\pi}{2} \right)^{n-1} \frac{(Q^2)^{n-2}}{\Gamma(n)\Gamma(n-1)}. \tag{159}$$

The phase space factorizes according to

$$\begin{aligned} &(2\pi)^D d\Phi_n(P, p_1, ..., p_n) = \\ &= (2\pi)^{D-1} dQ^2 d\Phi_j(Q, p_1, ..., p_j) d\Phi_{n-j+1}(P, Q, p_{j+1}, ..., p_n) \end{aligned} \tag{160}$$

where $Q = \sum_{i+1}^{j} p_i$.

4.2.2 Leading Terms in the Number of Colours

Within the phase space slicing method the integration region for real emission is divided into two regions : One small region, which contains all the singularities and where the calculation is done analytically but approximately. In the

remaining region the integration can be done exactly by numerical methods. It is convenient to define the inner cone via an invariant mass s_{min}. The approximation of the matrix elements within this small region by its soft and collinear limits introduces an error of $O(s_{min})$. Therefore one has to show, that one can choose s_{min} small enough that the systematical errors due to this approximation are negligible. On the other hand one wants to choose s_{min} as large as possible in order to reduce statistical errors in the Monte Carlo integration.

The formalism for phase space slicing is explained in detail in the paper by Giele and Glover [54]. Here I recall the basic features. In the soft limit each coloured-ordered amplitude factorizes according to

$$|A_{n+1}|^2 \;=\; \frac{g^2 N_C}{2}\left(2\mathrm{Eik}_{q1} + 2\mathrm{Eik}_{12} + ... + 2\mathrm{Eik}_{n\bar{q}}\right)|A_n|^2 \tag{161}$$

where the eikonal factors are

$$2\mathrm{Eik}_{ab} \;=\; 2\frac{2s_{ab}}{s_{ac}s_{cb}}. \tag{162}$$

The factor of 2 in front comes from the summation over the (unobserved) soft gluon helicities. The integration of an eikonal factor over the soft phase space yields

$$\int d\Phi_{\mathrm{soft}} \frac{2s_{ab}}{s_{ac}s_{cb}} \;=\; \frac{1}{(4\pi)^{2-\varepsilon}}\frac{1}{\Gamma(1-\varepsilon)}\frac{2}{\varepsilon^2}\left(\frac{\mu^2}{s_{min}}\right)^{\varepsilon}\left(\frac{s_{ab}}{s_{min}}\right)^{\varepsilon}. \tag{163}$$

Note that

$$\frac{1}{(4\pi)^{2-\varepsilon}}\frac{1}{\Gamma(1-\varepsilon)} \;=\; c_\Gamma + O(\varepsilon^3). \tag{164}$$

In the collinear case there is an overall factorization of the amplitudes (after averaging over angles):

$$|A(...,n,a,b,m,...)|^2 \;=\; g^2\frac{1}{s_{ab}}P_{c\to ab}\,|A(...,n,c,m,...)|^2\,. \tag{165}$$

The integration over the collinear phase space yields

$$\int d\Phi_{\mathrm{coll}} \frac{1}{s_{ab}}P_{c\to ab} \;=\; -\frac{1}{(4\pi)^{2-\varepsilon}}\frac{1}{\Gamma(1-\varepsilon)}\frac{4}{\varepsilon}\left(\frac{\mu^2}{s_{min}}\right)^{\varepsilon} I_{c\to ab} \tag{166}$$

where

$$I_{c\to ab} \;=\; \frac{1}{4}\int_{z_1}^{1-z_2} dz \frac{P_{c\to ab}}{(z(1-z))^{\varepsilon}} \tag{167}$$

and

$$z_1 = \frac{s_{min}}{s_{nc}}, \qquad z_2 = \frac{s_{min}}{s_{cm}}. \tag{168}$$

The integration over z is bounded by z_1 and $1-z_2$ in order to avoid the soft region, which was already accounted for. The splitting functions in the conventional scheme are given by

$$\begin{aligned}
P_{g\to gg} &= C_A \frac{1+z^4+(1-z)^4}{z(1-z)} \\
&= 2C_A \left(\frac{z}{1-z} + \frac{1-z}{z} + z(1-z) \right), \\
P_{q\to qg} &= 2C_F \frac{1+z^2-\varepsilon(1-z)^2}{1-z} \\
&= 2C_F \left(\frac{2z}{1-z} + (1-\varepsilon)(1-z) \right), \\
P_{g\to q\bar{q}} &= 2T_R N_f \frac{z^2+(1-z)^2-\varepsilon}{1-\varepsilon} \\
&= 2T_R N_f \left(1 - \frac{2z(1-z)}{1-\varepsilon} \right).
\end{aligned} \tag{169}$$

The integrated splitting functions in the conventional scheme are then

$$\begin{aligned}
I_{g\to gg} &= \frac{C_A}{2} \left(\frac{z_1^{-\varepsilon}+z_2^{-\varepsilon}-2}{\varepsilon} - \frac{11}{6} + \left(-\frac{67}{18} + \frac{\pi^2}{3} \right) \varepsilon + O(\varepsilon^2) \right) \\
&= \frac{C_A}{2} \left(-\ln z_1 - \ln z_2 - \frac{11}{6} + \left(\frac{1}{2}\ln^2 z_1 + \frac{1}{2}\ln^2 z_2 - \frac{67}{18} + \frac{\pi^2}{3} \right) \varepsilon + O(\varepsilon^2) \right), \\
I_{q\to qg} &= C_F \left(\frac{z_2^{-\varepsilon}-1}{\varepsilon} - \frac{3}{4} + \left(-\frac{7}{4} + \frac{\pi^2}{6} \right) \varepsilon + O(\varepsilon^2 \right) \\
&= C_F \left(-\ln z_2 - \frac{3}{4} + \left(\frac{1}{2}\ln^2 z_2 - \frac{7}{4} + \frac{\pi^2}{6} \right) \varepsilon + O(\varepsilon^2) \right),
\end{aligned} \tag{170}$$

$$\begin{aligned}
I_{g\to q\bar{q}} &= T_R N_f \left(\frac{1}{3} + \frac{5}{9}\varepsilon + O(\varepsilon^2) \right) \\
&= T_R N_f \left(\frac{1}{3} + \frac{5}{9}\varepsilon + O(\varepsilon^2) \right).
\end{aligned} \tag{171}$$

In the following we will write

$$I_{c\to ab} = I^0_{c\to ab} + \varepsilon I^1_{c\to ab} + O(\varepsilon^2). \tag{172}$$

Plugging everything together, the finite part of the multiplicative factor for a colour-ordered antenna with n gluons is :

$$
\begin{aligned}
g^2 c_\Gamma N_c \left(R_n - \frac{4}{N_c} n I_{g\to q\bar{q}} \right) = g^2 c_\Gamma N_c \Bigg\{ & (n+1) \ln^2 \left(\frac{\mu^2}{s_{min}} \right) \\
& + \ln^2 \left(\frac{s_{q1}}{s_{min}} \right) + ... + \ln^2 \left(\frac{s_{n\bar{q}}}{s_{min}} \right) \\
& + 2 \ln \left(\frac{\mu^2}{s_{min}} \right) \left(\ln \left(\frac{s_{q1}}{s_{min}} \right) + ... + \ln \left(\frac{s_{1\bar{q}}}{s_{min}} \right) \right) \\
& - \frac{4}{N_C} \Bigg[\frac{C_A}{2C_F} \left(I^1_{q\to qg} \left(\frac{s_{min}}{s_{q1}} \right) + \ln \left(\frac{\mu^2}{s_{min}} \right) I^0_{q\to qg} \left(\frac{s_{min}}{s_{q1}} \right) \right) \\
& + I^1_{g\to gg} \left(\frac{s_{min}}{s_{q1}}, \frac{s_{min}}{s_{12}} \right) + \ln \left(\frac{\mu^2}{s_{min}} \right) I^0_{g\to gg} \left(\frac{s_{min}}{s_{q1}}, \frac{s_{min}}{s_{12}} \right) \\
& + ... + \\
& + I^1_{g\to gg} \left(\frac{s_{min}}{s_{(n-1)n}}, \frac{s_{min}}{s_{n\bar{q}}} \right) + \ln \left(\frac{\mu^2}{s_{min}} \right) I^0_{g\to gg} \left(\frac{s_{min}}{s_{(n-1)n}}, \frac{s_{min}}{s_{n\bar{q}}} \right) \\
& + \frac{C_A}{2C_F} \left(I^1_{q\to qg} \left(\frac{s_{min}}{s_{n\bar{q}}} \right) + \ln \left(\frac{\mu^2}{s_{min}} \right) I^0_{q\to qg} \left(\frac{s_{min}}{s_{n\bar{q}}} \right) \right) \\
& n \left(I^1_{g\to q\bar{q}} + \ln \left(\frac{\mu^2}{s_{min}} \right) I^0_{g\to q\bar{q}} \right) \Bigg] \Bigg\}.
\end{aligned}
\tag{173}
$$

The factor $C_A/(2C_F) = N_c^2/(N_c^2-1)$ compensates the different colour factors in the definition of the splitting functions.

4.2.3 Subleading Terms in the Number of Colours

A partial amplitude factors in the soft gluon limit like

$$
A_{n+1} \to g \cdot \mathrm{Eik}^\lambda_{ab} \cdot A_n \tag{174}
$$

where the eikonal factors are

$$
\mathrm{Eik}^+_{ab} = \sqrt{2} \frac{\langle ab \rangle}{\langle as \rangle \langle sb \rangle}, \qquad \mathrm{Eik}^-_{ab} = -\sqrt{2} \frac{[ab]}{[as][sb]}. \tag{175}
$$

In subleading colour we have terms like

$$
\begin{aligned}
& \sum_{\text{soft gluon helicity } \lambda} A^{(2)*}_{n+1} A^{(1)}_{n+1} + A^{(1)*}_{n+1} A^{(2)}_{n+1} \\
& = \; g^2 \left(\mathrm{Eik}^{(2)-} \mathrm{Eik}^{(1)+} + \mathrm{Eik}^{(2)+} \mathrm{Eik}^{(1)-} \right) \left(A^{(2)*}_n A^{(1)}_n + A^{(1)*}_n A^{(2)}_n \right).
\end{aligned}
\tag{176}
$$

There are three different cases, depending how the soft gluon is inserted into the partial amplitude $A^{(1)}_{n+1}$ and $A^{(2)}_{n+1}$.

1. Two common legs

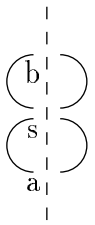

$$\sum_{\lambda} A^{(2)*}_{n+1}A^{(1)}_{n+1} + A^{(1)*}_{n+1}A^{(2)}_{n+1} \;=\; g^2\cdot 2\cdot 2\frac{s_{ab}}{s_{as}s_{sb}}\left(A^{(2)*}_{n}A^{(1)}_{n} + A^{(1)*}_{n}A^{(2)}_{n}\right) \tag{177}$$

2. One common leg.

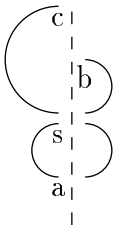

$$\begin{aligned}
&\sum_{\lambda} A^{(2)*}_{n+1}A^{(1)}_{n+1} + A^{(1)*}_{n+1}A^{(2)}_{n+1} = \\
&= \; g^2\cdot 2\left(\frac{\langle ab\rangle}{\langle as\rangle\langle sb\rangle}\frac{[ca]}{[cs][sa]} + \frac{[ab]}{[as][sb]}\frac{\langle ca\rangle}{\langle cs\rangle\langle sa\rangle}\right)\left(A^{(2)*}_{n}A^{(1)}_{n} + A^{(1)*}_{n}A^{(2)}_{n}\right) \\
&= \; g^2\cdot 2\left(\frac{s_{ab}}{s_{as}s_{sb}} - \frac{s_{bc}}{s_{bs}s_{sc}} + \frac{s_{ac}}{s_{as}s_{sc}}\right)\left(A^{(2)*}_{n}A^{(1)}_{n} + A^{(1)*}_{n}A^{(2)}_{n}\right)
\end{aligned} \tag{178}$$

3. No common legs.

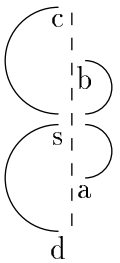

$$\begin{aligned}
&\sum_\lambda A_{n+1}^{(2)*} A_{n+1}^{(1)} + A_{n+1}^{(1)*} A_{n+1}^{(2)} = \\
&= g^2 \cdot 2 \left(\frac{\langle ab \rangle}{\langle as \rangle \langle sb \rangle} \frac{[cd]}{[cs][sd]} + \frac{[ab]}{[as][sb]} \frac{\langle cd \rangle}{\langle cs \rangle \langle sd \rangle} \right) \left(A_n^{(2)*} A_n^{(1)} + A_n^{(1)*} A_n^{(2)} \right) \\
&= g^2 \cdot 2 \left(\frac{s_{ac}}{s_{as} s_{sc}} - \frac{s_{ad}}{s_{as} s_{sd}} + \frac{s_{bd}}{s_{bs} s_{sd}} - \frac{s_{bc}}{s_{bs} s_{sc}} \right) \left(A_n^{(2)*} A_n^{(1)} + A_n^{(1)*} A_n^{(2)} \right)
\end{aligned} \tag{179}$$

In each case the last line indicates the different regions of phase space where the matrix element will be approximated by the appropriate eikonal approximations. Note that there are several soft regions.
In the collinear limit tree-level partial amplitudes factorize like

$$A_{n+1} \to g \sum_{\lambda=+/-} \mathrm{Split}_{-\lambda}(p_a^{\lambda_a}, p_b^{\lambda_b}) A_n(..., P^\lambda, ...) \tag{180}$$

where $P = p_a + p_b$, $p_a = zP$ and $p_b = (1-z)P$. λ, λ_a and λ_b denote the corresponding helicities. The splitting functions are given in the appendix.

4.2.4 Real Emission with Two Quarks and Three Gluons

The colour decomposition of the tree-level amplitude for $e^+e^- \to qggg\bar{q}$ is

$$\begin{aligned}
A_5 &= (T^1T^2T^3)_{q\bar{q}} A_5(q,1,2,3,\bar{q}) + (T^1T^3T^2)_{q\bar{q}} A_5(q,1,3,2,\bar{q}) \\
&\quad + (T^2T^3T^1)_{q\bar{q}} A_5(q,2,3,1,\bar{q}) + (T^2T^1T^3)_{q\bar{q}} A_5(q,2,1,3,\bar{q}) \\
&\quad + (T^3T^1T^2)_{q\bar{q}} A_5(q,3,1,2,\bar{q}) + (T^3T^2T^1)_{q\bar{q}} A_5(q,3,2,1,\bar{q}).
\end{aligned} \tag{181}$$

The partial amplitudes are given in [38]. The matrix element squared can be written as

$$|A_5|^2 = \vec{A}_5^\dagger C \vec{A}_5 \tag{182}$$

where

$$\vec{A}_5 = \begin{pmatrix} A_5(q,1,2,3,\bar{q}) \\ A_5(q,1,3,2,\bar{q}) \\ A_5(q,2,3,1,\bar{q}) \\ A_5(q,2,1,3,\bar{q}) \\ A_5(q,3,1,2,\bar{q}) \\ A_5(q,3,2,1,\bar{q}) \end{pmatrix} \tag{183}$$

and the colour matrix is given by

$$C = \begin{pmatrix} c_1^{(3)} & c_2^{(3)} & c_3^{(3)} & c_2^{(3)} & c_3^{(3)} & c_4^{(3)} \\ c_2^{(3)} & c_1^{(3)} & c_4^{(3)} & c_3^{(3)} & c_2^{(3)} & c_3^{(3)} \\ c_3^{(3)} & c_4^{(3)} & c_1^{(3)} & c_2^{(3)} & c_3^{(3)} & c_2^{(3)} \\ c_2^{(3)} & c_3^{(3)} & c_2^{(3)} & c_1^{(3)} & c_4^{(3)} & c_3^{(3)} \\ c_3^{(3)} & c_2^{(3)} & c_3^{(3)} & c_4^{(3)} & c_1^{(3)} & c_2^{(3)} \\ c_4^{(3)} & c_3^{(3)} & c_2^{(3)} & c_3^{(3)} & c_2^{(3)} & c_1^{(3)} \end{pmatrix} \tag{184}$$

where the colour factors are

$$\begin{aligned} c_1^{(3)} &= \left(\frac{1}{2}\right)^3 \frac{(N^2-1)^3}{N^2}, \\ c_2^{(3)} &= -\left(\frac{1}{2}\right)^3 \frac{(N^2-1)^2}{N^2}, \\ c_3^{(3)} &= \left(\frac{1}{2}\right)^3 \frac{N^2-1}{N^2}, \\ c_4^{(3)} &= \left(\frac{1}{2}\right)^3 \frac{(N^2-1)(N^2+1)}{N^2} = 2c_3^{(3)} - c_2^{(3)}. \end{aligned} \tag{185}$$

If one gluon becomes soft or collinear, the matrix element squared reduces to the one with one gluon less

$$|A_5|^2 \rightarrow \vec{A}_4^{\dagger} \begin{pmatrix} c_1^{(2)} R_{diag}(q,1,2,\bar{q}) & c_2^{(2)} R_{off}(q,1,2,\bar{q}) \\ c_2^{(2)} R_{off}(q,1,2,\bar{q}) & c_1^{(2)} R_{diag}(q,2,1,\bar{q}) \end{pmatrix} \vec{A}_4. \tag{186}$$

where the colour factors are

$$\begin{aligned} c_1^{(2)} &= \left(\frac{1}{2}\right)^2 \frac{(N^2-1)^2}{N}, \\ c_2^{(2)} &= -\left(\frac{1}{2}\right)^2 \frac{N^2-1}{N} \end{aligned} \tag{187}$$

The finite R-factors are given by

$$
\begin{aligned}
&R_{diag}(q,1,2,\bar{q}) = \\
&= g^2 c_\Gamma \left\{ \frac{N_c^2-1}{N_c} R_2(q,1,2,\bar{q}) \right. \\
&\quad + \frac{1}{N_c}\left(2R_2(q,1,2,\bar{q}) - R_1(q,1,\bar{q}) - R_1(q,2,\bar{q})\right) \\
&\quad + \frac{1}{N_c\,(N_c^2-1)}\left(R_2(q,1,2,\bar{q}) - R_1(q,1,\bar{q}) - R_1(q,2,\bar{q}) + R_0(q,\bar{q})\right) \\
&\quad \left. + 2I_{g\to q\bar{q}} \right\}, \\
&R_{off}(q,1,2,\bar{q}) = \\
&= g^2 c_\Gamma \left\{ \frac{N_c^2-1}{N_c}\left(R_1(q,1,\bar{q}) + R_1(q,2,\bar{q}) - R_0(q,\bar{q})\right) \right. \\
&\quad + \frac{1}{N_c}\left(R_1(q,1,\bar{q}) + R_1(q,2,\bar{q}) - 2R_0(q,\bar{q})\right) \\
&\quad \left. + 2I_{g\to q\bar{q}} \right\}. \qquad (188)
\end{aligned}
$$

The first three lines for R_{diag} give the separate contributions from the terms with the colour factors $c_1^{(3)}$,$c_2^{(3)}$ and $c_3^{(3)}$, respectively. ($c_4^{(3)}$ has been written as $c_4^{(3)} = 2c_3^{(3)} - c_2^{(3)}$.) The last line corresponds to the contribution from the $A(q,\bar{q},Q,\bar{Q},g)$ amplitudes, when one pair of quarks become collinear. The first two lines for R_{off} correspond to the contributions from $c_2^{(3)}$ and $c_3^{(3)}$. We have used the notation

$$
\begin{aligned}
S(a,b) &= \ln^2\left(\frac{\mu^2}{s_{min}}\right) + \ln^2\left(\frac{s_{ab}}{s_{min}}\right) + 2\ln\left(\frac{\mu^2}{s_{min}}\right)\ln\left(\frac{s_{ab}}{s_{min}}\right), \qquad (189) \\
I_{a\to bc}(z_1,z_2) &= I^1_{a\to bc}(z_1,z_2) + I^0_{a\to bc}(z_1,z_2)\ln\left(\frac{\mu^2}{s_{min}}\right), \qquad (190) \\
R_0(q,\bar{q}) &= S(q,\bar{q}) - \frac{4}{N_c}\frac{C_A}{2C_F} 2I_{q\to qg}\left(\frac{s_{min}}{s_{q\bar{q}}}\right), \qquad (191) \\
R_1(q,1,\bar{q}) &= S(q,1) + S(1,\bar{q}) - \frac{4}{N_c}\left[\frac{C_A}{2C_F} I_{q\to qg}\left(\frac{s_{min}}{s_{q1}}\right)\right. \\
&\quad \left. + I_{g\to gg}\left(\frac{s_{min}}{s_{q1}},\frac{s_{min}}{s_{1\bar{q}}}\right) + \frac{C_A}{2C_F} I_{q\to qg}\left(\frac{s_{min}}{s_{1\bar{q}}}\right)\right], \qquad (192) \\
R_2(q,1,2,\bar{q}) &= S(q,1) + S(1,2) + S(2,\bar{q}) - \frac{4}{N_c}\left[\frac{C_A}{2C_F} I_{q\to qg}\left(\frac{s_{min}}{s_{q1}}\right)\right. \\
&\quad + I_{g\to gg}\left(\frac{s_{min}}{s_{q1}},\frac{s_{min}}{s_{12}}\right) + I_{g\to gg}\left(\frac{s_{min}}{s_{12}},\frac{s_{min}}{s_{2\bar{q}}}\right) \\
&\quad \left. + \frac{C_A}{2C_F} I_{q\to qg}\left(\frac{s_{min}}{s_{2\bar{q}}}\right)\right]. \qquad (193)
\end{aligned}
$$

4.2.5 Real Emission with Four Quarks and One Gluon

The tree-level amplitude for $e^+e^- \to q\bar{q}Q\bar{Q}g$ can be written as

$$A_5 = \frac{1}{2}\delta_{14}T_{32}D_1 + \frac{1}{2}\delta_{32}T_{14}D_2 - \frac{1}{2}\delta_{12}T_{34}D_3 - \frac{1}{2}\delta_{34}T_{12}D_4 \qquad (194)$$

where the factor $1/2$ is due to the conventional normalization of T^a and

$$\begin{aligned}
D_1 &= c_0(1)B_1(0;1,2;3,4) + c_0(3)B_2(0;3,4;1,2) \\
&\quad +\delta_{flav}\frac{1}{N_C}\left(c_0(1)B_3(0;1,4;3,2) + c_0(3)B_4(0;3,2;1,4)\right), \\
D_2 &= c_0(1)B_2(0;1,2;3,4) + c_0(3)B_1(0;3,4;1,2) \\
&\quad +\delta_{flav}\frac{1}{N_C}\left(c_0(1)B_4(0;1,4;3,2) + c_0(3)B_3(0;3,2;1,4)\right), \\
D_3 &= c_0(1)\frac{1}{N_C}B_3(0;1,2;3,4) + c_0(3)\frac{1}{N_C}B_4(0;3,4;1,2) \\
&\quad +\delta_{flav}\left(c_0(1)B_1(0;1,4;3,2) + c_0(3)B_2(0;3,2;1,4)\right), \\
D_4 &= c_0(1)\frac{1}{N_C}B_4(0;1,2;3,4) + c_0(3)\frac{1}{N_C}B_3(0;3,4;1,2) \\
&\quad +\delta_{flav}\left(c_0(1)B_2(0;1,4;3,2) + c_0(3)B_1(0;3,2;1,4)\right). \qquad (195)
\end{aligned}$$

The partial amplitudes B_i are given in [38]. One can write

$$|A_5|^2 = \vec{D}^\dagger C\,\vec{D}. \qquad (196)$$

Then the colour matrix is given by

$$C = \begin{pmatrix} c_1^{(1)} & 0 & c_2^{(1)} & c_2^{(1)} \\ 0 & c_1^{(1)} & c_2^{(1)} & c_2^{(1)} \\ c_2^{(1)} & c_2^{(1)} & c_1^{(1)} & 0 \\ c_2^{(1)} & c_2^{(1)} & 0 & c_1^{(1)} \end{pmatrix} \qquad (197)$$

where

$$c_1^{(1)} = \frac{1}{8}N_C(N_C^2-1), \qquad c_2^{(1)} = -\frac{1}{8}(N_C^2-1) \qquad (198)$$

The colour decomposition of the four quark amplitude can be written as

$$\begin{aligned}
A_4 &= \frac{1}{2}\left(\delta_{12}\delta_{34} - \frac{1}{N_c}\delta_{14}\delta_{32}\right)\chi(1,2,3,4) \\
&\quad -\frac{1}{2}\left(\delta_{14}\delta_{32} - \frac{1}{N_c}\delta_{12}\delta_{34}\right)\delta_{flav}\chi(1,4,3,2) \qquad (199)
\end{aligned}$$

where

$$\chi(1,2,3,4) = A_4(1,2,3,4) + A_4(3,4,1,2). \qquad (200)$$

The matrix element squarred we may write as

$$|A_4|^2 \;=\; \vec{\chi}^{\dagger} \begin{pmatrix} c_1^{(0)} & c_2^{(0)} \\ c_2^{(0)} & c_1^{(0)} \end{pmatrix} \vec{\chi} \tag{201}$$

with

$$c_1^{(0)} = \frac{1}{4}\left(N_c^2 - 1\right), \qquad c_2^{(0)} = \frac{1}{4}\frac{N_c^2 - 1}{N_c} \tag{202}$$

and

$$\vec{\chi} \;=\; \begin{pmatrix} \chi(1,2,3,4) \\ \delta_{flav}\chi(1,4,3,2) \end{pmatrix}. \tag{203}$$

In the soft gluon limit, the functions B_i behave like

$$\begin{aligned} B_1(0;1,2;3,4) &\;\to\; g \cdot \mathrm{Eik}_{32} \cdot A(1,2;3,4), \\ B_2(0;1,2;3,4) &\;\to\; g \cdot \mathrm{Eik}_{14} \cdot A(1,2;3,4), \\ B_3(0;1,2;3,4) &\;\to\; g \cdot \mathrm{Eik}_{34} \cdot A(1,2;3,4), \\ B_4(0;1,2;3,4) &\;\to\; g \cdot \mathrm{Eik}_{12} \cdot A(1,2;3,4). \end{aligned} \tag{204}$$

In the limit where one pair of quarks becomes collinear, the amplitudes factorize as

$$\begin{aligned} B_1(0;1,2;3,4) &\;\to\; g\sum_{\lambda} \mathrm{Split}_P(3,4) A_4(1,P,0,2), \\ B_2(0;1,2;3,4) &\;\to\; g\sum_{\lambda} \mathrm{Split}_P(3,4) A_4(1,0,P,2), \\ B_3(0;1,2;3,4) &\;\to\; 0, \\ B_4(0;1,2;3,4) &\;\to\; g\sum_{\lambda} \mathrm{Split}_P(3,4) \left(A_4(1,P,0,2) + A_4(1,0,P,2)\right). \end{aligned} \tag{205}$$

One of the functions B_i is redundant, since

$$B_1 + B_2 - B_3 - B_4 = 0. \tag{206}$$

The contribution from unresolved phase space is written as

$$\vec{\chi}^{\dagger} \begin{pmatrix} c_1^{(0)} R_{diag}(1,2,3,4) & c_2^{(0)} R_{off}(1,2,3,4) \\ c_2^{(0)} R_{off}(1,2,3,4) & c_1^{(0)} R_{diag}(1,4,3,2) \end{pmatrix} \vec{\chi} \tag{207}$$

with

$$
\begin{aligned}
&R_{diag}(1,2,3,4) = \\
&\quad = \frac{1}{N_c}\left[N_c^2\left(R_0(1,4)+R_0(2,3)\right)+R_0(1,2)+R_0(3,4)\right. \\
&\qquad \left.+2\left(R_0(1,3)+R_0(2,4)-R_0(1,2)-R_0(2,3)-R_0(3,4)-R_0(1,4)\right)\right], \\
&R_{off}(1,2,3,4) = \\
&\quad = N_c\left(R_0(1,2)+R_0(2,3)+R_0(3,4)+R_0(1,4)\right) \\
&\qquad +\frac{N_c^2+1}{N_c}\left(R_0(1,3)+R_0(2,4)-R_0(1,2)-R_0(2,3)-R_0(3,4)-R_0(1,4)\right).
\end{aligned}
\tag{208}
$$

The first line gives the contribution from the colour factor $c_1^{(1)}$ while the second line gives the contribution from $c_2^{(1)}$.

4.2.6 Subtleties of Phase Space Slicing

Phase space slicing requires to split up the $(n+1)$-parton matrix element into terms with a definite singularity structure. For each of these terms only the regions of phase space have to be cut out in which singularities actually occur. These regions may be different for different terms. Cutting out additional regions may result in neglecting contributions which do not vanish in the $s_{min} \to 0$ limit but give a finite contribution. Therefore multiplying the squared amplitude by a product of Θ-functions $\prod \Theta(s_{ij} - s_{min})$ which cuts out all regions in which the integrand may have singularities may give a wrong result. To illustrate this point consider a simplified 4-parton matrix element

$$
|A|^2 = \frac{1}{s_{q1}s_{12}s_{2\bar{q}}} + \frac{1}{s_{q2}s_{21}s_{1\bar{q}}} \tag{209}
$$

The first terms has singularities in s_{q1}, s_{12} and $s_{2,\bar{q}}$, whereas the second has singularities in s_{q2}, s_{12} and $s_{1,\bar{q}}$. Assume that this matrix element gives the real emission to a 3-jet quantity. Cutting out additional phase space consists in considering integrals of the form

$$
\begin{aligned}
I = &\int d\Phi_4 \frac{1}{s_{q1}s_{12}s_{2\bar{q}}}\Theta(s_{q1}-s_{min})\Theta(s_{12}-s_{min})\Theta(s_{2\bar{q}}-s_{min}) \\
&\cdot\Theta(s_{min}-s_{q2})\Theta(3\text{ jets}).
\end{aligned}
\tag{210}
$$

Here we have taken only the first term of equation (209), the first three Θ - functions cut out the poles, whereas $\Theta(s_{min} - s_{q2})$ forces in addition $0 < s_{q2} < s_{min}$. $\Theta(3\text{ jets})$ denotes the jet defining function. It is easily verified numerically that this integral approaches a constant value in the limit $s_{min} \to 0$ and may therefore not be cut out.

In conclusion it is essential to decompose the matrix element into terms with definite singularity structure and to cut out for each term separately only the regions in which singularities actually occur.

4.3 The Dipole Formalism

The dipole formalism [57] is based on the subtraction method. The NLO cross section is written as

$$\begin{aligned} \sigma^{NLO} &= \int\limits_{n+1} d\sigma^R + \int\limits_n d\sigma^V \\ &= \int\limits_{n+1} \left(d\sigma^R - d\sigma^A \right) + \int\limits_n \left(d\sigma^V + \int\limits_1 d\sigma^A \right) \end{aligned} \tag{211}$$

where in the last line an approximation term $d\sigma^A$ has been added and subtracted. The approximation $d\sigma^A$ has to fulfill the following requirements:

- $d\sigma^A$ must be a proper approximation of $d\sigma^R$ such as to have the same pointwise singular behaviour (in D dimensions) as $d\sigma^R$ itself. Thus, $d\sigma^A$ acts as a local counterterm for $d\sigma^R$ and one can safely perform the limit $\varepsilon \to 0$. This defines a cross-section contribution

$$\sigma^{NLO}_{\{n+1\}} = \int\limits_{n+1} \left(d\sigma^R\Big|_{\varepsilon=0} - d\sigma^A\Big|_{\varepsilon=0} \right). \tag{212}$$

- Analytic integrability (in D dimensions) over the one-parton subspace leading to soft and collinear divergences. This gives the contribution

$$\sigma^{NLO}_{\{n\}} = \int\limits_n \left(d\sigma^V + \int\limits_1 d\sigma^A \right)_{\varepsilon=0}. \tag{213}$$

The final structure of a NLO calculation is then

$$\sigma^{NLO} = \sigma^{NLO}_{\{n+1\}} + \sigma^{NLO}_{\{n\}}. \tag{214}$$

Catani and Seymour derive the dipole formalism within the conventional dimensional regularization scheme (CDR). The approximation term is written as the n-parton Born term $d\sigma^B$ times the dipole factors :

$$d\sigma^A = \sum_{\text{dipoles}} d\sigma^B \otimes dV_{\text{dipole}}. \tag{215}$$

The integration over the $(n+1)$-parton phase space yields

$$\int\limits_{n+1} d\sigma^A = \sum \text{dipoles} \int\limits_n d\sigma^B \otimes \int\limits_1 dV_{\text{dipole}} = \int\limits_n \left[d\sigma^B \otimes I \right] \tag{216}$$

where the universal factor I is defined by

$$I = \sum_{\text{dipoles}} \int_1 dV_{\text{dipoles}}. \tag{217}$$

The $(n+1)$ matrix element is approximated by

$$\begin{aligned}
&\sum_{\text{pairs } i,j} \sum_{k \neq i,j} \mathcal{D}_{ij,k} = \\
&= \sum_{\text{pairs } i,j} \sum_{k \neq i,j} -\frac{1}{2p_i \cdot p_j} \langle 1, ..., (\tilde{ij}), ..., \tilde{k}, ... | \frac{T_k \cdot T_{ij}}{T_{ij}^2} V_{ij,k} | 1, ..., (\tilde{ij}), ..., \tilde{k}, ... \rangle
\end{aligned} \tag{218}$$

where the emitter parton is denoted by $\tilde{ij}$ and the spectator by $\tilde{k}$. The momenta are defined by

$$\begin{aligned}
\tilde{p}_k^\mu &= \frac{1}{1-y} p_k^\mu, \\
\tilde{p}_{ij}^\mu &= p_i^\mu + p_j^\mu - \frac{y}{1-y} p_k^\mu
\end{aligned} \tag{219}$$

where

$$y = \frac{p_i p_j}{p_i p_j + p_j p_k + p_k p_i}. \tag{220}$$

Both the emitter and the spectator are on-shell ($\tilde{p}_{ij}^2 = \tilde{p}_k^2 = 0$) and momentum conservation is implemented exactly

$$p_i^\mu + p_j^\mu + p_k^\mu = \tilde{p}_{ij}^\mu + \tilde{p}_k^\mu. \tag{221}$$

The T_k and T_{ij} are the colour charges of the spectator and the emitter, respectively. The colour charge operator is defined as if_{cab} if the emitting particle is a gluon, as T_{ij}^a if it is a quark and as $(T_{ij}^a)^\dagger = -T_{ji}^a$ if it is an anti-quark. The $V_{ij,k}$ are matrices in the helicity space of the emitter. They are related to the D-dimensional Altarelli-Parisi splitting functions and depend on y and the kinematic variables $\tilde{z}_i$, $\tilde{z}_j$, which are given by

$$\begin{aligned}
\tilde{z}_i &= \frac{p_i p_k}{p_j p_k + p_i p_k} = \frac{p_i \tilde{p}_k}{\tilde{p}_{ij} \tilde{p}_k}, \\
\tilde{z}_j &= 1 - \tilde{z}_i = \frac{p_j p_k}{p_j p_k + p_i p_k} = \frac{p_j \tilde{p}_k}{\tilde{p}_{ij} \tilde{p}_k}.
\end{aligned} \tag{222}$$

One finds

$$
\begin{aligned}
V_{q_i g_j,k} &= 8\pi\mu^{2\varepsilon}\alpha_s\delta_{ss'}C_F\left[\frac{2}{1-\tilde{z}_i(1-y)}-(1+\tilde{z}_i)-\varepsilon(1-\tilde{z}_i)\right], \\
V_{q_i\bar{q}_j,k} &= 8\pi\mu^{2\varepsilon}\alpha_s T_R\left[-g^{\mu\nu}-\frac{2}{p_ip_j}(\tilde{z}_ip_i^\mu-\tilde{z}_jp_j^\mu)(\tilde{z}_ip_i^\nu-\tilde{z}_jp_j^\nu)\right], \\
V_{g_i g_j,k} &= 8\pi\mu^{2\varepsilon}\alpha_s 2C_A\left[-g^{\mu\nu}\left(\frac{1}{1-\tilde{z}_i(1-y)}+\frac{1}{1-\tilde{z}_j(1-y)}-2\right)\right. \\
&\quad \left.+(1-\varepsilon)\frac{1}{p_ip_j}(\tilde{z}_ip_i^\mu-\tilde{z}_jp_j^\mu)(\tilde{z}_ip_i^\nu-\tilde{z}_jp_j^\nu)\right] \qquad (223)
\end{aligned}
$$

where s, s' are the spin indices of the fermion $\tilde{ij}$ and μ, ν are the spin indices of the gluon $\tilde{ij}$. Note that the spin correlation tensor

$$
\frac{1}{p_ip_j}(\tilde{z}_ip_i^\mu-\tilde{z}_jp_j^\mu)(\tilde{z}_ip_i^\nu-\tilde{z}_jp_j^\nu) \qquad (224)
$$

is orthogonal to both $\tilde{p}_{ij}^\mu$ and $\tilde{p}_{ij}^\nu$. Integrating the dipole factors over the dipole phase space and averaging over the polarizations of the emitter one obtains

$$
\int dp_i(\tilde{p}_{ij},\tilde{p}_k)\langle V_{ij,k}\rangle = \frac{\alpha_s}{2\pi}\frac{1}{\Gamma(1-\varepsilon)}\left(\frac{4\pi\mu^2}{2\tilde{p}_{ij}\tilde{p}_k}\right)^\varepsilon \mathcal{V}_{ij}(\varepsilon); \qquad (225)
$$

$$
\begin{aligned}
\mathcal{V}_{qg}(\varepsilon) &= \frac{\Gamma^3(1-\varepsilon)}{\Gamma(1-3\varepsilon)}C_F\left[\frac{1}{\varepsilon^2}+\frac{1}{\varepsilon}\frac{3+\varepsilon}{2(1-3\varepsilon)}\right] \\
&= C_F\left[\frac{1}{\varepsilon^2}+\frac{3}{2\varepsilon}+5-\frac{\pi^2}{2}+O(\varepsilon)\right], \\
\mathcal{V}_{q\bar{q}}(\varepsilon) &= \frac{\Gamma^3(1-\varepsilon)}{\Gamma(1-3\varepsilon)}T_R\left[-\frac{1}{\varepsilon}\frac{2(1-\varepsilon)}{(1-3\varepsilon)(3-2\varepsilon)}\right] \\
&= T_R\left[-\frac{2}{3\varepsilon}-\frac{16}{9}+O(\varepsilon)\right], \\
\mathcal{V}_{gg}(\varepsilon) &= \frac{\Gamma^3(1-\varepsilon)}{\Gamma(1-3\varepsilon)}2C_A\left[\frac{1}{\varepsilon^2}+\frac{1}{\varepsilon}\frac{11-7\varepsilon}{2(1-3\varepsilon)(3-2\varepsilon)}\right] \\
&= 2C_A\left[\frac{1}{\varepsilon^2}+\frac{11}{6\varepsilon}+\frac{50}{9}-\frac{\pi^2}{2}+O(\varepsilon)\right]. \qquad (226)
\end{aligned}
$$

By subtracting from the real emission part the fake contribution we obtain

$$
\begin{aligned}
d\sigma^R-d\sigma^A &= d\phi_{n+1}\left[|M(p_1,...,p_{n+1})|^2\theta_{n+1}^{cut}(p_1,...,p_{n+1})\right. \\
&\quad \left.-\sum_{\text{pairs }i,j}\sum_{k\neq i,j}\mathcal{D}_{ij,k}(p_1,...,p_{n+1})\theta_n^{cut}(p_1,...,\tilde{p}_{ij},...,\tilde{p}_k,...,p_{n+1})\right]. \qquad (227)
\end{aligned}
$$

Both $d\sigma^R$ and $d\sigma^A$ are integrated over the same $(n+1)$ parton phase space, but it should be noted that $d\sigma^R$ is proportional to θ_{n+1}^{cut}, whereas $d\sigma^A$ is proportional to θ_n^{cut}. Here θ_n^{cut} denotes the jet-defining function for n-partons.

The integral over the subtraction term is written as

$$\int_{n+1} d\sigma^A = \int_n \left[d\sigma^B \cdot I(\varepsilon) \right] \tag{228}$$

where

$$I(p_1, ..., p_n) = -\frac{\alpha_s}{2\pi} \frac{1}{\Gamma(1-\varepsilon)} \sum_i \frac{1}{T_i^2} \mathcal{V}_i(\varepsilon) \sum_{k \neq i} T_i \cdot T_k \left(\frac{4\pi\mu^2}{2p_i \cdot p_k} \right)^{\varepsilon} \tag{229}$$

where

$$\mathcal{V}_i = T_i^2 \left(\frac{1}{\varepsilon^2} - \frac{\pi^2}{3} \right) + \frac{\gamma_i}{\varepsilon} + \gamma_i + K_i + O(\varepsilon) \tag{230}$$

with

$$\begin{aligned} \gamma_{i=q,\bar{q}} &= \frac{3}{2} C_F, \qquad \gamma_{i=g} = \frac{11}{6} C_A - \frac{2}{3} T_R N_f, \\ K_{i=q,\bar{q}} &= \left(\frac{7}{2} - \frac{\pi^2}{6} \right) C_F, \qquad K_{i=g} = \left(\frac{67}{18} - \frac{\pi^2}{6} \right) C_A - \frac{10}{9} T_R N_f. \end{aligned} \tag{231}$$

Note that the T_i are acting on the colour space of the amplitudes. In summary the dipole formalism needs

- a set of independent colour projections of the matrix element squared at the tree level in D dimensions, summed over parton polarizations.
- the one-loop matrix element in D dimensions;
- an additional projection of the Born level matrix element over the helicity of each external gluon in four dimensions;
- the tree-level $(n+1)$-matrix element in four dimensions.

4.3.1 Spin Correlation

In this subsection I give the relevant formulae for the implementation of the spin correlation using helicity amplitudes. Let A^μ denote the n-parton amplitude, where the polarization vector ε_μ of the emitter gluon has been amputated. Using

$$\left(\varepsilon_+^\mu\right)^* \varepsilon_+^\nu + \left(\varepsilon_-^\mu\right)^* \varepsilon_-^\nu = -g^{\mu\nu} + \frac{\tilde{p}_{ij}^\mu q^\nu + \tilde{p}_{ij}^\nu q^\mu}{\tilde{p}_{ij} \cdot q}, \tag{232}$$

where q is an arbitrary reference momentum, we obtain

$$(A^\mu)^* \left(-g_{\mu\nu}\right) A^\nu \;=\; A_+^* A_+ + A_-^* A_- \tag{233}$$

where $A_\pm$ denotes the helicity amplitude where the emitter gluon has positive or negative helicity. The dependence on the reference momentum q drops out, since $\left(\tilde{p}_{ij}\right)_\mu A^\mu = 0$ (gauge invariance), $q_\mu \varepsilon^\mu = 0$ (property of the polarization vectors) and $\left(\tilde{p}_{ij}\right)^2 = 0$ (the gluon is on mass-shell). For the spin correlation we obtain

$$(A_\mu)^* \left(\tilde{z}_i p_i^\mu - \tilde{z}_j^\mu p_j^\mu\right) \left(\tilde{z}_i p_i^\nu - \tilde{z}_j^\nu p_j^\nu\right) A_\nu \;=\; \left|E A_+ + E^* A_-\right|^2 , \tag{234}$$

where

$$E \;=\; \frac{\langle q+|\tilde{z}_i \not{p}_i - \tilde{z}_j \not{p}_j|\tilde{p}_{ij}+\rangle}{\sqrt{2}[q\tilde{p}_{ij}]} \tag{235}$$

As reference momentum one may choose $q = p_j$, in that case E reduces to

$$E \;=\; \frac{\tilde{z}_i [q p_i] \langle p_i \tilde{p}_{ij}\rangle}{\sqrt{2}[q\tilde{p}_{ij}]} \tag{236}$$

Using the fact that the spin correlation tensor is orthogonal to $\tilde{p}_{ij}$ one shows again that the dependence on the reference momentum drops out.

4.3.2 Colour Correlation

The colour correlation matrices may be obtained by two ways. The first approach is the one given by Catani and Seymour. Within this approach one acts with the colour charge operators on the n-parton amplitudes. For example

$$\begin{aligned}\langle q,1,2,\bar{q}|T_q \cdot T_1|q,1,2,\bar{q}\rangle = \left(T^2_{\bar{q}j} T^{1'}_{jq'} A(q,1,2,\bar{q})^*, T^{1'}_{\bar{q}j} T^2_{jq'} A(q,2,1,\bar{q})^*\right) \\ \cdot T^a_{q'q} \cdot 2\mathrm{Tr}\left(T^{1'} T^a T^1 - T^a T^{1'} T^1\right) \cdot \begin{pmatrix} T^1_{qi} T^2_{i\bar{q}} A(q,1,2,\bar{q}) \\ T^2_{qi} T^1_{i\bar{q}} A(q,2,1,\bar{q}) \end{pmatrix}\end{aligned} \tag{237}$$

Here the colour charge operator for the gluon has been written as

$$i f^{cab} \;=\; 2\mathrm{Tr}\left(T^c T^a T^b - T^a T^c T^b\right) \tag{238}$$

On the other hand one may start from the colour decomposition of the $(n+1)$ -parton matrix element in the form of equations (182) and (196). One then considers the soft and collinear limits using the partial fraction decompositions (177) - (179). This procedure is identical to the one followed in the phase space slicing approach. With the help of the identity

$$\frac{s_{ab}}{s_{as} s_{sb}} \;=\; \frac{s_{ab}}{s_{as}(s_{as}+s_{sb})} + \frac{s_{ab}}{s_{sb}(s_{as}+s_{sb})} \tag{239}$$

the colour correlation matrix can then be read off from equations (186) and (207). This approach has the advantage that it makes the connection between each divergent term in the $(n+1)$ -parton matrix element and the corresponding subtraction term transparent.

The leading order matrix element $e^+e^- \to qg_1g_2g_3\bar{q}$ needs 27 dipole factors. There are six terms where the quark is the emitter and a gluon the spectator and three terms where the role of the emitter and spectator are exchanged. The colour correlation matrices are invariant under the exchange of emitter and spectator. The colour correlation matrix for the case $T_q \cdot T_1$ is given by

$$T_q \cdot T_1 = \begin{pmatrix} c_2^{(3)} - c_1^{(3)} & \frac{1}{2}\left(c_4^{(3)} - c_2^{(3)}\right) \\ \frac{1}{2}\left(c_4^{(3)} - c_2^{(3)}\right) & c_3^{(3)} - c_2^{(3)} \end{pmatrix} \tag{240}$$

If the antiquark $\bar{q}$ is the spectator we obtain

$$T_q \cdot T_{\bar{q}} = \begin{pmatrix} -c_3^{(3)} & -c_4^{(3)} \\ -c_4^{(3)} & -c_3^{(3)} \end{pmatrix} \tag{241}$$

Finally the colour correlation matrix where both emitter and spectator are gluons is given by

$$T_1 \cdot T_2 = \begin{pmatrix} -c_1^{(3)} + 2c_2^{(3)} - c_3^{(3)} & 0 \\ 0 & -c_1^{(3)} + 2c_2^{(3)} - c_3^{(3)} \end{pmatrix} \tag{242}$$

All other colour correlation matrices can be obtained by a permutation of indices.

The leading order matrix element $e^+e^- \to q\bar{q}Q\bar{Q}g$ needs 12 dipole factors associated with the splitting $g \to q\bar{q}$ and 12 dipole factors assocoiated to the splitting $q \to qg$ or $\bar{q} \to g\bar{q}$. The relevant colour correlation matrices for the first case where already given above. The colour correlation matrices for the latter case are

$$T_q \cdot T_{\bar{q}} = \begin{pmatrix} -\frac{c_1^{(1)}}{N_c^2} - 2\frac{c_2^{(1)}}{N_c} & -\frac{c_1^{(1)}}{N_c} - c_2^{(1)}\left(1 + \frac{1}{N_c^2}\right) \\ -\frac{c_1^{(1)}}{N_c} - c_2^{(1)}\left(1 + \frac{1}{N_c^2}\right) & -c_1^{(1)} - 2\frac{c_2^{(1)}}{N_c} \end{pmatrix} \tag{243}$$

$$T_q \cdot T_{\bar{Q}} = \begin{pmatrix} -c_1^{(1)} - 2\frac{c_2^{(1)}}{N_c} & -\frac{c_1^{(1)}}{N_c} - c_2^{(1)}\left(1 + \frac{1}{N_c^2}\right) \\ -\frac{c_1^{(1)}}{N_c} - c_2^{(1)}\left(1 + \frac{1}{N_c^2}\right) & -\frac{c_1^{(1)}}{N_c^2} - 2\frac{c_2^{(1)}}{N_c} \end{pmatrix} \tag{244}$$

$$T_q \cdot T_Q = \begin{pmatrix} 2\frac{c_2^{(1)}}{N_c} & c_2^{(1)}\left(1 + \frac{1}{N_c^2}\right) \\ c_2^{(1)}\left(1 + \frac{1}{N_c^2}\right) & 2\frac{c_2^{(1)}}{N_c} \end{pmatrix} \tag{245}$$

4.4 Comparison between Phase Space Slicing and the Dipole Formalism

Both phase space slicing and the dipole formalism provide a general algorithm for the cancellation of infrared divergences. Apart from that they have several advantages and disadvantages.

- Within the dipole formalism the matrix elements of the real contributions, the virtual corrections, the subtraction term and the integrated subtraction term can be put in different subroutines and tested separately. In particular the integrand $d\sigma^R - d\sigma^A$ can be checked in each collinear limit.

- In order to construct the subtraction term colour correlated (and helicity projected) amplitudes are only needed for the n-parton configuration.

- The subtraction term requires the evaluation of many dipole factors (51 for $e^+e^- \to 4$ jets). Although $d\sigma^R - d\sigma^A$ does not give large numerical values, this term tends to give large statistical errors. This requires a high number of integrand evaluations. It turns out that a straightforward implementation of the dipole formalism requires roughly the same computer time as the phase space slicing method with a remapping of phase space.

- Within the phase space slicing method the $(n+1)$-parton matrix element has to be broken up to implement the $\theta(s_{ij} - s_{min})$-functions, which cut out the singular regions. In the colour subleading part, the implementation of the θ-functions has to be done according to the partial fraction decomposition of the eikonal factors. Care has to be taken that no finite region of phase space is cut out.

- Within phase space slicing one has to reproduce a logarithmic term by numerical integration. This is not always easily achieved. The problem can be cured by a remapping of phase space, as explained in the next chapter, such that the poles of the integrand are absorbed into the integral measure.

- Using phase space slicing the result will be a difference between two large numbers, which therefore have to be computed with high precision. A possible way to circumvent this problem is to cancel the logarithmic terms on a point-by-point basis. Starting from a "hard" n-parton configuration, one integrates numerically the real emission part over all "soft" one-parton configurations. The sum of the real emission part and the virtual contributions is then integrated over the "hard" phase space. The mapping of the "hard" n-parton phase space into all "soft" $(n+1)$-parton configurations is in some sense the inverse mapping of the dipole formalism, which maps a $(n+1)$ -parton configuration into all possible n-parton configurations.

- Using the phase space slicing method one has to show that the result is independent of s_{min}.

4.5 Regularization Schemes and Splitting Functions

Theoretical calculations of infrared-safe quantities in QCD should lead to unambiguous results, independent of the chosen regularization scheme. Regularization schemes are needed in order to handle ultraviolet and infrared singularities. Since the results are only calculated within perturbation theory, numerical differences between results obtained in different regularization schemes are attributed to uncalculated higher orders. In a NLO calculation infrared singularities cancel between one-loop integrals and phase space integrals of tree-level matrix elements. The independency of physical quantities is only achieved if the regularization scheme is unitary. Unitarity means that the amplitudes have to fullfill the condition

$$2\mathrm{Abs}T_{aa} \;=\; \sum_b |T_{ab}|^2 \tag{246}$$

up to the relevant order in perturbation theory. In particular, at NLO the discontinuity of the one-loop matrix element on left-hand side provides a constraint on the squares of the tree-level matrix elements on the right-hand side. Unitarity demands therefore that unobserved particles are treated uniformly. Unobserved particles are virtual, collinear or soft particles. Catani, Seymour and Trócsányi [61] have shown that this recipe enforces unitarity up to the calculated order. Terms sensitive to the precise definition of the regularization scheme enter the calculation usually in the virtual part through tensor loop integrals, and in the real emission part through the splitting functions, which enter the dipole factors (in the dipole formalism) as well as the contribution from unresolved phase space (within phase space slicing).

4.5.1 Dimensional Regularization Schemes

All schemes entail continuing the momentum integrals (both the loop integrals and the integrals over soft and collinear phase space) to $4-2\varepsilon$ dimensions in order to render them finite. Having done this, one is left with a lot of freedom how to treat the momenta of the observed particles and the polarization vectors of all particles. As a pratical matter the observable external momenta can be effectively taken to be four-dimensional by taking the momentum components in the (-2ε)-dimensions to vanish in a given scattering process. Various regularization schemes are :

- Conventional dimensional regularization (CDR) [63]: All momenta and all polarization vectors are taken to be in D dimensions.

- 't Hooft-Veltman scheme [64]: The momenta and the helicities of the unobserved particles are D dimensional, whereas the momenta and the helicities of the observed particles are 4 dimensional.

- Four-dimensional helicity scheme (FDH) [32]: All polarization vectors are kept in four dimensions, as well as the momenta of the observed particles. Only the momenta of the unobserved particles are continued to D dimensions. Today most calculations are carried out in this scheme, mainly because it fits nicely with the spinor helicity method and respects supersymmetry.

4.5.2 Splitting Functions

The probability of finding a particle b inside a particle a with fraction z of the longitudinal momentum of a in the p_∞-frame to lowest order in α_s is given by [60]

$$d\mathcal{P}_{a\to b+c}(z)dz = \frac{\alpha_s}{4\pi}P_{a\to b+c}(z)dzdt \tag{247}$$

where $t = \ln(Q^2/Q_0^2)$. The splitting function $P_{a\to b+c}(z)$ is given by

$$P_{a\to b+c}(z) = z(1-z)\sum_{\substack{\text{spins,}\\ \text{colours}}}\frac{|A_{a\to b+c}|^2}{k_\perp^2} \tag{248}$$

where a sum over the spins and colours of b and c and an average over the spin and colours of a is taken (if the case).
In QCD one has the following symmetries:

$$\begin{aligned} P_{q\to q+g}(z) &= P_{q\to g+q}(1-z), \\ P_{g\to q+\bar{q}}(z) &= P_{g\to q+\bar{q}}(1-z), \\ P_{g\to g+g}(z) &= P_{g\to g+g}(1-z). \end{aligned} \tag{249}$$

The limit where p_i and p_j become collinear is precisely defined as

$$\begin{aligned} p_i^\mu &= zp^\mu + k_\perp^\mu - \frac{k_\perp^2}{z}\frac{n^\mu}{2p\cdot n}, \\ p_j^\mu &= (1-z)p^\mu - k_\perp^\mu - \frac{k_\perp^2}{1-z}\frac{n^\mu}{2p\cdot n}. \end{aligned} \tag{250}$$

n^μ is an auxiliary light-like vector which is necesarry to specify the transverse component $k_\perp$ ($k_\perp\cdot p = k_\perp\cdot n = 0$) or, equivalently, how the collinear limit is

approached. The polarized splitting functions are [57]:

$$\begin{aligned}
\hat{P}_{q\to qg}(z,k_\perp,\varepsilon) &= 2\delta_{ss'}C_F\left(\frac{1+z^2}{1-z}-\varepsilon(1-z)\right),\\
\hat{P}_{g\to gg}(z,k_\perp,\varepsilon) &= 2C_A\left[-g^{\mu\nu}\left(\frac{z}{1-z}+\frac{1-z}{z}\right)-2(1-\varepsilon)z(1-z)\frac{k_\perp^\mu k_\perp^\nu}{k_\perp^2}\right],\\
\hat{P}_{g\to q\bar{q}}(z,k_\perp,\varepsilon) &= 2T_R\left(-g^{\mu\nu}+4z(1-z)\frac{k_\perp^\mu k_\perp^\nu}{k_\perp^2}\right) \qquad (251)
\end{aligned}$$

where the spin indices of the parent parton a have been denoted by s, s' if a is a fermion and μ, ν if a is a gluon. A statistical factor of $1/2!$ for two identical particles is included in the $g \to gg$ case. The D-dimensional splitting functions are obtained after averaging over the polarizations of the parton a. They are according to Catani, Seymour and Trócsányi [61] given by

$$\begin{aligned}
P_{g\to gg} &= 2C_A\left(\frac{z}{1-z}+\frac{1-z}{z}+\frac{h_g}{1-\varepsilon}z(1-z)\right),\\
P_{q\to qg} &= 2C_F\left(\frac{2z}{1-z}+h_g(1-z)\right),\\
P_{g\to q\bar{q}} &= 2T_R N_f\left(1-\frac{2}{1-\varepsilon}z(1-z)\right) \qquad (252)
\end{aligned}$$

where the parameter depends on the scheme and is equal to $h_g = 1-\varepsilon$ in the conventional dimensional regularization scheme and the 't Hooft-Veltman scheme and $h_g = 1$ for dimensional reduction. In particular they obtain the same splitting functions in the conventional scheme and in the 't Hooft-Veltman scheme. The integrated splitting functions, entering the contribution from the unresolved phase space within the phase space slicing method, are then as follows (only the terms I^1 are scheme-dependent) :

$$\begin{aligned}
I^1_{g\to gg}(CDR) &= \frac{C_A}{2}\left(\frac{1}{2}\ln^2 z_1+\frac{1}{2}\ln^2 z_2-\frac{67}{18}+\frac{\pi^2}{3}\right),\\
I^1_{q\to qg}(CDR) &= C_F\left(\frac{1}{2}\ln^2 z_2-\frac{7}{4}+\frac{\pi^2}{6}\right),\\
I^1_{g\to q\bar{q}}(CDR) &= T_R N_f\frac{5}{9}. \qquad (253)
\end{aligned}$$

In the FDH-scheme one obtains, using the results from Catani, Seymour and Trócsányi :

$$\begin{aligned}
I^1_{g\to gg}(FDH) &= \frac{C_A}{2}\left(\frac{1}{2}\ln^2 z_1+\frac{1}{2}\ln^2 z_2-\frac{32}{9}+\frac{\pi^2}{3}\right),\\
I^1_{q\to qg}(FDH) &= C_F\left(\frac{1}{2}\ln^2 z_2-\frac{3}{2}+\frac{\pi^2}{6}\right),\\
I^1_{g\to q\bar{q}}(FDH) &= T_R N_f\frac{5}{9}. \qquad (254)
\end{aligned}$$

In the literature there is some disagreement concerning the splitting functions in the 't Hooft-Veltman scheme. The splitting functions in the HV scheme given in the paper by Giele and Glover [54] as well as in the paper by Kunszt, Signer and Trócsányi [62] disagree with the result from Catani, Seymour and Trócsányi. Since the results from Catani et al. are manifest unitarity, they appear to be correct. (D.A. Kosower has rechecked the splitting function for $g \to gg$ in the HV scheme and agrees with Catani et al.) Further confirmation is certainly desirable.

4.5.3 Conversion to the 't Hooft – Veltman Scheme

The one-loop amplitudes have been calculated in the four-dimensional helicity scheme. The transition rules between one-loop amplitudes calculated in the FDH scheme and the corresponding ones calculated in the HV scheme are [52]

$$A_{FDH}^{one-loop} - A_{HV}^{one-loop} = c_\Gamma g^2 A^{tree} \left(\frac{N_c}{3} - \frac{n_q}{4N_c} + \frac{n_q N_c}{12} \right) \tag{255}$$

where n_q is the number of quarks. The one-loop amplitude for $e^+e^- \to q\bar{q}gg$ is converted into the 't Hooft-Veltman scheme by

$$A_{HV}^{\text{one-loop}} = A^{\text{one-loop}} - c_\Gamma \frac{1}{2} g^2 N_C \left(1 - \frac{1}{N_C^2} \right) A^{\text{tree}}, \tag{256}$$

whereas the one-loop amplitude for $e^+e^- \to q\bar{q}Q\bar{Q}$ is converted by

$$A_{HV}^{\text{one-loop}} = A^{\text{one-loop}} - c_\Gamma g^2 N_C \left(\frac{2}{3} - \frac{1}{N_C^2} \right) A^{\text{tree}}. \tag{257}$$

4.5.4 Procedure Adopted in the Numerical Program

The procedure adopted in the numerical program is as follows : The one-loop amplitudes have been calculated in the FDH scheme and are converted in the HV-scheme with the formulae quoted above. The splitting functions entering the contribution from the unresolved phase space or the integrals over the dipole factors have then to be taken in the 't Hooft-Veltman scheme as well. We take the formulae for the splitting functions in the HV-scheme from Catani, Seymour and Trócsányi (which are identical to the ones in the CDR scheme).

5 Monte Carlo Integration Techniques

Due to the complicated excluded phase space regions (due to the experimental cuts and the jet algorithm) and the complicated expressions involved, the integration over phase space has usually to be done by Monte Carlo techniques. Reducing the statistical errors involves a variety of techniques. First I give an overview of the basic principles of Monte Carlo integration, based on the review by F.James [66].
The heart of Monte Carlo integration is a pseudorandom number generator. The default random number generators provided by the standard libraries are quite often not appropriate for these purposes. As an example, the standard random number generator of the C implementation at our institute has a period of $2^{15} - 1 = 32767$, certainly not enough, if one integration involves up to 10^8 calls to the random number generator. Subsection 5.2 deals therefore with pseudorandom number generators and is based on [67] and [68].
Monte Carlo integration of complicated functions in high dimensions is most efficiently done with the VEGAS-algorithm ([69], [70]), briefly described in section 5.3.
The numerical NLO program requires the integration of the virtual corrections (and the Born contribution) over an n-parton phase space. I will call an n-parton phase space configuration a hard phase space configuration. Mapping a hypercube of random numbers in the intervall $[0, 1]$ and of dimension $4n$ into a set of n physical four-momenta is done with the RAMBO-algorithm [71], described in section 5.4. Furthermore the integration of the real emission part requires the integration over an $(n + 1)$-parton phase space. Using phase space slicing it is desirable to generate phase space configurations which are "close" to the s_{min}-boundary of phase space slicing. I will call such an $(n+1)$-parton configuration a soft phase space configuration. Although originally developped for phase space slicing, this remapping is also useful to improve the efficiency of the dipole formalism. The remapping of phase space is described in section 5.5 and the application to the dipole formalism is given in section 5.5.1.

5.1 Basic Monte Carlo Techniques

- Crude Monte Carlo : Choose randomly values of x and average the values of $f(x)$.

- Stratified sampling : This technique consists of dividing the full integration space into subspaces, performing a Monte Carlo integration in each subspace, and adding up the partial results in the end. If the subspace and the number of points in each subspace are chosen carefully, this can lead to a dramatic reduction in the variance compared with crude Monte Carlo, but it should be noted that it can also lead to a larger variance if the choice is

not appropriate. Without further improvement this method is limited to a small number of dimensions.

- Importance sampling : Mathematically, importance sampling corresponds to a change of integration variables :

$$f(x)dx \to f(x)\frac{dG(x)}{g(x)}, \qquad g(x) = \frac{dG(x)}{dx}. \tag{258}$$

The relevant variance is now $\mathrm{var}(f/g)$, which will be small if g is chosen to be close to f in shape. The function g has to fullfill the following criteria:

1. $g(x)$ is a probability density function, e.g. $g(x) \geq 0$ for all x and g is normalized

$$\int dx g(x) = 1. \tag{259}$$

2. $G(x)$, the integral of $g(x)$ is known analytically.
3. $G(x)$ can be inverted (e.g. solved for x) analytically, or a g-distributed random number generator is available.
4. the ratio $f(x)/g(x)$ is as constant as possible, so that the variance $\mathrm{var}(f/g)$ is small compared with $\mathrm{var}(f)$.

One disadvantage of importance sampling is the fact, that it is dangerous to choose functions g, which vanish somewhere. If g vanishes somewhere where f is not zero, $\mathrm{var}(f/g)$ may be infinite and the usual technique of estimating the variance from the sample points may not detect this fact if the region where $g = 0$ is small.

- Control variates : As in importance sampling one seeks an integrable function g which approximates the function f to be integrated, but this time the two functions are subtracted rather than divided,

$$\int dx f(x) \;\; = \;\; \int dx \, (f(x) - g(x)) + \int dx g(x). \tag{260}$$

If the integral of g is known, the only uncertainty comes from the integral of $(f - g)$, which will have smaller variance than f if g has been chosen carefully. The method of control variates is more stable than importance sampling, since zeros in g cannot induce singularities in $(f-g)$. Another advantage over importance sampling is that the integral of the approximating function g need not be inverted analytically.

- Antithetic variates : Usually Monte Carlo calculations use random points, which are independent of each other. The method of antithetic variates

deliberately makes use of correlated points, taking advantage of the fact that such a correlation may be negative. Mathematically this is based on the fact that

$$\mathrm{var}(f_1 + f_2) \quad = \quad \mathrm{var}(f_1) + \mathrm{var}(f_2) + 2\mathrm{covar}(f_1, f_2). \tag{261}$$

If we can arrange to choose points such that f_1 and f_2 are negative correlated, a substantial reduction in variance may be realized. The most trivial example for the application of the method of antithetic variates would be a Monte Carlo integration of the function $f(x) = x$ in the interval $[0, 1]$ by evaluating the integrand at the points x_i and $1 - x_i$.

5.2 Pseudorandom Number Generators

Pseudorandom numbers are produced in the computer by a simple algorithm, and are therefore not truly random.

So-called "quasirandom" numbers are also produced by a numerical algorithm, but are not designed to appear to be random, but rather to be distributed as uniformly as possible, in order to reduce the errors in numerical integration.

A good random number generator should have the following properties:

- Good distribution. For pseudorandom numbers, this means good randomness. For quasirandom numbers, the desired quality is uniformity.
- Long period. Both pseudorandom and quasirandom generators always have a period, after which they begin to generate the same sequence of numbers over again. To avoid undesired correlations one should in any practical calculation not come anywhere near exhausting the period.
- Repeatability. For testing and development, it may be necessary to repeat a calculation with exactly the same random numbers as in the previous run. Furthermore the generator should allow the possibility of repeating a part of a calculation without having to start at the very beginning. This requires to be able to store the state of a generator.
- Long disjoint subsequences. For large problems it is extremely convenient to be able to perform independent subsimulations whose results can later be combined assuming statistical indepedence.
- Portability. This means not only that the code should be portable (i.e. in a high-level language like Fortran or C), but that it should generate exactly the same sequence of numbers on different machines.
- Efficiency. This was considered very important in the early days.

Some algorithms for pseudo-random number generators:

- Multiplicative linear congruential generator. Each succesive integer is obtained by multiplying the previous one by a well chosen multiplier, optionally adding another constant, and throwing away the most significant digits of the result:

$$s_i = (as_{i-1} + c) \bmod m. \tag{262}$$

  One choice for the constants [68] would be $a = 69069$, $c = 0$ and $m = 2^{32}$. Other choices are $a = 1812433253$, $c = 0$ and $m = 2^{32}$ or $a = 1566083941$, $c = 0$ and $m = 2^{32}$.

- Fibonacci-type generators. Each number is the result of an arithmetic or logical operation (addition, subtraction or exclusive-or) between two numbers which have occured somewhere earlier in the sequence, not necessarily the last two :

$$s_i = (s_{i-p} \circ s_{i-q}) \bmod m. \tag{263}$$

  The generator used in the program is of this type:

$$s_i = (s_{i-24} + s_{i-55}) \bmod 2^{32}. \tag{264}$$

  It was proposed in 1958 by G.J. Mitchell and D.P. Moore. This generator has a period of

$$2^f \left(2^{55} - 1\right) \tag{265}$$

  where $0 \leq f < 32$.

- Shift register or tausworthe. This class of generators is based on the same formula as lagged Fibonacci generators, but with $m = 2$ and the $\circ$-operation is exclusive-or.

5.3 VEGAS - Monte Carlo Integration in High Dimensions

Whereas the variance-reducing techniques described above require some advance knowledge of the behaviour of the function to be integrated, the VEGAS algorithm ([69], [70]) is adaptive, e.g. it learns about the function as it proceeds. The algorithm combines the basic ideas of importance sampling and stratified sampling into an iterative algorithm, which automatically concentrates evaluations of the integrand in those regions where the integrand is largest in magnitude. The algorithm starts by subdividing the integration space into a rectangular grid and

performs an integration in each subspace. These results are then used to adjust the grid for the next iteration, according to where the integral receives dominant contributions. Eventually after a few iterations the optimal grid is found. After this initial exploratory phase, the grid may be frozen and in a second evaluation phase the integral may be evaluated with high precision according to the optimized grid. The separation into an exploratory phase and an evaluation phase allows one to use fewer integrand evaluations in the first phase and to ignore the numerical estimates from this phase (which will in general have a larger variance).

5.4 Generating Hard Phase Space Configurations

The RAMBO algorithm [71] is used to map a hypercube $[0,1]^{4n}$ of random numbers into n physical four-momenta with center-of-mass energy w. Massless fourvectors can be generated with uniform weight and this routine is used in the Monte Carlo integration. In order to test the program, it is also useful to be able to generate phase space configuration, where two particles are collinear. This is done by first generating an $(n-1)$-parton configuration with one massive particle, and letting this particle subsequently decay.

5.4.1 Massless Particles

The phase space measure for a system of n massless particles with center-of-mass energy w is

$$d\Phi_n(w) = \prod_{i=1}^{n} \frac{d^4p_i}{(2\pi)^3}\delta(p_i^2)\theta(p_i^0)(2\pi)^4\delta^4\left(P - \sum_{i=1}^{n} p_i\right). \tag{266}$$

The RAMBO algorithm generates a set of massless four-momenta p_i^μ according to the phase-space measure (266) as follows:

- Generate independently n massless four-momenta q_i^μ with isotropic angular distribution and energies q_i^0 distributed according to the density $q_i^0 e^{-q_i} dq_i^0$. Using $4n$ random numbers ρ_i uniformly distributed in $[0,1]$ this is done as follows:

$$\begin{aligned} c_i &= 2\rho_{i_1} - 1, & \varphi_i &= 2\pi\rho_{i_2}, & q_i^0 &= -\ln(\rho_{i_3}\rho_{i_4}), \\ q_i^x &= q_i^0\sqrt{1-c_i^2}\cos\varphi_i, & q_i^y &= q_i^0\sqrt{1-c_i^2}\sin\varphi_i, & q_i^z &= q_i^0 c_i. \end{aligned} \tag{267}$$

- The four-vectors q_i^μ are then transformed into the desired four-vectors p_i^μ, using the following Lorentz and scaling transformations:

$$\begin{aligned} p_i^0 &= x\left(\gamma q_i^0 + \vec{b}\cdot\vec{q_i}\right), \\ \vec{p_i} &= x\left(\vec{q_i} + \vec{b}q_i^0 + a\left(\vec{b}\cdot\vec{q_i}\right)\vec{b}\right) \end{aligned} \tag{268}$$

where

$$\vec{b} = -\frac{1}{M}\vec{Q}, \qquad x = \frac{w}{M}, \qquad \gamma = \frac{Q^0}{M} = \sqrt{1+\vec{b}^2},$$
$$a = \frac{1}{1+\gamma}, \qquad Q^\mu = \sum_{i=1}^{n} q_i^\mu, \qquad M = \sqrt{Q^2}. \tag{269}$$

5.4.2 Massive Particles

Phase-space configurations corresponding to massive particles can be generated by starting from a massless configuration and then transforming this configuration into one with the desired masses. This is done as follows : Let p_i^μ be a set of massless momenta. The p_i^μ are transformed into the four-momenta k_i^μ as follows:

$$\begin{aligned} k_i^0 &= \sqrt{m_i^2 + \xi^2 (p_i^0)^2}, \\ \vec{k}_i &= \xi \vec{p}_i \end{aligned} \tag{270}$$

where ξ is a solution of the equation

$$w = \sum_{i=1}^{n} \sqrt{m_i^2 + \xi^2 (p_i^0)^2}. \tag{271}$$

It should be noted that in the general case no analytic expression for ξ exists and ξ has to be computed numerically. The phase space integral can be written as

$$\Phi_n(\{p\}) = \int \prod_{i=1}^{n} \frac{d^4 p_i}{(2\pi)^3} \delta(k_i^2 - m_i^2)\theta(k_i^0)(2\pi)^4 \delta^4 \left(P - \sum_{i=1}^{n} k_i \right) \cdot W(\{p\},\{k\}) \tag{272}$$

where the weight is given by

$$W_m = \left(\frac{1}{w} \sum_{i=1}^{n} |\vec{k}_i| \right)^{2n-3} \left(\prod_{i=1}^{n} \frac{|\vec{k}_i|}{k_i^0} \right) \left(\sum_{i=1}^{n} \frac{|\vec{k}_i|^2}{k_i^0} \right)^{-1}. \tag{273}$$

In contrast to the massless case, the weight is no longer constant but varies over phase space.

This algorithm is used to generate events with n massless particles, such that m particles have an invariant mass λ. For $m = 2$ and $\lambda \to 0$ this gives a useful routine to check collinear limits of amplitudes numerically. The algorithm consists of the following steps :

- Generate an event with $(n - m + 1)$ massless particles.

- Find ξ by solving $f(\xi) = 0$, e.g.

$$f(\xi) = w - \sum \sqrt{m_i^2 + (\xi p_i^0)^2} = 0 \tag{274}$$

  where $m_1 = \lambda$ and $m_i = 0$ for $i > 1$.

- Transform to k_i and m_i.
- Generate an event with m massless particles and $w = \lambda$.
- Do a Lorentz transformation such that $Q = \Lambda^{-1}(\lambda, \vec{0})$.

5.5 Remapping of Phase Space

The remapping of phase space is due to D.A.Kosower [72] and was originally intended for the phase space slicing method. The application to the dipole formalism is straightforward and given in the next subsection. Within the phase space slicing approach one wants to improve the efficiency of the Monte Carlo integration of the real emission part by absorbing the poles of the matrix element into the integral measure. Soft and collinear singularities appear in the real emission part of the squared amplitudes as poles $1/(s_{ab}s_{bc})$ (soft) or $1/s_{ab}$ (collinear). For example the leading colour contribution to the real emission part from $e^+e^- \to qg_1g_2g_3\bar{q}$ is a incoherent sum of cyclic-ordered partial amplitudes. A specific term in this sum has singularities in

$$s_{q1}, s_{12}, s_{23}, s_{3\bar{q}} \tag{275}$$

where the indices correspond to the specific cyclic order. (The other terms are obtained by a permutation of the gluons.) Soft singularities occur only when two adjacent invariants become small. Let us consider the set of products of invariants

$$\mathcal{S} \;=\; \{(s_{(i-1)i} \cdot s_{i(i+1)})\}, \tag{276}$$

such that for every soft or collinear pole, the corresponding combination is included into the set. In the example above we would consider the set

$$\{(s_{q1}s_{12}), (s_{12}s_{23}), (s_{23}s_{3\bar{q}})\} \tag{277}$$

In the region where $s_{as}s_{sb}$ is the smallest product, we remap the phase space as follows: Let k'_a, k_s and k'_b be the corresponding momenta such that $s_{as} = (k'_a + k_s)^2$, $s_{sb} = (k'_b + k_s)^2$ and $s_{ab} = (k'_a + k_s + k'_b)^2$. We want to relate this $(n+1)$ particle configuration to a nearby "hard" n-particle configuration with $(k_a + k_b)^2 = (k'_a + k_s + k'_b)^2$, where k_a and k_b are the corresponding "hard" momenta. Using the factorization of the phase space, we have

$$d\Phi_{n+1} \;=\; d\Phi_{n-1} \frac{dK^2}{2\pi} d\Phi_3(K, k'_a, k_s, k'_b). \tag{278}$$

The three-particle phase space is given by

$$\begin{aligned} d\Phi_3(K, k'_a, k_s, k'_b) &= \frac{1}{32(2\pi)^5 s_{ab}} ds_{as} ds_{sb} d\Omega'_b d\phi_s \\ &= \frac{1}{4(2\pi)^3 s_{ab}} ds_{as} ds_{sb} d\phi_s d\Phi_2(K, k_a, k_b) \end{aligned} \tag{279}$$

and therefore

$$d\Phi_{n+1} = d\Phi_n \frac{ds_{as} ds_{sb} d\phi_s}{4(2\pi)^3 s_{ab}}. \tag{280}$$

The region of integration for s_{as} and s_{sb} is $s_{as} > s_{min}$, $s_{sb} > s_{min}$ (from the Θ-functions of phase space slicing) and $s_{as} + s_{sb} < s_{ab}$ (Dalitz plot for massless particles). It is desirable to absorb poles in s_{as} and s_{sb} into the measure. (Using phase space slicing these poles will give after integration numerically large terms with $\ln^2 s_{min}$ and $\ln s_{min}$. A naive numerical integration of these poles without any remapping results in a poor accuracy.) This is done by changing the variables according to

$$\begin{aligned} s_{as} &= s_{ab} \left(\frac{s_{min}}{s_{ab}} \right)^{u_1}, \\ s_{sb} &= s_{ab} \left(\frac{s_{min}}{s_{ab}} \right)^{u_2} \end{aligned} \tag{281}$$

where $0 \leq u_1, u_2 \leq 1$. Note that $u_1, u_2 > 0$ enforces $s_{as}, s_{sb} > s_{min}$. Therefore this transformation of variables may only be applied to invariants s_{ij} where the region $0 < s_{ij} < s_{min}$ is cut out. The phase space measure becomes

$$d\Phi_{n+1} = d\Phi_n \frac{1}{4(2\pi)^3} \frac{s_{as} s_{sb}}{s_{ab}} \ln^2 \left(\frac{s_{min}}{s_{ab}} \right) \Theta(s_{as} + s_{sb} < s_{ab}) du_1 du_2 d\phi_s. \tag{282}$$

This give the following algorithm for generating a $(n+1)$-parton configuration:

- Take a "hard" n-parton configuration and pick out two momenta k_a and k_b. Use three uniformly distributed random number u_1, u_2, u_3 and set

$$\begin{aligned} s_{ab} &= (k_a + k_b)^2, \\ s_{as} &= s_{ab} \left(\frac{s_{min}}{s_{ab}} \right)^{u_1}, \\ s_{sb} &= s_{ab} \left(\frac{s_{min}}{s_{ab}} \right)^{u_2}, \\ \phi_s &= 2\pi u_3. \end{aligned} \tag{283}$$

- If $(s_{as} + s_{sb}) > s_{ab}$, reject the event.

- If not, solve for k'_a, k'_b and k_s. If $s_{as} < s_{sb}$ we want to have $k'_b \to k_b$ as $s_{as} \to 0$. Define

$$E_a = \frac{s_{ab} - s_{sb}}{2\sqrt{s_{ab}}}, \quad E_s = \frac{s_{as} + s_{sb}}{2\sqrt{s_{ab}}}, \quad E_b = \frac{s_{ab} - s_{as}}{2\sqrt{s_{ab}}}, \tag{284}$$

$$\theta_{ab} = \arccos\left(1 - \frac{s_{ab} - s_{as} - s_{sb}}{2E_a E_b}\right), \qquad \theta_{sb} = \arccos\left(1 - \frac{s_{sb}}{2E_s E_b}\right) \tag{285}$$

It is convenient to work in a coordinate system which is obtained by a Lorentz transformation to the center of mass of $k_a + k_b$ and a rotation such that k'_b is along the positive z-axis. In that coordinate system

$$\begin{aligned} p'_a &= E_a(1, \sin\theta_{ab}\cos(\phi_s + \pi), \sin\theta_{ab}\sin(\phi_s + \pi), \cos\theta_{ab}), \\ p_s &= E_s(1, \sin\theta_{sb}\cos\phi_s, \sin\theta_{sb}\sin\phi_s, \cos\theta_{sb}), \\ p'_b &= E_b(1, 0, 0, 1). \end{aligned} \tag{286}$$

The momenta p'_a, p_s and p'_b are related to the momenta k'_a, k_s and k'_b by a sequence of Lorentz transformations back to the original frame

$$k'_a = \Lambda_{boost}\Lambda_{xy}(\phi)\Lambda_{xz}(\theta)p'_a \tag{287}$$

and analogous for the other two momenta. The explicit formulae for the Lorentz transformations are obtained as follows :

Denote by $K = \sqrt{(k_a + k_b)^2}$ and by p_b the coordinates of the hard momentum k_b in the center of mass system of $k_a + k_b$. p_b is given by

$$p_b = \left(\frac{Q^0}{K}k_b^0 - \frac{\vec{k}_b \cdot \vec{Q}}{K}, \vec{k}_b + \left(\frac{\vec{k}_b \cdot \vec{Q}}{K(Q^0 + K)} - \frac{k_b^0}{K}\right)\vec{Q}\right) \tag{288}$$

with $Q = k_a + k_b$. The angles are then given by

$$\begin{aligned} \theta &= \arccos\left(1 - \frac{p_b \cdot p'_b}{2p_b^t p_b^{t'}}\right), \\ \phi &= \arctan\left(\frac{p_b^y}{p_b^x}\right) \end{aligned} \tag{289}$$

The explicit form of the rotations is

$$\begin{aligned} \Lambda_{xz}(\theta) &= \begin{pmatrix} 1 & 0 & 0 & 0 \\ 0 & \cos\theta & 0 & \sin\theta \\ 0 & 0 & 1 & 0 \\ 0 & -\sin\theta & 0 & \cos\theta \end{pmatrix}, \\ \Lambda_{xy}(\phi) &= \begin{pmatrix} 1 & 0 & 0 & 0 \\ 0 & \cos\phi & -\sin\phi & 0 \\ 0 & \sin\phi & \cos\phi & 0 \\ 0 & 0 & 0 & 1 \end{pmatrix}. \end{aligned} \tag{290}$$

The boost $k' = \Lambda_{boost} q$ is given by

$$k' = \left(\frac{Q^0}{K} q^0 + \frac{\vec{q} \cdot \vec{Q}}{K}, \vec{q} + \left(\frac{\vec{q} \cdot \vec{Q}}{K(Q^0 + K)} + \frac{q^0}{K} \right) \vec{Q} \right) \tag{291}$$

with $Q = k_a + k_b$ and $K = \sqrt{(k_a + k_b)^2}$.

- If $s_{as} > s_{sb}$, exchange a and b in the formulae above.
- The "soft" event has then the weight

$$W_{n+1} = \frac{\pi}{2} \frac{1}{(2\pi)^3} \frac{s_{as} s_{sb}}{s_{ab}} \ln^2 \left(\frac{s_{min}}{s_{ab}} \right) W_n \tag{292}$$

where W_n is the weight of the original "hard" event.

Note that the set $\mathcal{S}$ contains only invariants in which the integrand has actually poles. This set is different for different terms obtained from the $(n+1)$-parton matrix element after decomposition into terms with definite singularity structure.

5.5.1 Improving the Dipole Formalism

Within the dipole formalism we have to evaluate the terms

$$\int_n \left(d\sigma^V + d\sigma^B \otimes I \right) \quad \text{and} \quad \int_{n+1} d\sigma^R - d\sigma^A. \tag{293}$$

The first term is most efficiently integrated by splitting this term into a leading colour piece and a subleading colour piece. The leading-colour piece gives the numerically dominant contribution. The leading-colour one-loop amplitudes are relative simple and can therefore be integrated without further problems. The subleading-colour one-loop amplitudes are more complicated and need therefore more computer time. On the other hand they will result in numerical smaller contributions and therefore can be evaluated with fewer integrand evaluations. Although the second term $d\sigma^R - d\sigma^A$ gives usually only a modest numerical contribution, a naive Monte Carlo integration will give large statistical errors. A simplified model for this term would be

$$F = \int_0^1 dx \left(\frac{f(x)}{x} - \frac{g(x)}{x} \right) \tag{294}$$

with the additional condition $f(0) = g(0)$. The integral can be rewritten as

$$F = \int_0^{s_{min}} dx \frac{f(x) - g(x)}{x} + \int_{\ln s_{min}}^0 dy \left(f(e^y) - g(e^y) \right) \tag{295}$$

Using the Taylor expansion for $f(x) - g(x)$ one sees that the first term gives a contribution of order $O(s_{min})$. In the second term the $1/x$ behaviour has been absorbed into integral measure by a change of variables $y = \ln x$, and the integrand tends to be more flat. This may reduce the statistical error in a Monte Carlo integration. The precise implementation for the term $d\sigma^R - d\sigma^A$ is done as follows: Consider a set of products of invariants, including all the invariants in which the (unsubtracted) matrix elements has poles (and which may give rise to logarithms therefore). The relevant set of products of invariants for the two-quark, three-gluon final state consists of the pairs

$$\begin{aligned}\mathcal{S}_g &= \{s_{q1}s_{12}, s_{q1}s_{13}, s_{q2}s_{21}, s_{q2}s_{23}, s_{q3}s_{31}, s_{q3}s_{32} \\ &\quad s_{23}s_{3\bar{q}}, s_{32}s_{2\bar{q}}, s_{13}s_{3\bar{q}}, s_{31}s_{1\bar{q}}, s_{12}s_{2\bar{q}}, s_{21}s_{1\bar{q}} \\ &\quad s_{12}s_{23}, s_{13}s_{32}, s_{21}s_{13} \\ &\quad s_{q1}s_{1\bar{q}}, s_{q2}s_{2\bar{q}}, s_{q2}s_{2\bar{q}}\} . \end{aligned} \tag{296}$$

Singularities associated with the last three pairs appear only in the colour-subleading part.
The set for the four-quark, one-gluon final state consists of the pairs

$$\begin{aligned}\mathcal{S}_q &= \Big\{s_{qg}s_{g\bar{q}}, s_{Qg}s_{g\bar{Q}}, s_{qg}s_{g\bar{Q}}, s_{Qg}s_{g\bar{q}} \\ &\quad s_{q\bar{q}}s_{\bar{q}Q}, s_{q\bar{Q}}s_{\bar{Q}q}, s_{\bar{q}q}s_{q\bar{Q}}, s_{\bar{q}Q}s_{Q\bar{Q}} \\ &\quad s_{qg}s_{gQ}, s_{\bar{q}g}s_{g\bar{Q}}\Big\} . \end{aligned} \tag{297}$$

The second line takes care of the collinear singularities when two quarks become collinear. The phase space is then partitioned according to

$$\Phi_{n+1} = \sum_{\mathcal{S}} \Theta(a,b,c)\Phi_{n+1} \tag{298}$$

where $\Theta(a,b,c) = 1$ if $s_{ab}s_{bc}$ is the smallest product in the set $\mathcal{S}$, and $\Theta(a,b,c) = 0$ otherwise. The sum is over all products in the set $\mathcal{S}$. We may use the symmetries under permutations in order to reduce the number of summands which need to be evaluated. For the two-quark, three-gluon case we have to evaluate the terms with $\Theta(q,1,2)$ and $\Theta(2,3,\bar{q})$ with weight 6, as well as the terms with $\Theta(1,2,3)$ and $\Theta(q,3,\bar{q})$ which are weighted by a factor of 3. For the four quark, one gluon case we evaluate the terms with $\Theta(q,g,\bar{Q})$ and $\Theta(q,g,\bar{q})$, which are weighted by a factor 2, the term with $\Theta(q,\bar{q},Q)$ weighted by a factor 4 and the terms with $\Theta(q,g,Q)$ and $\Theta(\bar{q},g,\bar{q})$ with unit weight.

If $s_{as}s_{sb}$ is the smallest product in the set the phase space is split into two regions: the first region is defined as the region where $s_{as} > s_{min}$ and $s_{sb} > s_{min}$ where s_{min} is now an arbitrary parameter. In this region the phase space mapping of the previous section is applied.

The second region is necessarily defined as the complement of the first region: $s_{as} < s_{min}$ or $s_{sb} < s_{min}$. In this region the integration is performed without any phase space mapping.

In summary the term $d\sigma^R - d\sigma^A$ is calculated as follows:

$$\begin{aligned} d\sigma^R - d\sigma^A &= \sum_{\mathcal{S}} \left(d\sigma^R - d\sigma^A \right) \Theta(s_{as} - s_{min}) \Theta(s_{sb} - s_{min}) \Theta(a, s, b) \\ &\quad + \sum_{\mathcal{S}} \left(d\sigma^R - d\sigma^A \right) \left(1 - \Theta(s_{as} - s_{min}) \Theta(s_{sb} - s_{min}) \right) \Theta(a, s, b) \end{aligned} \tag{299}$$

Note that this slicing does not involve any approximations and is exact whatever value s_{min} might take. The aim is of course to choose s_{min} such that the statistical errors are reduced.
It turns out that by choosing s_{min} small enough the second region gives a vanishing contribution. The result obtained from the first region has a statistical error reduced roughly by a factor of 10 compared to the result without any remapping and the same number of integrand evaluations. Empirically

$$\eta = \frac{s_{min}/Q^2}{y_{cut}} = 10^{-3} \tag{300}$$

is a good value.

6 Phenomenology

6.1 Exact General Purpose Programs at NLO for $e^+e^- \to 4$ Jets

The numerical program developed in this work is a general purpose program for calculating four-, three- and two-jet quantities to next-to-leading order (NLO) in α_s (and five-jet quantities at leading order). I will call it MERCUTIO. It is similar to MENLO PARC [92], DEBRECEN [97] and EERAD2 [100]. The main difference among the programs is the technique used for the cancellation of real and virtuel singularities: MERCUTIO uses the dipole formalism [57]. The cancellation of the infrared singularities in the program MENLO PARC is based on the subtraction method according to [56], the program DEBRECEN uses the dipole formalism whereas the cancellation in the program EERAD2 is done with the help of phase space slicing. The only approximations which have been made are the neglect of the light quark masses and terms which are suppressed by $1/m_{top}^4$ or higher powers of the top quark mass. MERCUTIO calculates the quantities in fixed order in α_s, no resummation of terms of $\ln y_{cut}$ or $\ln y_{cut}$ has been implemented. Therefore our results are reliable only for values of y_{cut} which are not too small. The program calculates the jet quantities at the partonic level, and no hadronization is done.

The program is designed to calculate any infrared-safe observable. An observable is called infrared-safe, if its actual value does not change when an arbitrarily soft gluon is emitted, nor when a parton splits into a pair of collinear partons.

6.1.1 Power Corrections

An infrared-safe observable R that depends on some large momentum scale $\sqrt{s}$ has the following form

$$R\left(\sqrt{s}\right) \;=\; R_{pert}\left(\alpha_s\left(\sqrt{s}\right)\right) + R_{non-pert}\left(\sqrt{s}\right). \qquad (301)$$

The term R_{pert} denotes the perturbative component that can be calculated as a power-series expansion in $\alpha_s(\sqrt{s})$ and, thus behaves as $(1/\ln\sqrt{s})^n$. This is exactly what the program MERCUTIO does, calculating the perturbative component to NLO. The remaining contribution $R_{non-pert}$ is due to non-perturbative phenomena (hadronization) and is power-behaved, i.e. proportional to $(1/\sqrt{s})^p$. Since the power p is positive, $R_{non-pert}$ is suppressed when $s \to \infty$ but can be quantitatively relevant at finite values of $\sqrt{s}$. Techniques to estimate the size of the power corrections are the operator product expansion (where it is applicable), the renormalon approach and the estimation based on event generators.

6.1.2 Small y_{cut}

At small y_{cut} one hopes to probe the interface between perturbative and non-perturbative QCD. There are two obstacles to that :
First of all the perturbative expansion in not only an expansion in α_s, but also in $\ln^2 y_{cut}$ and $\ln y_{cut}$. At small y_{cut} the logarithms become large and the jet algorithm has to allow a resummation of these terms to all orders. The factorization properties of the Durham algorithm allow such a resummation, while the JADE algorithm does not.
Secondly hadronization corrections might be substantial.

6.1.3 Differences to Event Generators

The NLO programs like MERCUTIO shall not be confused with Monte Carlo event generators like HERWIG [89] or JETSET [90]. These event generators basically consist of a hard subprocess (with LO matrix elements), final state parton shower descriptions and a non-perturbative component, at a certain scale of the order of 1GeV, where the partons from the shower are converted into hadrons according to some phenomenological model. The hadronization parameters are tuned in order to reproduce the experimental data. The parton shower description usually simplifies the kinematics and the helicity structure and neglects interference effects. In contrast to QED, where the photon emission is incoherent due to the eikonal identity, the gluon emission in QCD is coherent beyond the leading logarithmic approximation. This is sometimes referred to as the angular ordering property of QCD.

Furthermore the final state radiation and the hard matrix element can in principle not be treated separately. This is also an approximation.
The event generators may be used to estimate the size of hadronization corrections.

6.1.4 Colour Coherence

In QED the photon emission is incoherent : The photons know only about their source, i.e. a fermion line, but they don't know about each other. Up to an overall factor, the probability for the emission of n photons is just the product of the probabilities for the independent emission of each of them in the soft photon limit.

The situation is different in QCD : The gluon emission is incoherent only in leading order in the number of colours, but becomes coherent beyond this approximation. This is illustrated by the following example : The amplitude for a $q\bar{q}$ pair plus n gluons, where one gluon has opposite helicity as the others, is

given by

$$A(q^+,1^+,...,j^-,...,\bar{q}^-) \;=\; ig^n \sum_{\{1,2,...,n\}} \left(T^1...T^n\right)_{q\bar{q}} \frac{\langle jq\rangle\langle j\bar{q}\rangle^3}{\langle q\bar{q}\rangle}\frac{1}{\langle q1\rangle...\langle n\bar{q}\rangle} \tag{302}$$

where the sum is over all permutations of the gluon legs. In the case for the corresponding QED-amplitude for the emission of n photons one replaces the colour matrices by a unit matrix $1_{q\bar{q}}$. With the help of the eikonal identity

$$\sum_{\{1,...,n\}} \frac{\langle q\bar{q}\rangle}{\langle q1\rangle...\langle n\bar{q}\rangle} \;=\; \prod_{i=1}^{n} \frac{\langle q\bar{q}\rangle}{\langle qi\rangle\langle i\bar{q}\rangle} \tag{303}$$

the squared matrix element in the QED case may be written as

$$\begin{aligned}\sum_{colours} &= e^{2n}N_c\frac{s_{qj}^3 s_{\bar{q}j}}{s_{q\bar{q}}^2}\sum_{\{1,...,n\}}\frac{1}{s_{q1}s_{12}...s_{n\bar{q}}} + \text{ interference terms}\\ &= e^{2n}N_c\frac{s_{qj}^3 s_{\bar{q}j}}{s_{q\bar{q}}^2}\prod_{i=1}^{n}\frac{s_{q\bar{q}}}{s_{qi}s_{i\bar{q}}}.\end{aligned} \tag{304}$$

In contrast in QCD the interference terms are suppressed by a factor of $1/N_c^2$ and they therefore no longer sum up to cancel the coherence inherent in the sum of squares.

6.2 Jet Algorithms

A jet is qualitatively a large amount of hadronic energy in a small angular region. In e^+e^--annihilation the initial state is purely electromagnetic and therefore all hadrons in the final state can be associated with the hard scattering process. A jet algorithm has to be infrared safe. Given a set of four-momenta (which may either correspond to the measured four-momenta of particles in an experiment or to the four-momenta of partons obtained from a theoretical calculation) a jet-algorithm assigns in e^+e^--collisions each four-momentum to a jet. Usually this is done by introducing a resolution variable y_{ij}, where a smaller value of y_{ij} means that the particles i and j are "closer" to each other. The clustering procedure of a jet algorithm is in most cases defined through the following steps:

1. Define a resolution parameter y_{cut}.

2. For every pair (p_k, p_l) of final-state hadron momenta compute the corresponding resolution variable y_{kl}.

3. If y_{ij} is the smallest value of y_{kl} computed above and $y_{ij} < y_{cut}$ then combine (p_i, p_j) into a single jet ('pseudo-particle') with momentum p_{ij} according to a recombination prescription.

4. Repeat until all pairs of objects (particles and/or pseudo-particles) have $y_{kl} > y_{cut}$.

The various jet algorithms differ in the precise definition of the resolution variable and the recombination prescription.

It is desirable that a jet algorithm also have some additional features :

- A jet algorithm should have small hadronization corrections.
- A jet algorithm should allow the possibility of resumming large logarithmic terms to all orders in perturbation theory.
- A jet algorithm should have a reduced renormalization scale dependence in fixed order in perturbation theory.

6.2.1 Definition of the Resolution Variable

- Minimum mass cut:

$$y_{ij} = \frac{(p_i + p_j)^2}{s_{min}}. \tag{305}$$

- JADE algorithm [73]:

$$y_{ij} = \frac{2E_iE_j\,(1 - \cos\Theta_{ij})}{Q^2}. \tag{306}$$

  where E_i is the energy of particle i and Θ_{ij} is the relative angle in the e^+e^--centre-of-mass frame. The JADE-algorithm merges soft particles first, even if they are far apart in angle.

- DURHAM algorithm (or k_T algorithm) [74]:

$$y_{ij} = \frac{2\min(E_i^2, E_j^2)\,(1 - \cos\Theta_{ij})}{Q^2}. \tag{307}$$

  The DURHAM-algorithm merges a soft particle with the energetic particle closest in angle.

- GENEVA algorithm [75]:

$$y_{ij} = \frac{8}{9}\frac{2E_iE_j\,(1 - \cos\Theta_{ij})}{(E_i + E_j)^2}. \tag{308}$$

The factor 8/9 is provided so that the maximum value for y_{cut} for which three-jet events can still be obtained from three partons is $y_{cut} = 1/3$, as it is for the JADE and DURHAM versions. The GENEVA algorithm merges soft particles together only if the angle is much smaller than the angle they make with a high-energetic particle.

6.2.2 Recombination Prescriptions

- E-scheme:

$$\begin{aligned} E_{ij} &= E_i + E_j, \\ \vec{p}_{ij} &= \vec{p}_i + \vec{p}_j. \end{aligned} \tag{309}$$

The E-scheme conserves energy and momentum, but the recombined momentum is not massless.

- $E0$-scheme:

$$\begin{aligned} E_{ij} &= E_i + E_j, \\ \vec{p}_{ij} &= \frac{E_i + E_j}{|\vec{p}_i + \vec{p}_j|} (\vec{p}_i + \vec{p}_j). \end{aligned} \tag{310}$$

The $E0$-scheme conserves energy, but not momentum. The recombined momentum is massless.

- P-scheme:

$$\begin{aligned} E_{ij} &= \frac{|\vec{p}_i + \vec{p}_j|}{E_i + E_j} (E_i + E_j) = |\vec{p}_i + \vec{p}_j|, \\ \vec{p}_{ij} &= \vec{p}_i + \vec{p}_j. \end{aligned} \tag{311}$$

The P-scheme conserves momentum, but not energy. The recombined momentum is massless, as in the $E0$-scheme.

6.2.3 Angular-Ordered Durham Algorithm

The jet algorithms described above may be modified by distinguishing an ordering variable v_{ij} and a resolution variable y_{ij}. The alogrithm works as follows :

- Select a pair of objects (ij) with the minimal value of the ordering variable v_{ij}.
- If $y_{ij} < y_{cut}$ they are combined, one recomputes the relevant values of the ordering variable and goes back to the first step.

- If $y_{ij} \geq y_{cut}$, then the pair (if any) with the next smallest value of the ordering variable is considered. If no such pair exists, then clustering is finished.

For the angular-ordered Durham algorithm one takes for the ordering variable

$$v_{ij} \quad = \quad 2(1 - \cos\theta_{ij}) \tag{312}$$

where θ_{ij} is the relative angle between the particles i and j in the e^+e^- c.m. frame. The angular ordering corresponds to the fact, that a soft gluon emitted at some angle to the jet axis cannot resolve the colours of jet constituents at smaller angles. The resolution variable y_{ij} is the same as in the usual Durham algorithm.

6.2.4 The Cambridge Algorithm

While the angular-ordered Durham algorithm already avoids a lot of spurious junk-jet formation, one weakness of the angular-ordered Durham algorithm is the possible wrong assignment of soft wide-angle radiation to already-resolved jets [76]. For example consider the parton-level application of the algorithm to the splitting $q_1 \to q_1 + g_2$, accompanied by a soft large-angle gluon g_3, such that

$$E_1 >> E_2 >> E_3, \qquad \theta_{12} << \theta_{13} \approx \theta_{23}. \tag{313}$$

According to the angular ordering property the soft gluon g_3 is radiated coherently and the corresponding radiation intensity is proportional to the total colour charge of the system $q_1 + g_2$, which is just that of the initial quark. However, in half of the events the algorithm will erroneously assign g_3 to the gluon jet g_2 because the latter happens to lie a little bit closer in angle. If at some y_{cut} the jets q_1 and g_2 are resolved as two jets, the gluon jet will be overpopulated. Dokshitzer, Leder, Moretti and Webber [76] therefore proposed modifying the angular-ordered Durham algorithm by freezing the softer of two already resolved objects in order to prevent it from attracting any other extra partners among the remaining objects with large emission angles. The Cambridge algorithm is defined as follows:

- Select a pair of objects (ij) with the minimal value of the ordering variable v_{ij}.
- If $y_{ij} < y_{cut}$ they are combined, one recomputes the relevant values of the ordering variable and goes back to the first step.
- If $y_{ij} \geq y_{cut}$ and $E_i < E_j$ then i is defined as a resolved jet and deleted from the table.
- Repeat until only one object is left in the table. This object is also defined as a jet and clustering is finished.

This procedure suffices to prevent mis-clustering in the dominant region of phase space where, in the above example, the gluon g_2 is softer then the quark q_1. It will still cluster the partons incorrectly in the subleading configuration where the gluon is accidentally harder than the quark.

6.3 Global Event Shape Variables

Event shape variables describe the topology of an event. They may be calculated without reference to a jet defining algorithm. Like jet algorithms they have to be infrared safe. Examples for event shape variables are:

6.3.1 Thrust

The thrust T is defined as [78]

$$T = \max_{\hat{n}} \frac{\sum_i |\vec{p}_i \cdot \hat{n}|}{\sum_i |\vec{p}_i|} \tag{314}$$

and maximizes the total longitudinal momentum (along the unit vector $\hat{n}$) of the final state particle p_i in a given event. The direction of $\hat{n}$ that produces the maximum is known as the thrust axis. The range of the values for the thrust is :

$$\frac{1}{2} \leq T \leq 1. \tag{315}$$

$T = 1$ corresponds to an (ideal) collinear two-jet event (e.g. all momenta are along one line), whereas $T = 1/2$ corresponds to the topology of a sphere (e.g. the momenta of the n final state particles are equally distributed and n approaches infinity).

6.3.2 The C- and D-Parameters

The C- and D-parameters are derived from the eigenvalues of the momentum tensor [82]

$$\theta^{ij} = \frac{\sum_a \frac{p_a^i p_a^j}{|\vec{p}_a|}}{\sum_a |\vec{p}_a|} \tag{316}$$

where the sum runs over all final state particles and p_a^i is the i-th component of the three-momentum $\vec{p}_a$ of particle a in the c.m. system. The tensor θ is normalized to have unit trace. In terms of the eigenvalues of the θ tensor, λ_1, λ_2, λ_3, with $\lambda_1 + \lambda_2 + \lambda_3 = 1$, one defines

$$C = 3\left(\lambda_1\lambda_2 + \lambda_2\lambda_3 + \lambda_3\lambda_1\right),$$

$$D = 27\lambda_1\lambda_2\lambda_3 \tag{317}$$

$$= 27 \det\theta^{ij}. \tag{318}$$

The range of values is $0 \leq C, D \leq 1$. The D-parameter measures aplanarity, since one needs at least four final-state particles to obtain a non-vanishing value.

6.4 Jet Shape Variables

6.4.1 Four-Jet Angular Shape Variables

After having defined jets as pseudo-particles with the help of a jet algorithm, one may consider angular correlations between them. The jets are labelled in order of descending jet energy, such that jet 1 has the highest energy and jet 4 has the smallest. The definitions of various four-jet angular shape variables are:

1. the Körner-Schierholz-Willrodt variable [84], $\cos\phi_{KSW}$, is the cosine of the average of two angles between planes spanned by the jets,

$$\begin{aligned} \phi_{KSW} &= \frac{1}{2}\left[\arccos\left(\frac{(\vec{p}_1\times\vec{p}_4)\cdot(\vec{p}_2\times\vec{p}_3)}{|\vec{p}_1\times\vec{p}_4||\vec{p}_2\times\vec{p}_3|}\right)\right. \\ &\left. + \arccos\left(\frac{(\vec{p}_1\times\vec{p}_3)\cdot(\vec{p}_2\times\vec{p}_4)}{|\vec{p}_1\times\vec{p}_3||\vec{p}_2\times\vec{p}_4|}\right)\right]; \end{aligned} \tag{319}$$

2. the modified Nachtmann-Reiter variable [85], $|\cos\theta^*_{NR}|$, is the absolute value of the cosine of the angle between the vectors $\vec{p}_1-\vec{p}_2$ and $\vec{p}_3-\vec{p}_4$,

$$\cos\theta^*_{NR} = \frac{(\vec{p}_1-\vec{p}_2)\cdot(\vec{p}_3-\vec{p}_4)}{|\vec{p}_1-\vec{p}_2||\vec{p}_3-\vec{p}_4|}; \tag{320}$$

3. $\cos\alpha_{34}$, the cosine of the angles between the two smallest energy jets [86],

$$\cos\alpha_{34} = \frac{\vec{p}_3\cdot\vec{p}_4}{|\vec{p}_3||\vec{p}_4|}; \tag{321}$$

4. the Bengtsson-Zerwas correlation [87], $|\cos\chi_{BZ}|$ is the absolute value of the cosine of the angle between the plane spanned by jets 1 and 2 and that by jets 3 and 4,

$$\cos\chi_{BZ} = \frac{(\vec{p}_1\times\vec{p}_2)\cdot(\vec{p}_3\times\vec{p}_4)}{|\vec{p}_1\times\vec{p}_2||\vec{p}_3\times\vec{p}_4|}. \tag{322}$$

6.4.2 Three-Jet Shape Variables

With the numerical program for $e^+e^- \to 4$ jets one may also study the internal structure of 3 jets events. One example is the jet broadening variable defined as

$$B_{jet} = \frac{\sum_i |p^i_\perp|}{\sum_i |p^i|} \tag{323}$$

Here $p^i_\perp$ is the momentum of particle i transverse to the jet axis, and the sum extends over all particles in the jet.

6.5 Numerical Analysis

As our nominal choice of input parameters we use $N_c = 3$ colours and $N_f = 5$ massless quarks. We take the electromagnetic coupling to be $\alpha(m_Z) = 1/127.9$ and the strong coupling to be $\alpha_s(m_Z) = 0.118$. The numerical values of the Z^0-mass and width are $m_Z = 91.187$ GeV and $\Gamma_Z = 2.490$ GeV. For the top mass we take $m_t = 174$ GeV and for the weak mixing angle $\sin^2\theta_W = 0.230$. Unless stated otherwise, we take the center of mass energy to be $\sqrt{Q^2} = m_Z$ and we set the renormalization scale equal to $\mu^2 = Q^2$.

The numerical program is based on the dipole formalism. In addition I implemented for the leading colour contribution also phase space slicing. The results from the two methods agree with each other.

6.5.1 Four-Jet Fraction

The four-jet fraction has been calculated by each group which has provided a numerical NLO four-jet program and serves as a cross-check. The four-jet fraction is defined as by

$$R_4 = \frac{\sigma_{4-jet}}{\sigma_{tot}} \tag{324}$$

where σ_{tot} is the total hadronic cross-section at $O(\alpha_s)$ given by

$$\sigma_{tot} = \sigma_{2-jet}^{Born}\left(1 + \frac{\alpha_s}{\pi}\right). \tag{325}$$

The values obtained for the four-jet fraction for different jet algorithms and varying y_{cut} are given in table 1, together with the corresponding values from the programs MENLO PARC by L. Dixon and A. Signer [92], DEBRECEN by Z. Nagy and Z. Trócsányi [97] and EERAD2 by E.W.N. Glover [100].

6.5.2 The D-Parameter

At NLO the D-parameter distribution is expanded as

$$\frac{1}{\sigma_{tot}} D \frac{d\sigma}{dD} = \left(\frac{\alpha_s}{2\pi}\right)^2 B_D + \left(\frac{\alpha_s}{2\pi}\right)^3 C_D. \tag{326}$$

The average of the shape variable is defined as

$$\langle D \rangle = \frac{1}{\sigma_{tot}} \int_0^1 D \frac{d\sigma}{dD} dD. \tag{327}$$

In leading order I find for the average value for the D-parameter

Algorithm	y_{cut}	MERCUTIO	MENLO PARC
JADE-E0	0.005	$(3.90 \pm 0.22) \cdot 10^{-1}$	$(3.79 \pm 0.08) \cdot 10^{-1}$
	0.01	$(1.93 \pm 0.01) \cdot 10^{-1}$	$(1.88 \pm 0.03) \cdot 10^{-1}$
	0.03	$(3.37 \pm 0.02) \cdot 10^{-2}$	$(3.46 \pm 0.05) \cdot 10^{-2}$
	y_{cut}	DEBRECEN	EERAD2
	0.005	$(3.88 \pm 0.07) \cdot 10^{-1}$	$(3.87 \pm 0.03) \cdot 10^{-1}$
	0.01	$(1.92 \pm 0.01) \cdot 10^{-1}$	$(1.93 \pm 0.01) \cdot 10^{-1}$
	0.03	$(3.37 \pm 0.01) \cdot 10^{-2}$	$(3.35 \pm 0.01) \cdot 10^{-2}$
Algorithm	y_{cut}	MERCUTIO	MENLO PARC
DURHAM	0.005	$(1.05 \pm 0.02) \cdot 10^{-1}$	$(1.04 \pm 0.02) \cdot 10^{-1}$
	0.01	$(4.73 \pm 0.07) \cdot 10^{-2}$	$(4.70 \pm 0.06) \cdot 10^{-2}$
	0.03	$(6.94 \pm 0.08) \cdot 10^{-3}$	$(6.82 \pm 0.08) \cdot 10^{-3}$
	y_{cut}	DEBRECEN	EERAD2
	0.005	$(1.05 \pm 0.01) \cdot 10^{-1}$	$(1.05 \pm 0.01) \cdot 10^{-1}$
	0.01	$(4.66 \pm 0.02) \cdot 10^{-2}$	$(4.65 \pm 0.02) \cdot 10^{-2}$
	0.03	$(6.87 \pm 0.04) \cdot 10^{-3}$	$(6.86 \pm 0.03) \cdot 10^{-3}$
Algorithm	y_{cut}	MERCUTIO	MENLO PARC
GENEVA	0.02	$(2.74 \pm 0.19) \cdot 10^{-1}$	$(2.56 \pm 0.06) \cdot 10^{-1}$
	0.03	$(1.80 \pm 0.06) \cdot 10^{-1}$	$(1.71 \pm 0.03) \cdot 10^{-1}$
	0.05	$(8.54 \pm 0.15) \cdot 10^{-2}$	$(8.58 \pm 0.15) \cdot 10^{-2}$
	y_{cut}	DEBRECEN	EERAD2
	0.02	$(2.63 \pm 0.06) \cdot 10^{-1}$	$(2.61 \pm 0.05) \cdot 10^{-1}$
	0.03	$(1.75 \pm 0.03) \cdot 10^{-1}$	$(1.72 \pm 0.03) \cdot 10^{-1}$
	0.05	$(8.37 \pm 0.12) \cdot 10^{-2}$	$(8.50 \pm 0.06) \cdot 10^{-2}$

Table 1: The four-jet fraction as calculated by MERCUTIO, MENLO PARC, DEBRECEN and EERAD2, for different jet algorithms and varying y_{cut}.

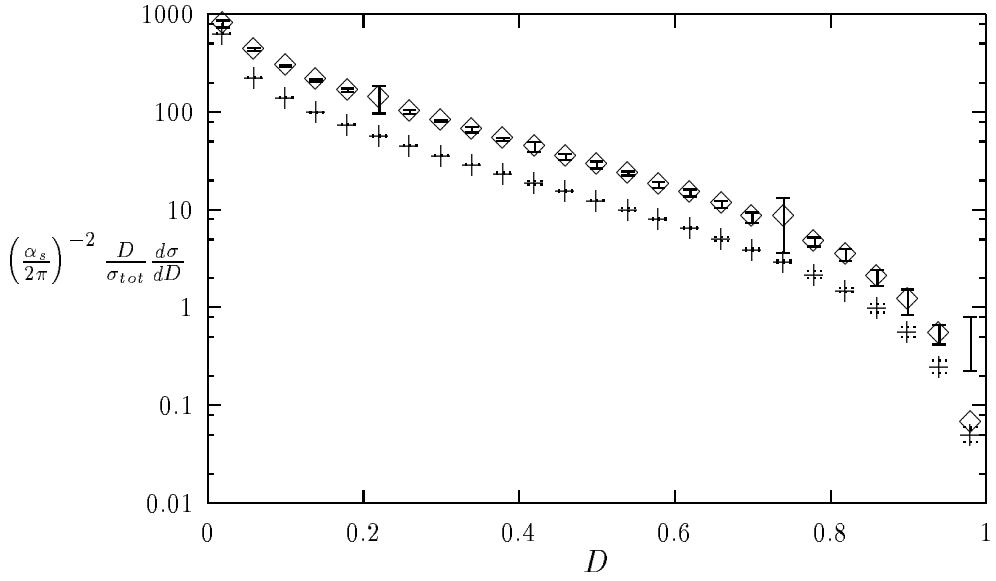

Figure 1: The D-parameter distribution at NLO (diamonds) and LO (crosses).

$$\left\langle \frac{D}{\sigma_{2-jet}^{Born}} \frac{d\sigma}{dD} \right\rangle = (60.4 \pm 0.2) \left(\frac{\alpha_s}{2\pi}\right)^2 \tag{328}$$

which is in perfect agreement with the value given by Ellis, Ross and Terrano [91]:

$$60.5 \left(\frac{\alpha_s}{2\pi}\right)^2 \tag{329}$$

The values for the functions B_D and C_D are given in table 2. These numbers agree with the ones given by Nagy and Trócsányi as published in [97] after taking care of different normalizations (σ_{tot} in our case and σ_{2-jet}^{Born} in [97]). (In the first preprint version of [97] there was a mismatch of factors C_F.) Figure 1 shows the D-parameter distribution. For the average I obtain

$$\langle D \rangle = \left(\frac{\alpha_s}{2\pi}\right)^2 (58.2 \pm 0.2) + \left(\frac{\alpha_s}{2\pi}\right)^3 (2.32 \pm 0.18) \cdot 10^3. \tag{330}$$

6.5.3 The Jet Broadening Variable

At NLO the B_{jet}-distribution is expanded as

$$\frac{1}{\sigma_{tot}} \frac{B_{jet}}{n_{jets}} \frac{d\sigma}{dB_{jet}} = \left(\frac{\alpha_s}{2\pi}\right)^2 B_{B_{jet}} + \left(\frac{\alpha_s}{2\pi}\right)^3 C_{B_{jet}}. \tag{331}$$

D	B_D	C_D
0.02	$(6.36 \pm 0.04) \cdot 10^2$	$(8.21 \pm 3.53) \cdot 10^3$
0.06	$(2.23 \pm 0.02) \cdot 10^2$	$(1.14 \pm 0.07) \cdot 10^4$
0.10	$(1.42 \pm 0.01) \cdot 10^2$	$(8.17 \pm 0.29) \cdot 10^3$
0.14	$(9.93 \pm 0.05) \cdot 10^1$	$(6.00 \pm 0.36) \cdot 10^3$
0.18	$(7.44 \pm 0.06) \cdot 10^1$	$(4.95 \pm 0.42) \cdot 10^3$
0.22	$(5.71 \pm 0.08) \cdot 10^1$	$(4.44 \pm 2.37) \cdot 10^3$
0.26	$(4.53 \pm 0.05) \cdot 10^1$	$(2.90 \pm 0.22) \cdot 10^3$
0.30	$(3.59 \pm 0.04) \cdot 10^1$	$(2.40 \pm 0.14) \cdot 10^3$
0.34	$(2.90 \pm 0.05) \cdot 10^1$	$(1.97 \pm 0.23) \cdot 10^3$
0.38	$(2.36 \pm 0.06) \cdot 10^1$	$(1.54 \pm 0.12) \cdot 10^3$
0.42	$(1.89 \pm 0.06) \cdot 10^1$	$(1.35 \pm 0.28) \cdot 10^3$
0.46	$(1.56 \pm 0.03) \cdot 10^1$	$(1.01 \pm 0.12) \cdot 10^3$
0.50	$(1.25 \pm 0.02) \cdot 10^1$	$(8.68 \pm 1.26) \cdot 10^2$
0.54	$(1.01 \pm 0.03) \cdot 10^1$	$(7.14 \pm 0.59) \cdot 10^2$
0.58	$(8.09 \pm 0.22) \cdot 10^0$	$(5.27 \pm 0.70) \cdot 10^2$
0.62	$(6.54 \pm 0.16) \cdot 10^0$	$(4.43 \pm 0.62) \cdot 10^2$
0.66	$(5.06 \pm 0.24) \cdot 10^0$	$(3.32 \pm 0.48) \cdot 10^2$
0.70	$(3.91 \pm 0.12) \cdot 10^0$	$(2.37 \pm 0.56) \cdot 10^2$
0.74	$(2.93 \pm 0.08) \cdot 10^0$	$(2.94 \pm 2.56) \cdot 10^2$
0.78	$(2.21 \pm 0.18) \cdot 10^0$	$(1.33 \pm 0.25) \cdot 10^2$
0.82	$(1.52 \pm 0.07) \cdot 10^0$	$(1.03 \pm 0.25) \cdot 10^2$
0.86	$(9.94 \pm 0.96) \cdot 10^{-1}$	$(5.52 \pm 1.96) \cdot 10^1$
0.90	$(5.64 \pm 0.63) \cdot 10^{-1}$	$(3.32 \pm 1.85) \cdot 10^1$
0.94	$(2.49 \pm 0.37) \cdot 10^{-1}$	$(1.55 \pm 0.63) \cdot 10^1$
0.98	$(5.11 \pm 0.93) \cdot 10^{-2}$	$(0.77 \pm 8.47) \cdot 10^0$

Table 2: The Born level and next-to-leading order functions B_D and C_D for the D-parameter.

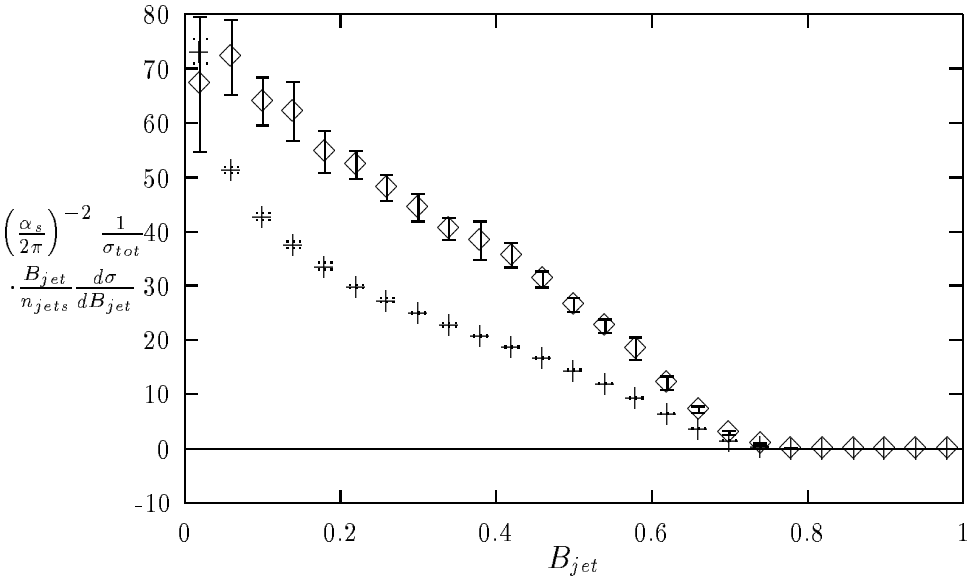

Figure 2: The B_{jet}- distribution at NLO (diamonds) and LO (crosses).

The average of the shape variable is defined as

$$\langle B_{jet} \rangle = \frac{1}{\sigma_{tot}} \int_0^1 \frac{B_{jet}}{n_{jets}} \frac{d\sigma}{dB_{jet}} dB_{jet}. \tag{332}$$

The jet broadening variable is calculated for three-jet events defined by the DURHAM algorithm and $y_{cut} = 0.1$. For the average I obtain

$$\langle B_{jet} \rangle = \left(\frac{\alpha_s}{2\pi}\right)^2 (17.9 \pm 0.1) + \left(\frac{\alpha_s}{2\pi}\right)^3 (5.25 \pm 0.31) \cdot 10^2. \tag{333}$$

The values for the functions $B_{B_{jet}}$ and $C_{B_{jet}}$ are given in table 3. Figure 2 shows the distribution of the jet broadening variable.

B_{jet}	$B_{B_{jet}}$	$C_{B_{jet}}$
0.02	$(7.31 \pm 0.22) \cdot 10^1$	$(-6.34 \pm 5.49) \cdot 10^2$
0.06	$(5.13 \pm 0.05) \cdot 10^1$	$(9.24 \pm 2.68) \cdot 10^2$
0.10	$(4.27 \pm 0.06) \cdot 10^1$	$(1.05 \pm 0.16) \cdot 10^3$
0.14	$(3.75 \pm 0.06) \cdot 10^1$	$(1.28 \pm 0.18) \cdot 10^3$
0.18	$(3.36 \pm 0.06) \cdot 10^1$	$(1.14 \pm 0.16) \cdot 10^3$
0.22	$(2.99 \pm 0.03) \cdot 10^1$	$(1.18 \pm 0.09) \cdot 10^3$
0.26	$(2.74 \pm 0.03) \cdot 10^1$	$(1.10 \pm 0.10) \cdot 10^3$
0.30	$(2.50 \pm 0.02) \cdot 10^1$	$(1.05 \pm 0.08) \cdot 10^3$
0.34	$(2.28 \pm 0.03) \cdot 10^1$	$(9.50 \pm 0.93) \cdot 10^2$
0.38	$(2.08 \pm 0.02) \cdot 10^1$	$(9.14 \pm 1.69) \cdot 10^2$
0.42	$(1.87 \pm 0.01) \cdot 10^1$	$(8.74 \pm 0.62) \cdot 10^2$
0.46	$(1.67 \pm 0.02) \cdot 10^1$	$(7.59 \pm 0.59) \cdot 10^2$
0.50	$(1.44 \pm 0.02) \cdot 10^1$	$(6.52 \pm 0.61) \cdot 10^2$
0.54	$(1.20 \pm 0.01) \cdot 10^1$	$(5.76 \pm 0.54) \cdot 10^2$
0.58	$(9.42 \pm 0.18) \cdot 10^0$	$(4.90 \pm 1.06) \cdot 10^2$
0.62	$(6.46 \pm 0.12) \cdot 10^0$	$(3.07 \pm 0.64) \cdot 10^2$
0.66	$(3.76 \pm 0.07) \cdot 10^0$	$(1.77 \pm 0.28) \cdot 10^2$
0.70	$(1.60 \pm 0.04) \cdot 10^0$	$(7.77 \pm 1.60) \cdot 10^1$
0.74	$(3.39 \pm 0.28) \cdot 10^{-1}$	$(2.45 \pm 0.94) \cdot 10^1$
0.78	$(1.11 \pm 0.31) \cdot 10^{-2}$	$(2.42 \pm 2.45) \cdot 10^0$
0.82	0.00	$(0.43 \pm 1.36) \cdot 10^{-2}$
0.86	0.00	0.00
0.90	0.00	0.00
0.94	0.00	0.00
0.98	0.00	0.00

Table 3: The Born level and next-to-leading order functions $B_{B_{jet}}$ and $C_{B_{jet}}$ for the jet broadening variable.

7 Conclusions

In this thesis the QCD corrections to $e^+e^- \to$ 4 jets have been considered. Relatively compact expressions for the one-loop amplitudes have been obtained with the help of modern techniques for the calculation of loop amplitudes: Colour decomposition, spinor helicity method, the unitarity based cut-technique, techniques using supersymmetry or inspired by string theory, as well as the factorization in collinear limits.
I also developped an efficient algorithm for the reduction of tensor loop integrals, which makes use of the facts that (a) loop momenta are usually sandwiched between Dirac spinors and that (b) in four dimensions there can be only four independent vectors.

In the second part of the thesis I described the numerical program "MERCUTIO", which can be used to calculate any infrared safe four-jet quantity in electron-positron annihilation at next-to-leading order. The program is based on the dipole formalism and uses a remapping of phase-space in order to improve the efficiency of the Monte Carlo integration.

Numerical results were given for the four-jet fraction R_4, the D-parameter and the jet broadening variable B_{jet}. The numerical values for the first two quantities agree with the results from other groups. The NLO-correction to the jet broadening variable is a new result.

A Feynman Rules

A.1 QCD Lagrange Density

The Lagrange density for QCD is given by:

$$\mathcal{L} = \mathcal{L}_F + \mathcal{L}_G + \mathcal{L}_{GF} + \mathcal{L}_{FP}, \tag{334}$$

$$\begin{aligned}
\mathcal{L}_F &= \sum_{flavours} \bar{\psi}^i (i\gamma^\mu D_\mu^{ij} - m_f \delta^{ij}) \psi^j, \\
\mathcal{L}_G &= -\frac{1}{4} F^a_{\mu\nu} F^{a\mu\nu}, \\
\mathcal{L}_{GF} &= -\frac{1}{2\xi} (\partial^\mu A^a_\mu)^2, \\
\mathcal{L}_{FP} &= (\partial^\mu \chi^{a*}) D^{ab}_\mu \chi^b,
\end{aligned} \tag{335}$$

$$F^a_{\mu\nu} = \partial_\mu A^a_\nu - \partial_\nu A^a_\mu + g f^{abc} A^b_\mu A^c_\nu, \tag{336}$$

$$\begin{aligned}
D^{ij}_\mu &= \delta^{ij} \partial_\mu - ig (T^a)^{ij} A^a_\mu, \\
D^{ab}_\mu &= \delta^{ab} \partial_\mu - g f^{abc} A^c_\mu.
\end{aligned} \tag{337}$$

The colour indices i and j run from 1 to 3, whereas the indices a, b and c label the generators of $SU(3)$ and run from 1 to 8. D_μ is the covariant derivative. It appears in the fermionic part of the Lagrange density in the fundamental representation (D^{ij}_μ), whereas it appears in the ghost-part in the adjoint representation (D^{ab}_μ).

A.2 Conventional Feynman Rules

Fermion propagator:

$$\frac{i}{\not{p}} \delta_{ij}$$

Gluon propagator:

$$\frac{-i \left(g_{\mu\nu} - (1-\xi) \frac{k_\mu k_\nu}{k^2} \right)}{k^2} \delta_{ab}$$

Ghost propagator:

$$\frac{i}{k^2} \delta^{ab}$$

Quark-gluon-vertex:

$$ig\gamma_\mu T^a_{ij}$$

3-gluon-vertex :

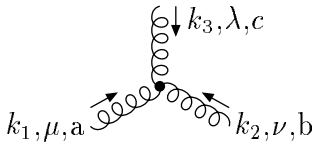

$$gf^{abc}\left[(k_3-k_2)_\mu g_{\nu\lambda}+(k_1-k_3)_\nu g_{\lambda\mu}+(k_2-k_1)_\lambda g_{\mu\nu}\right]$$

4-gluon-vertex :

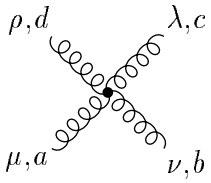

$$-ig^2\left[f^{abe}f^{ecd}\left(g_{\mu\lambda}g_{\nu\rho}-g_{\mu\rho}g_{\nu\lambda}\right)+f^{ace}f^{ebd}\left(g_{\mu\nu}g_{\lambda\rho}-g_{\mu\rho}g_{\lambda\nu}\right)+f^{ade}f^{ecb}\left(g_{\mu\nu}g_{\lambda\rho}-g_{\mu\lambda}g_{\nu\rho}\right)\right]$$

Gluon-ghost-vertex :

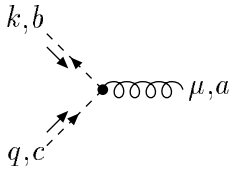

$$gf^{abc}k_\mu$$

A.3 External Particles

By convention we take outgoing particles to have no phase factor.

Outgoing fermion with positive helicity : $\langle p+|$
Outgoing fermion with negative helicity : $\langle p-|$
Outgoing antifermion with positive helicity : $|p-\rangle$
Outgoing antifermion with negative helicity : $|p+\rangle$

Then we have to include a phase factor i for particles with incoming momenta.

Incoming antifermion with negative helicity : $i\langle p+|$
Incoming antifermion with positive helicity : $i\langle p-|$
Incoming fermion with negative helicity : $i|p-\rangle$
Incoming fermion with positive helicity : $i|p+\rangle$

Polarization vectors for gluons :

$$\begin{aligned} \varepsilon_\mu^+(k,q) &= \frac{\langle q-|\gamma_\mu|k-\rangle}{\sqrt{2}\langle qk\rangle}. \\ \varepsilon_\mu^-(k,q) &= \frac{\langle q+|\gamma_\mu|k+\rangle}{\sqrt{2}\,[kq]} \end{aligned}$$

where q is an arbitrary null reference momentum.

B Spinor Algebra

We take the contravariant vector as

$$p^\mu = (p_t, p_x, p_y, p_z) \tag{338}$$

and the signs of the metric as

$$g_{\mu\nu} = \mathrm{diag}\,(+1, -1, -1, -1)\,. \tag{339}$$

The two-dimensional antisymmetric tensor needed to raise and lower indices of two-component spinors is given by:

$$\varepsilon_{AB} = \begin{pmatrix} 0 & 1 \\ -1 & 0 \end{pmatrix}, \qquad \varepsilon_{BA} = -\varepsilon_{AB}. \tag{340}$$

The two-dimensional antisymmetric tensor satisfies the Schouten identity:

$$\varepsilon_{AB}\varepsilon_{CD} + \varepsilon_{AC}\varepsilon_{DB} + \varepsilon_{AD}\varepsilon_{BC} = 0. \tag{341}$$

It is also useful to have the four-dimensional antisymmetric tensor $\varepsilon_{\mu\nu\rho\sigma}$. We define the sign as

$$\varepsilon_{0123} = +1. \tag{342}$$

The Pauli matrices are

$$\sigma_x = \begin{pmatrix} 0 & 1 \\ 1 & 0 \end{pmatrix}, \quad \sigma_y = \begin{pmatrix} 0 & -i \\ i & 0 \end{pmatrix}, \quad \sigma_z = \begin{pmatrix} 1 & 0 \\ 0 & -1 \end{pmatrix}. \tag{343}$$

We define the four-dimensional σ^μ-matrices as

$$\sigma^\mu_{A\dot{B}} = (1, -\sigma_i)\,, \qquad \bar{\sigma}^{\mu\dot{A}B} = (1, \sigma_i)\,. \tag{344}$$

The Weyl representation for the Dirac matrices is then given by

$$\gamma^\mu = \begin{pmatrix} 0 & \sigma^\mu \\ \bar{\sigma}^\mu & 0 \end{pmatrix}, \qquad \gamma_5 = \begin{pmatrix} 1 & 0 \\ 0 & -1 \end{pmatrix}. \tag{345}$$

Using the commutation relation for the Pauli matrices it is easily verified that the γ^μ satisfy indeed the Dirac algebra

$$\{\gamma_\mu, \gamma_\nu\} = 2g_{\mu\nu}. \tag{346}$$

The Fierz identity for the Dirac matrices is:

$$(\gamma^\mu)_{ij}(\gamma_\mu)_{kl} + (\gamma^\mu\gamma_5)_{ij}(\gamma_\mu\gamma_5)_{kl} = -\left[(\gamma^\mu)_{il}(\gamma_\mu)_{kj} + (\gamma^\mu\gamma_5)_{il}(\gamma_\mu\gamma_5)_{kj}\right]. \tag{347}$$

Two-component spinors : There are two types of notations used in the literature to denote Weyl spinors : The one with dotted and undotted indices as well as the bra- and ket-vector notation. While the former is more useful when indices are left uncontracted, the latter is more convenient in expressions where all indices are contracted.

$$\begin{aligned} |p+\rangle = p_B, \qquad & \langle q+| = q_{\dot{A}}, \\ |p-\rangle = p^{\dot{B}}, \qquad & \langle q-| = q^A. \end{aligned} \tag{348}$$

Four-component Dirac spinors can be constructed out of two Weyl spinors:

$$\begin{aligned} u(p) &= \begin{pmatrix} p_A \\ p^{\dot{B}} \end{pmatrix}, \\ \overline{u}(p) &= \left(p^A, p_{\dot{B}}\right). \end{aligned} \tag{349}$$

Raising and lowering of indices is done with the help of the antisymmetric tensor ε_{AB}:

$$\begin{aligned} p^B = \varepsilon^{BA} p_A, \qquad & q^{\dot{A}} = \varepsilon^{\dot{A}\dot{B}} q_{\dot{B}}, \\ p_{\dot{B}} = p^{\dot{A}} \varepsilon_{\dot{A}\dot{B}}, \qquad & q_A = q^B \varepsilon_{BA}. \end{aligned} \tag{350}$$

Each four-vector gets a bispinor representation :

$$P^{\dot{A}B} = p_\mu \bar{\sigma}^{\mu \dot{A} B} \quad \text{or} \quad P_{A\dot{B}} = p_\mu \sigma^\mu_{A\dot{B}}. \tag{351}$$

The Fierz identities are

$$\begin{aligned} \sigma^\mu_{A\dot{A}} \bar{\sigma}^{\dot{B}B}_\mu &= 2\delta_A^{\ B} \delta_{\dot{A}}^{\ \dot{B}}, \\ \sigma^\mu_{A\dot{A}} \sigma_{\mu B\dot{B}} &= 2\varepsilon_{AB} \varepsilon_{\dot{A}\dot{B}}, \\ \bar{\sigma}^{\mu \dot{A} A} \bar{\sigma}^{\dot{B}B}_\mu &= 2\varepsilon^{\dot{A}\dot{B}} \varepsilon^{AB}. \end{aligned} \tag{352}$$

Other useful identities :

$$\begin{aligned} \sigma^\mu_{A\dot{C}} \bar{\sigma}^{\nu \dot{C} B} + \sigma^\nu_{A\dot{C}} \bar{\sigma}^{\mu \dot{C} B} &= 2\delta_A^{\ B} g^{\mu\nu}, \\ \bar{\sigma}^{\mu \dot{A} C} \sigma^\nu_{C\dot{B}} + \bar{\sigma}^{\nu \dot{A} C} \sigma^\mu_{C\dot{B}} &= 2\delta^{\dot{A}}_{\ \dot{B}} g^{\mu\nu}. \end{aligned} \tag{353}$$

Spinor products are defined as

$$\begin{aligned} \langle pq \rangle &= p^A q_A, \\ [pq] &= p_{\dot{A}} q^{\dot{A}}. \end{aligned} \tag{354}$$

The normalization of spinors is given by

$$\langle p \pm | \gamma_\mu | p \pm \rangle = 2p_\mu. \tag{355}$$

Useful formulas in the bra-ket notation:

$$\begin{aligned}\langle p\pm|\gamma_{\mu_1}...\gamma_{\mu_{2n+1}}|q\pm\rangle &= \langle q\mp|\gamma_{\mu_{2n+1}}...\gamma_{\mu_1}|p\mp\rangle,\\ \langle p\pm|\gamma_{\mu_1}...\gamma_{\mu_{2n}}|q\mp\rangle &= -\langle q\pm|\gamma_{\mu_{2n}}...\gamma_{\mu_1}|p\mp\rangle.\end{aligned} \tag{356}$$

Schouten identity:

$$\begin{aligned}\langle AB\rangle\langle CD\rangle &= \langle AD\rangle\langle CB\rangle+\langle AC\rangle\langle BD\rangle,\\ [AB]\,[CD] &= [AD][CB]+[AC][BD].\end{aligned} \tag{357}$$

Fierz identity:

$$\langle A+|\gamma_\mu|B+\rangle\langle C-|\gamma^\mu|D-\rangle = 2[AD]\langle CB\rangle. \tag{358}$$

Given the four-momentum p^μ, we can obtain the corresponding two-component spinor up to an arbitrary phase α. For positive energy spinors we have

$$p_A = \frac{e^{i\alpha}}{\sqrt{p^+}}\begin{pmatrix} p^+\\ p^\perp\end{pmatrix} \tag{359}$$

where we used light-cone coordinates

$$p^+=p^t+p^z,\quad p^-=p^t-p^z,\quad p^\perp=p^x+ip^y. \tag{360}$$

Since p^μ is a null-vector, we have

$$p^{\perp^*}p^\perp = p^+p^-. \tag{361}$$

It is easily verified that p_A satisfies

$$p_\mu\bar\sigma^{\mu\dot BA}p_A=0\quad\text{and}\quad p_{\dot B}\bar\sigma^{\mu\dot BA}p_A=2p^\mu. \tag{362}$$

For negative energy spinors we have

$$p_A = i\frac{e^{i\alpha}}{\sqrt{|p^+|}}\begin{pmatrix}|p^+|\\ p^\perp\end{pmatrix}. \tag{363}$$

The spinor products are then given by

$$\begin{aligned}\langle pq\rangle &= \frac{(-i)^n}{\sqrt{|p^+q^+|}}\left(q^+p^\perp-p^+q^\perp\right),\\ [qp] &= \langle pq\rangle^*\mathrm{sign}(pq)\end{aligned} \tag{364}$$

where n is the number of negative energy spinors.

C Splitting Amplitudes

The expressions for the tree- and loop-splitting amplitudes are given in [28].

C.1 Tree Splitting Amplitudes

In the collinear limit tree-level partial amplitudes factorize

$$A_{n+1}^{tree} \xrightarrow{p_a||p_b} \sum_{\lambda=+/-} \mathrm{Split}_{-\lambda}^{tree}(p_a^{\lambda_a}, p_b^{\lambda_b}) A_n^{tree}(..., P^{\lambda}, ...) \tag{365}$$

where p_a and p_b are the momenta of two adjacent legs, $P = p_a + p_b$, $p_a = zP$ and $p_b = (1-z)P$. λ, λ_a and λ_b denote the corresponding helicities. The splitting functions are:

$$\begin{aligned}
\mathrm{Split}_{g^+}(g^+, g^+) &= 0 & \mathrm{Split}_{g^-}(g^-, g^-) &= 0 \\
\mathrm{Split}_{g^+}(g^+, g^-) &= \sqrt{2}\frac{(1-z)^{\frac{3}{2}}}{\sqrt{z}\langle ab\rangle} & \mathrm{Split}_{g^-}(g^-, g^+) &= -\sqrt{2}\frac{(1-z)^{\frac{3}{2}}}{\sqrt{z}[ab]} \\
\mathrm{Split}_{g^+}(g^-, g^+) &= \sqrt{2}\frac{z^{\frac{3}{2}}}{\sqrt{(1-z)}\langle ab\rangle} & \mathrm{Split}_{g^-}(g^+, g^-) &= -\sqrt{2}\frac{z^{\frac{3}{2}}}{\sqrt{(1-z)}[ab]} \\
\mathrm{Split}_{g^+}(g^-, g^-) &= -\sqrt{2}\frac{1}{\sqrt{z(1-z)}[ab]} & \mathrm{Split}_{g^-}(g^+, g^+) &= \sqrt{2}\frac{1}{\sqrt{z(1-z)}\langle ab\rangle} \\
\mathrm{Split}_{q^-}(q^+, g^+) &= \sqrt{2}\frac{1}{\sqrt{1-z}\langle ab\rangle} & \mathrm{Split}_{q^+}(q^-, g^-) &= -\sqrt{2}\frac{1}{\sqrt{1-z}[ab]} \\
\mathrm{Split}_{q^-}(q^+, g^-) &= -\sqrt{2}\frac{z}{\sqrt{1-z}[ab]} & \mathrm{Split}_{q^+}(q^-, g^+) &= \sqrt{2}\frac{z}{\sqrt{1-z}\langle ab\rangle} \\
\mathrm{Split}_{\bar{q}^-}(g^+, \bar{q}^+) &= \sqrt{2}\frac{1}{\sqrt{z}\langle ab\rangle} & \mathrm{Split}_{\bar{q}^+}(g^-, \bar{q}^-) &= -\sqrt{2}\frac{1}{\sqrt{z}[ab]} \\
\mathrm{Split}_{\bar{q}^-}(g^-, \bar{q}^+) &= -\sqrt{2}\frac{1-z}{\sqrt{z}[ab]} & \mathrm{Split}_{\bar{q}^+}(g^+, \bar{q}^-) &= \sqrt{2}\frac{1-z}{\sqrt{z}\langle ab\rangle} \\
\mathrm{Split}_{g^+}(q^+, \bar{q}^-) &= \sqrt{2}\frac{1-z}{\langle ab\rangle} & \mathrm{Split}_{g^-}(q^-, \bar{q}^+) &= -\sqrt{2}\frac{1-z}{[ab]} \\
\mathrm{Split}_{g^+}(q^-, \bar{q}^+) &= -\sqrt{2}\frac{z}{\langle ab\rangle} & \mathrm{Split}_{g^-}(q^+, \bar{q}^-) &= \sqrt{2}\frac{z}{[ab]}
\end{aligned} \tag{366}$$

C.2 Loop Splitting Amplitudes

Loop amplitudes factorize according to

$$\begin{aligned}
A_{n+1}^{loop} \xrightarrow{p_a||p_b} & \sum_{\lambda=+/-} \mathrm{Split}_{-\lambda}^{tree}(p_a^{\lambda_a}, p_b^{\lambda_b}) A_n^{loop}(..., P^{\lambda}, ...) \\
& + \mathrm{Split}_{-\lambda}^{loop}(p_a^{\lambda_a}, p_b^{\lambda_b}) A_n^{tree}(..., P^{\lambda}, ...).
\end{aligned} \tag{367}$$

The loop splitting amplitudes are expressed as

$$\mathrm{Split}^{loop}_{-\lambda}(p_a^{\lambda_a}, p_b^{\lambda_b}) \;=\; c_\Gamma \cdot \mathrm{Split}^{tree}_{-\lambda}(p_a^{\lambda_a}, p_b^{\lambda_b}) \cdot r_{-\lambda}(p_a^{\lambda_a}, p_b^{\lambda_b}) \tag{368}$$

with the exception of the $g^+ \to g^- g^-$ and the $g^- \to g^+ g^+$ splitting amplitudes. In this case the tree splitting amplitudes vanish. The loop splitting amplitudes depend also on the particle circulating in the loop. $\mathrm{Split}^{[J]}$ denotes the contribution from an adjoint spin-J particle (with two helicity states). To obtain the splitting amplitudes where the internal particle is in the fundamental representation one divides by N_c.
We have

$$\mathrm{Split}^{[1]}_{+}(p_a^+, p_b^+) \;=\; -\frac{1}{48\pi^2}\sqrt{z(1-z)}\frac{[ab]}{\langle ab\rangle^2}, \tag{369}$$

$$\mathrm{Split}^{[1]}_{+}(p_a^+, p_b^+) = -\mathrm{Split}^{[1/2]}_{+}(p_a^+, p_b^+) = \mathrm{Split}^{[0]}_{+}(p_a^+, p_b^+). \tag{370}$$

The remaining $g \to gg$ loop splitting amplitudes are

$$\begin{aligned}
r^{[1]}_{-}(p_a^+, p_b^+) &= -\frac{1}{\varepsilon^2}\left(\frac{\mu^2}{z(1-z)(-s_{ab})}\right)^{\varepsilon} + 2\ln z \ln(1-z) + \frac{1}{3}z(1-z) - \frac{\pi^2}{6}, \\
r^{[1/2]}_{-}(p_a^+, p_b^+) &= -\frac{1}{3}z(1-z), \\
r^{[0]}_{-}(p_a^+, p_b^+) &= +\frac{1}{3}z(1-z), \\
r^{[1]}_{+}(p_a^\pm, p_b^\mp) &= -\frac{1}{\varepsilon^2}\left(\frac{\mu^2}{z(1-z)(-s_{ab})}\right)^{\varepsilon} + 2\ln z \ln(1-z) - \frac{\pi^2}{6}, \\
r^{[1/2]}_{+}(p_a^\pm, p_b^\mp) &= 0, \\
r^{[0]}_{+}(p_a^\pm, p_b^\mp) &= 0.
\end{aligned} \tag{371}$$

The loop splitting amplitudes for $q \to qg$ and $\bar{q} \to g\bar{q}$ are given by

$$\begin{aligned}
r_+(q^-, g^+) = r_-(q^+, g^-) &= f(1-z, s_{qg}), \\
r_+(q^-, g^-) = r_-(q^+, g^+) &= f(1-z, s_{qg}) + \left(1 + \frac{1}{N_c^2}\right)\frac{1-z}{2}, \\
r_-(g^+, \bar{q}^+) = r_+(g^-, \bar{q}^-) &= f(z, s_{g\bar{q}}) + \left(1 + \frac{1}{N_c^2}\right)\frac{z}{2}, \\
r_-(g^-, \bar{q}^+) = r_+(g^+, \bar{q}^-) &= f(z, s_{g\bar{q}})
\end{aligned} \tag{372}$$

where

$$\begin{aligned}
f(z,s) \;=\; & -\frac{1}{\varepsilon^2}\left(\frac{\mu^2}{z(-s)}\right)^{\varepsilon} - \mathrm{Li}_2(1-z) \\
& -\frac{1}{N_c^2}\left[-\frac{1}{\varepsilon^2}\left(\frac{\mu^2}{(1-z)(-s)}\right)^{\varepsilon} + \frac{1}{\varepsilon^2}\left(\frac{\mu^2}{(-s)}\right)^{\varepsilon} - \mathrm{Li}_2(z)\right].
\end{aligned} \tag{373}$$

The loop splitting amplitudes for $g \to q\bar{q}$ are given by

$$\begin{aligned}
r_{\pm}^{[1]}(q^{\pm},\bar{q}^{\mp}) &= -\frac{1}{\varepsilon^2}\left[\left(\frac{\mu^2}{z(-s_{q\bar{q}})}\right)^{\varepsilon}+\left(\frac{\mu^2}{(1-z)(-s_{q\bar{q}})}\right)^{\varepsilon}-2\left(\frac{\mu^2}{(-s_{q\bar{q}})}\right)^{\varepsilon}\right] \\
&\quad +\frac{13}{6\varepsilon}\left(\frac{\mu^2}{(-s_{q\bar{q}})}\right)^{\varepsilon}+\ln(z)\ln(1-z)-\frac{\pi^2}{6}+\frac{83}{18}-\frac{\delta_R}{6} \\
&\quad -\frac{1}{N_c^2}\left[-\frac{1}{\varepsilon^2}\left(\frac{\mu^2}{(-s_{q\bar{q}})}\right)^{\varepsilon}-\frac{3}{2\varepsilon}\left(\frac{\mu^2}{(-s_{q\bar{q}})}\right)^{\varepsilon}-\frac{7}{2}-\frac{\delta_R}{2}\right], \\
r_{\pm}^{[1/2]}(q^{\pm},\bar{q}^{\mp}) &= -\frac{2}{3\varepsilon}\left(\frac{\mu^2}{(-s_{q\bar{q}})}\right)^{\varepsilon}-\frac{10}{9}, \\
r_{\pm}^{[0]}(q^{\pm},\bar{q}^{\mp}) &= -\frac{1}{3\varepsilon}\left(\frac{\mu^2}{(-s_{q\bar{q}})}\right)^{\varepsilon}-\frac{8}{9}. \qquad (374)
\end{aligned}$$

Here δ_R is a parameter depending on the dimensional regularization scheme used. $\delta_R = 0$ for the FDH-scheme and $\delta_R = 1$ for the CDR-scheme.

D Renormalization

Let g be the unrenormalized coupling constant, g_r the renormalized coupling constant and g_R the dimensionless renormalized coupling constant. They are related by

$$\begin{aligned} g &= Z_g g_r, \\ g_r &= g_R \mu^{\varepsilon}. \end{aligned} \tag{375}$$

The β-function is defined by

$$\beta = \mu \frac{d}{d\mu} g_R. \tag{376}$$

As usual, denote $\alpha_s = \frac{g_R^2}{4\pi}$. Then

$$\mu \frac{d}{d\mu} \alpha_s = -\frac{1}{2\pi}\beta_0 \alpha_s^2 - \frac{1}{8\pi^2}\beta_1 \alpha_s^3 - \frac{1}{32\pi^3}\beta_2 \alpha_s^4 - ... \tag{377}$$

where the first few coefficients of the β-function are given by [101] - [103]

$$\begin{aligned} \beta_0 &= \frac{11}{3} C_A - \frac{4}{3} T_R N_f, \\ \beta_1 &= \frac{34}{3} C_A^2 - 4 \left(\frac{5}{3} C_A + C_F \right) T_R N_f, \\ \beta_2 &= \frac{2857}{54} C_A^3 - \left(\frac{1415}{27} C_A^2 + \frac{205}{9} C_A C_F - 2 C_F^2 \right) T_R N_f \\ &\quad + \left(\frac{158}{27} C_A + \frac{44}{9} C_F \right) T_R^2 N_f^2. \end{aligned} \tag{378}$$

For a group $SU(N_C)$ the fundamental and the adjoint Casimirs are given by

$$\begin{aligned} \left(T^a T^a\right)_{ij} &= C_F \delta_{ij} = \frac{N_C^2 - 1}{2N_C} \delta_{ij}, \\ f^{abc} f^{dbc} &= C_A \delta^{ad} = N_C \delta^{ad}. \end{aligned} \tag{379}$$

The standard normalization is

$$\mathrm{Tr}\left(T^a T^b\right) = T_R \delta^{ab} = \frac{1}{2} \delta^{ab}. \tag{380}$$

An approximate solution for α_s at NLO is

$$\frac{\alpha_s(\mu)}{4\pi} = \frac{1}{\beta_0 L} \left(1 - \frac{\beta_1}{\beta_0^2} \frac{\ln L}{L} \right) \tag{381}$$

where $L = \ln(\mu^2 / \Lambda_{QCD}^2)$. The one-loop amplitudes presented in the papers [34] and [35] are bare ones, i.e. no ultraviolet subtraction has been performed. The renormalized amplitudes are obtained from the unrenormalized ones by

$$A_R^{\text{one-loop}} = A^{\text{one-loop}} - \frac{1}{\varepsilon} c_\Gamma g^2 N_C \left(\frac{11}{3} - \frac{2}{3}\frac{N_f}{N_C} - \frac{1}{3}\frac{N_S}{N_C} \right) A^{\text{tree}} \tag{382}$$

where N_S is the number of scalars ($N_S = 0$ in QCD).

E Integral Functions

E.1 Loop Integrals

A general loop integral is denoted by

$$I_n\left[P(k)\right] = (-1)^n (4\pi)^{2-\varepsilon} \int \frac{d^{4-2\varepsilon}k}{(2\pi)^{4-2\varepsilon} i} \frac{P(k)}{k^2(k-p_1)^2 ... (k-p_1-...-p_{n-1})^2} \tag{383}$$

where $P(k)$ denotes a polynomial in the loop momentum. The bubbles are given by

$$\begin{aligned} I_2[1] &= \frac{r_\Gamma}{\varepsilon(1-2\varepsilon)} (-s)^{-\varepsilon}, \\ I_2[k^\mu] &= \frac{p_1^\mu}{2} I_2[1] \end{aligned} \tag{384}$$

where

$$r_\Gamma = \frac{\Gamma(1+\varepsilon)\Gamma^2(1-\varepsilon)}{\Gamma(1-2\varepsilon)}. \tag{385}$$

The one- and two-mass scalar triangles are

$$\begin{aligned} I_3^{1m}[1](m_1^2 = s, m_2^2 = 0, m_3^2 = 0) &= \frac{r_\Gamma}{\varepsilon^2} \frac{(-s)^{-\varepsilon}}{-s}, \\ I_3^{2m}[1](m_1^2 = s, m_2^2 = t, m_3^2 = 0) &= \frac{r_\Gamma}{\varepsilon^2} \frac{(-s)^{-\varepsilon} - (-t)^{-\varepsilon}}{(-s)-(-t)}. \end{aligned} \tag{386}$$

Sometimes it is convenient to give the explicit expression for the scalar box integrals $I_4[1]$ in terms of a scalar box function $F_4^{D=4-2\varepsilon}$ times a kinematical factor

$$I_4[1] = -\frac{r_\Gamma}{2\sqrt{\det S}} F_4 \tag{387}$$

where $S_{ij} = -\frac{1}{2}(p_i + ... p_{j-1})^2$ for $i \neq j$ and $S_{ii} = 0$.
We have

$$\begin{aligned} \sqrt{\det S} &= \frac{1}{4}\sqrt{B^2 - 4\prod_{i=1}^{4} m_i^2}, \\ B &= st - m_1^2 m_3^2 - m_2^2 m_4^2 \end{aligned} \tag{388}$$

where $s = (p_1+p_2)^2$, $t = (p_2+p_3)^2$ and $m_i^2 = p_i^2$. If at least one external mass vanishes, $\det(S)$ factorizes as $\det(S) = (\frac{1}{2}B)^2$ and we have the relation

$$I_4[1] = -\frac{2r_\Gamma}{B} F_4^{D=4-2\varepsilon} \quad \text{one external mass zero.}$$

Sometimes it's also useful to define the six-dimensional scalar box function via

$$2r_\Gamma(1-2\varepsilon)\sqrt{B^2-4\prod_{i=1}^{4}m_i^2}\,F_4^{D=6-2\varepsilon} = (4\pi)^{2-\varepsilon}\int\frac{d^{4-2\varepsilon}k}{(2\pi)^{4-2\varepsilon}i}\frac{\varepsilon(k,p_1,p_2,p_3)\varepsilon(k,p_1,p_2,p_3)}{k^2(k-p_1)^2(k-p_1^2-p_2^2)^2(k-p_1^2-p_2^2-p_3^2)^2}. \tag{389}$$

The no-mass box :

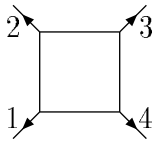

$$s=(p_1+p_2)^2, \qquad t=(p_2+p_3)^2,$$

$$I_4^{0m}[1] = -2r_\Gamma\frac{1}{st}\left\{-\frac{1}{\varepsilon^2}\left[(-s)^{-\varepsilon}+(-t)^{-\varepsilon}\right]+\frac{1}{2}\ln^2\left(\frac{-s}{-t}\right)\right\}. \tag{390}$$

The one-mass box :

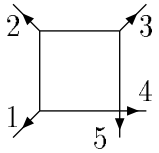

$$I_4^{1m}[1] = -2r_\Gamma\frac{1}{s_{12}s_{23}}\left\{-\frac{1}{\varepsilon^2}\left[(-s_{12})^{-\varepsilon}+(-s_{23})^{-\varepsilon}-(-s_{123})^{-\varepsilon}\right]+\mathrm{Li}_2\left(1-\frac{-s_{123}}{-s_{12}}\right)+\mathrm{Li}_2\left(1-\frac{-s_{123}}{-s_{23}}\right)+\frac{1}{2}\ln^2\left(\frac{-s_{12}}{-s_{23}}\right)+\frac{\pi^2}{6}\right\}, \tag{391}$$

$$(1-2\varepsilon)F_4^{1m,D=6-2\varepsilon} = \mathrm{Ls}_{-1}\left(\frac{-s}{-m^2},\frac{-t}{-m^2}\right). \tag{392}$$

Two-mass boxes :

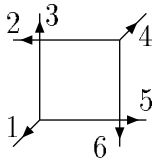

$$
\begin{aligned}
s &= s_{123}, \qquad m_2^2 = s_{23}, \\
t &= s_{234}, \qquad m_4^2 = s_{56},
\end{aligned}
$$

$$
\begin{aligned}
I_4^{2me} = & \\
= \quad & -2r_\Gamma \frac{1}{st - m_2^2 m_4^2} \left\{ -\frac{1}{\varepsilon^2} \left[(-s)^{-\varepsilon} + (-t)^{-\varepsilon} - (-m_2^2)^{-\varepsilon} - (-m_4^2)^{-\varepsilon} \right] \right. \\
& + \mathrm{Li}_2 \left(1 - \frac{-m_2^2}{-s} \right) + \mathrm{Li}_2 \left(1 - \frac{-m_4^2}{-s} \right) + \mathrm{Li}_2 \left(1 - \frac{-m_2^2}{-t} \right) + \mathrm{Li}_2 \left(1 - \frac{-m_4^2}{-t} \right) \\
& \left. + \mathrm{Li}_2 \left(1 - \frac{m_2^2 m_4^2}{st} \right) + \frac{1}{2} \ln^2 \left(\frac{-s}{-t} \right) \right\},
\end{aligned} \tag{393}
$$

$$
(1-2\varepsilon) F_4^{2me, D=6-2\varepsilon} = \mathrm{Ls}_{-1}^{2me} \left(s, t, m_2^2, m_4^2 \right). \tag{394}
$$

Two adjacent massive legs :

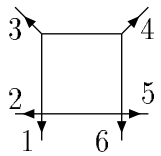

$$
\begin{aligned}
s &= s_{123}, \qquad m_1^2 = s_{12}, \\
t &= s_{34}, \qquad m_4^2 = s_{56},
\end{aligned}
$$

$$
\begin{aligned}
I_4^{2mh}[1] = & \\
= \quad & -2r_\Gamma \frac{1}{st} \left\{ -\frac{1}{\varepsilon^2} \left[(-s)^{-\varepsilon} + (-t)^{-\varepsilon} - (-m_1^2)^{-\varepsilon} - (-m_4^2)^{-\varepsilon} \right] \right. \\
& - \frac{1}{2\varepsilon^2} \frac{(-m_1^2)^{-\varepsilon} (-m_4^2)^{-\varepsilon}}{(-t)^{-\varepsilon}} \\
& \left. + \mathrm{Li}_2 \left(1 - \frac{-m_1^2}{-s} \right) + \mathrm{Li}_2 \left(1 - \frac{-m_4^2}{-s} \right) + \frac{1}{2} \ln^2 \left(\frac{-t}{-s} \right) \right\},
\end{aligned} \tag{395}
$$

$$
(1-2\varepsilon) F_4^{2mh, D=6-2\varepsilon} = \mathrm{Ls}_{-1}^{2mh} \left(t, s, m_1^2, m_4^2 \right). \tag{396}
$$

The integral functions Ls_{-1} are given below. The integral functions appearing in the final result of the loop amplitude are

$$
\begin{aligned}
\mathrm{L}_0 \left(\frac{-s}{-t} \right) &= \frac{\ln \left(\frac{-s}{-t} \right)}{1 - \frac{s}{t}}, \\
\mathrm{L}_1 \left(\frac{-s}{-t} \right) &= \frac{\mathrm{L}_0 \left(\frac{-s}{-t} \right) + 1}{1 - \frac{s}{t}}.
\end{aligned} \tag{397}
$$

These function are related to two-mass triangles. The functions related to box integrals are

$$\begin{aligned}
\mathrm{Ls}_{-1}\left(\frac{-s_1}{-t_1},\frac{-s_2}{-t_2}\right) &= \mathrm{Li}_2\left(1-\frac{-s_1}{-t_1}\right)+\mathrm{Li}_2\left(1-\frac{-s_2}{-t_2}\right)\\
&\quad +\ln\left(\frac{-s_1}{-t_1}\right)\ln\left(\frac{-s_2}{-t_2}\right)-\frac{\pi^2}{6},\\
\mathrm{Ls}_0\left(\frac{-s_1}{-t_1},\frac{-s_2}{-t_2}\right) &= \frac{\mathrm{Ls}_{-1}\left(\frac{-s_1}{-t_1},\frac{-s_2}{-t_2}\right)}{1-\frac{s_1}{t_1}-\frac{s_2}{t_2}},\\
\mathrm{Ls}_1\left(\frac{-s_1}{-t_1},\frac{-s_2}{-t_2}\right) &= \frac{\mathrm{Ls}_0\left(\frac{-s_1}{-t_1},\frac{-s_2}{-t_2}\right)+\mathrm{L}_0\left(\frac{-s_1}{-t_1}\right)+\mathrm{L}_0\left(\frac{-s_2}{-t_2}\right)}{1-\frac{s_1}{t_1}-\frac{s_2}{t_2}},\\
\mathrm{Ls}_{-1}^{2\mathrm{m}e}\left(s,t,m_1^2,m_3^2\right) &= -\mathrm{Li}_2\left(1-\frac{-m_1^2}{-s}\right)-\mathrm{Li}_2\left(1-\frac{-m_1^2}{-t}\right)-\mathrm{Li}_2\left(1-\frac{-m_3^2}{-s}\right)\\
&\quad -\mathrm{Li}_2\left(1-\frac{-m_3^2}{-t}\right)+\mathrm{Li}_2\left(1-\frac{m_1^2m_3^2}{st}\right)-\frac{1}{2}\ln^2\left(\frac{-s}{-t}\right),\\
\tilde{\mathrm{Ls}}_{-1}^{2\mathrm{m}h}\left(s,t,m_1^2,m_2^2\right) &= -\mathrm{Li}_2\left(1-\frac{-m_1^2}{-t}\right)-\mathrm{Li}_2\left(1-\frac{-m_2^2}{-t}\right)-\frac{1}{2}\ln^2\left(\frac{-s}{-t}\right)\\
&\quad +\frac{1}{2}\ln\left(\frac{-s}{-m_1^2}\right)\ln\left(\frac{-s}{-m_2^2}\right),\\
\mathrm{Ls}_{-1}^{2\mathrm{m}h}\left(s,t,m_1^2,m_2^2\right) &= \tilde{\mathrm{Ls}}_{-1}^{2\mathrm{m}h}\left(s,t,m_1^2,m_2^2\right)\\
&\quad +\left[\frac{1}{2}\left(s-m_1^2-m_2^2\right)+\frac{m_1^2m_2^2}{t}\right]I_3^{3\mathrm{m}}\left(s,m_1^2,m_2^2\right).
\end{aligned} \tag{398}$$

The imaginary parts of the logarithm and the dilogarithm are given by

$$\begin{aligned}
\ln\left(\frac{-s}{-t}\right) &= \ln\left(\left|\frac{s}{t}\right|\right)-i\pi\left(\theta(s)-\theta(t)\right),\\
\mathrm{Li}_2\left(1-\frac{-s}{-t}\right) &= \mathrm{ReLi}_2\left(1-\frac{s}{t}\right)-i\theta\left(-\frac{s}{t}\right)\ln\left(1-\frac{s}{t}\right)\mathrm{Im}\ln\left(\frac{-s}{-t}\right)
\end{aligned} \tag{399}$$

where the step function $\theta(s)$ is defined as $\theta(s)=1$ for $s>0$ and $\theta(s)=0$ otherwise. The three-mass triangle is defined by

$$I_3^{3\mathrm{m}}\left(s_{12},s_{34},s_{56}\right) = \int_0^1 d^3\alpha_i \frac{\delta\left(1-\alpha_1-\alpha_2-\alpha_3\right)}{-\alpha_1\alpha_2 s_{12}-\alpha_2\alpha_3 s_{34}-\alpha_3\alpha_1 s_{56}}. \tag{400}$$

With the notation

$$\begin{aligned}
\delta_{12} &= s_{12} - s_{34} - s_{56}, \\
\delta_{34} &= s_{34} - s_{56} - s_{12}, \\
\delta_{56} &= s_{56} - s_{12} - s_{34}, \\
\Delta_3 &= s_{12}^2 + s_{34}^2 + s_{56}^2 - 2s_{12}s_{34} - 2s_{34}s_{56} - 2s_{56}s_{12}
\end{aligned} \tag{401}$$

the three-mass triangle $I_3^{3\mathrm{m}}$ is expressed in the region $s_{12}, s_{34}, s_{56} < 0$ and $\Delta_3 < 0$ by [42]

$$\begin{aligned}
I_3^{3\mathrm{m}} &= \frac{2}{\sqrt{-\Delta_3}} \left[\mathrm{Cl}_2\left(2\arctan\left(\frac{\sqrt{-\Delta_3}}{\delta_{12}}\right)\right) + \mathrm{Cl}_2\left(2\arctan\left(\frac{\sqrt{-\Delta_3}}{\delta_{34}}\right)\right) \right. \\
&\quad \left. + \mathrm{Cl}_2\left(2\arctan\left(\frac{\sqrt{-\Delta_3}}{\delta_{56}}\right)\right)\right].
\end{aligned} \tag{402}$$

In the region $s_{12}, s_{34}, s_{56} < 0$ and $\Delta_3 > 0$ as well as in the region $s_{12}, s_{56} < 0$, $s_{34} > 0$ (for which Δ_3 is always positive) the integral $I_3^{3\mathrm{m}}$ is given by [53]

$$\begin{aligned}
I_3^{3\mathrm{m}} &= -\frac{1}{\sqrt{\Delta_3}} \mathrm{Re}\left[2\left(\mathrm{Li}_2(-\rho x) + \mathrm{Li}_2(-\rho y)\right) + \ln(\rho x)\ln(\rho y)\right. \\
&\quad \left. + \ln\left(\frac{y}{x}\right)\ln\left(\frac{1+\rho x}{1+\rho y}\right) + \frac{\pi^2}{3}\right] \\
&\quad - \frac{i\pi\theta(s_{34})}{\sqrt{\Delta_3}} \ln\left(\frac{\left(\delta_{12}+\sqrt{\Delta_3}\right)\left(\delta_{56}+\sqrt{\Delta_3}\right)}{\left(\delta_{12}-\sqrt{\Delta_3}\right)\left(\delta_{56}-\sqrt{\Delta_3}\right)}\right)
\end{aligned} \tag{403}$$

where

$$x = \frac{s_{12}}{s_{56}}, \quad y = \frac{s_{34}}{s_{56}}, \quad \rho = \frac{2s_{56}}{\delta_{56} + \sqrt{\Delta_3}}. \tag{404}$$

The Clausen function $\mathrm{Cl}_2(x)$ is defined by

$$\mathrm{Cl}_2(x) = \sum_{n=1}^{\infty} \frac{\sin(nx)}{n^2} = -\int_0^x dt \ln\left(\left|2\sin\left(\frac{t}{2}\right)\right|\right). \tag{405}$$

In the axial vector contribution the integral

$$f(m; s_{12}, s_{34}, s_{56}) = \int_0^1 d^3a_i \frac{a_2 a_3 \delta(1 - a_1 - a_2 - a_3)}{m^2 - s_{12}a_1a_2 - s_{34}a_2a_3 - s_{56}a_3a_1} \tag{406}$$

appears. For $m = 0$ we get

$$\begin{aligned} f(0; s_{12}, s_{34}, s_{56}) &= \left(\frac{3 s_{34}\delta_{34}}{\Delta_3^2} - \frac{1}{\Delta_3}\right) s_{12} s_{56} I_3^{3m}(s_{12}, s_{34}, s_{56}) \\ &+ \left(\frac{3 s_{56}\delta_{56}}{\Delta_3^2} - \frac{1}{2\Delta_3}\right) s_{12} \ln\left(\frac{-s_{12}}{-s_{34}}\right) \\ &+ \left(\frac{3 s_{12}\delta_{12}}{\Delta_3^2} - \frac{1}{2\Delta_3}\right) s_{56} \ln\left(\frac{-s_{56}}{-s_{34}}\right) - \frac{\delta_{34}}{2\Delta_3}. \end{aligned} \tag{407}$$

For $m = m_t$ the integral is approximated by its Taylor expansion

$$f(m_t; s_{12}, s_{34}, s_{56}) = \frac{1}{24 m_t^2} + \frac{(2 s_{34} + s_{12} + s_{56})}{360 m_t^4} + ... \tag{408}$$

E.2 Numerical Implementation

E.2.1 The Dilogarithm

The real part of the dilogarithm $\mathrm{Li}_2(x)$ is numerically evaluated as follows [40] : Using the relations

$$\begin{aligned} \mathrm{Li}_2(x) &= -\mathrm{Li}_2(1-x) + \frac{\pi^2}{6} - \ln(x)\ln(1-x), \\ \mathrm{Li}_2(x) &= -\mathrm{Li}_2\left(\frac{1}{x}\right) - \frac{\pi^2}{6} - \frac{1}{2}(\ln(-x))^2 \end{aligned} \tag{409}$$

the argument is shifted into the range $-1 \le x \le 1/2$. Then

$$\begin{aligned} \mathrm{Li}_2(x) &= \sum_{i=0}^{\infty} \frac{B_i}{(i+1)!} z^{i+1} \\ &= B_0 z + \frac{B_1}{2} z^2 + \sum_{n=1}^{\infty} \frac{B_{2n}}{(2n+1)!} z^{2n+1} \end{aligned} \tag{410}$$

with $z = -\ln(1-x)$ and the B_i are the Bernoulli numbers. The Bernoulli numbers B_i are defined through the generating function

$$\frac{t}{e^t - 1} = \sum_{i=0}^{\infty} B_n \frac{t^n}{n!}. \tag{411}$$

E.2.2 The Clausen Function

The numerical evaluation of the Clausen function is done as follows [42] : Using the symmetry

$$\mathrm{Cl}_2(-x) = -\mathrm{Cl}_2(x), \tag{412}$$

the periodicity

$$\mathrm{Cl}_2(x + 2n\pi) \quad = \quad \mathrm{Cl}_2(x), \tag{413}$$

and the duplication formula

$$\mathrm{Cl}_2(2x) \quad = \quad 2\mathrm{Cl}_2(x) - 2\mathrm{Cl}_2(\pi - x) \tag{414}$$

the argument may be shifted into the range $0 \leq x \leq 2\pi/3$. Then

$$\mathrm{Cl}_2(x) \quad = \quad -x\ln(x) + x + \sum_{n=1}^{\infty} \frac{(-1)^{n+1} B_{2n}}{2n(2n+1)!} x^{2n+1}. \tag{415}$$

References

[1] M. Mangano and S. Parke, Phys.Rep. 200, (1991), 301

[2] Z. Bern, UCLA/93/TEP/5, TASI 1992, hep-ph/9304249

[3] L.Dixon, TASI 1995, hep-ph/9601359

[4] Z.Kunszt, TASI 1995, hep-ph/9603235

[5] Z.Bern, L.Dixon and D.A.Kosower, Ann.Rev.Nucl.Part.Sci. 46, (1996), 109

[6] G.Sterman, TASI 1995, hep-ph/9606312

[7] G.Altarelli, Phys.Rep. 81, (1982),1

[8] S.Catani, CERN-TH/97-371,hep-ph/9712442

[9] Report of the Workshop on Physics at LEP2, CERN 96-01, 1996

[10] P.Cvitanović, P.G.Lauwers and P.N.Scharbach, Nucl.Phys. B186, (1981), 165

[11] F.A. Berends and W.T. Giele, Nucl. Phys. B294, (1987), 700

[12] Z. Bern and D.A. Kosower, Nucl. Phys. B362, (1991), 389

[13] M. Mangano, S. Parke and Z. Xu, Nucl. Phys. B298, (1988), 653

[14] D.A.Kosower, B.-H. Lee and V.P.Nair, Phys.Lett. 201B, (1988), 85

[15] G.'t Hooft, Nucl.Phys. B72, (1974), 461

[16] P.De Causmaecker, R.Gastmans, W.Troost and T.T.Wu, Nucl.Phys. B206, (1982), 53

[17] R.Kleiss and W.J.Stirling, Nucl.Phys. B262, (1985), 235

[18] Z.Xu, D.-H. Zhang and L.Chang, Nucl.Phys. B291, (1987), 392

[19] J.F.Gunion and Z.Kunszt, Phys.Lett. 161B, (1985), 333

[20] S.J.Parke and T.R.Taylor, Phys.Rev.Lett. 56, (1986), 2459

[21] F.A.Berends and W.T.Giele, Nucl.Phys. B306, (1988), 759

[22] D.A. Kosower, Nucl.Phys. B335, (1990), 23

[23] S.J.Parke and T.Taylor, Phys.Lett. 157 B, (1985), 81

[24] M.T.Grisaru and H.N.Pendleton, Nucl.Phys. B124, (1977), 81

[25] R.E.Cutkosky, J. Math. Phys. 1, (1960), 429

[26] Z.Bern, L.Dixon, D.C. Dunbar and D.A.Kosower, Nucl.Phys. B435, (1995), 59

[27] Z.Bern and A.G.Morgan, Nucl.Phys B467, (1996), 479

[28] Z.Bern, L.Dixon, D.C. Dunbar and D.A.Kosower, Nucl.Phys. B425, (1994), 217

[29] Z.Koba and H.B.Nielsen, Nucl.Phys. B10, (1969), 633

[30] J.L.Gervais and A.Neveu, Nucl.Phys. B46, (1972), 381

[31] H.Kawai, D.C.Lewellen and S.H.Tye, Nucl.Phys. B288, (1987), 1

[32] Z.Bern and D.A.Kosower, Nucl.Phys. B379, (1992), 451

[33] Z.Bern and D.C.Dunbar, Nucl.Phys. B379, (1992), 562

[34] Z.Bern,L.Dixon,D.A.Kosower and S.Weinzierl, Nucl.Phys. B489, (1997), 3

[35] Z.Bern,L.Dixon and D.A.Kosower, Nucl.Phys. B513, (1998), 3

[36] E.W.N.Glover and D.J.Miller, Phys.Lett. B396, (1997), 257

[37] J.M.Campbell, E.W.N.Glover and D.J.Miller, Phys.Lett. B409, (1997), 503

[38] F.A.Berends, W.T.Giele and H.Kuijf, Nucl. Phys. B321, (1989), 39

[39] K.Hagiwara, T.Kuruma and Y.Yamada, Nucl.Phys. B358, (1991), 80

[40] G. 't Hooft and M. Veltman, Nucl.Phys. B153, (1979),365

[41] A. Denner, U. Nierste and R. Scharf, Nucl.Phys. B367, (1991), 637

[42] H. J. Lu and C.A. Perez, SLAC-PUB-5809

[43] G. Passarino and M.Veltman, Nucl.Phys. B160, (1979), 151

[44] R.G. Stuart, Comp.Phys.Comm. 48, (1988), 367

[45] R.G. Stuart and A. Góngora-T., Comp.Phys.Comm. 56, (1990), 337

[46] W.L. van Neerven and J.A.M.Vermaseren, Phys. Lett. 137B, (1984),241

[47] G.J. van Oldenborgh and J.A.M.Vermaseren, Z. Phys. C 46, (1990),425

[48] Z. Bern, L. Dixon and D. Kosower, Nucl. Phys. B412, (1994), 751

[49] J.M. Campbell, E.W.N. Glover and D.J. Miller, Nucl.Phys. B498, (1997), 397

[50] R.Pittau, Comput.Phys.Commun. 104, (1997), 23

[51] A.J.Davydychev, Phys.Lett. B263, (1991), 107

[52] A.Signer, Ph.D. thesis, Diss. ETH Nr. 11143

[53] N.I.Ussyukina and A.I.Davydychev, Phys.Lett. 298B, (1993), 363

[54] W.T.Giele and E.W.N.Glover, Phys. Rev. D 46, (1992), 1980

[55] W.L. van Neerven and J.A.M. Vermaseren, Nucl.Phys. B238, (1984), 73

[56] S.Frixione, Z.Kunszt and A.Signer, Nucl.Phys. B467, (1996), 399

[57] S. Catani, M.H. Seymour, Nucl.Phys. B485, (1997), 291, Erratum-ibid. B510, (1997), 503,

[58] N.Byers and C.N.Yang, Rev. Mod. Phys. 36, (1964), 595

[59] E.Byckling and K.Kajantie, Particle Kinematics, John Wiley & Sons, London, 1973

[60] G.Altarelli and G.Parisi, Nucl.Phys. B126, (1977), 298

[61] S.Catani, M.H.Seymour and Z.Trócsányi, Phys.Rev. D55, (1997), 6819

[62] Z.Kunszt, A.Signer and Z.Trócsányi, Nucl.Phys. B411, (1994), 397

[63] J.C. Collins, Renormalization, Cambridge University Press, 1984

[64] G. 't Hooft and M.Veltman, Nucl.Phys. B44, (1972), 189

[65] W.Siegel, Phys.Lett. 84B, (1979), 193

[66] F.James, Rep.Prog.Phys. 43, (1980), 1145

[67] F.James, Comp.Phys.Comm. 60, (1990), 329

[68] D.E.Knuth, Semi-numerical algorithms, vol.2 in : The Art of Computer Programming, 2nd ed. (Addison-Wesley,1981)

[69] G.P.Lepage, Cornell preprint, (1980), CLNS-80/447

[70] G.P.Lepage, J. Comp. Phys. 27, (1978), 192

[71] R.Kleiss, W.J.Stirling and S.D.Ellis, Comp.Phys.Comm. 40, (1986), 359

[72] D.A.Kosower, unpublished notes

[73] W.Bartel et al., Z.Phys. C 33, (1986), 23

[74] *Report of the Hard QCD Working Group*, in Proc. Durham Workshop on Jet Studies at LEP and HERA, J.Phys. G17, (1991), 1537

[75] S.Bethke, Z.Kunszt, D.E.Soper and W.J.Stirling, Nucl.Phys B370, (1992), 310

[76] Y.L.Dokshitzer, G.D.Leder, S.Moretti and B.R.Webber, hep-ph/9707323

[77] S.Moretti, L.Lönnblad and T.Sjöstrand, hep-ph/9804296

[78] E.Fahri, Phys.Rev.Lett. 39, (1977), 1587

[79] H.Georgi and M.Machacek, Phys.Rev.Lett. 39, (1977), 1237

[80] MARK J collaboration, Phys.Rep. 63, (1980), 340

[81] A. De Rujula, J.Ellis, E.G.Floratos and M.K.Gaillard, Nucl.Phys. B138, (1978), 387

[82] G.Parisi, Phys.Lett. 74B, (1978), 65

[83] G.C.Fox and S.Wolfram, Phys.Lett. 82B, (1979), 134

[84] J.G.Körner, G.Schierholz and J.Willrodt, Nucl.Phys. B185, (1981), 365

[85] O.Nachtmann and A.Reiter, Zeit.Phys. C 16, (1982), 45

[86] P.Abreu et al. DELPHI Collaboration, Phys.Lett. 255, (1991), 466

[87] M.Bengtsson and P.M.Zerwas, Phys.Lett. B208, (1988), 306

[88] L.Lönnblad, Comp.Phys.Comm. 71, (1992), 15

[89] G.Marchesini et al., Comp.Phys.Comm. 67, (1992), 465

[90] T.Sjöstrand, Comp.Phys.Comm 82, (1994), 74

[91] R.K.Ellis, D.A.Ross and A.E.Terrano, Nucl.Phys. B178, (1981), 421

[92] L.Dixon and A. Signer, Phys.Rev. D56, (1997), 4031

[93] L.Dixon and A. Signer, Phys.Rev.Lett. 78, (1997), 811

[94] Z.Nagy and Z.Trócsányi, Nucl. Phys. B486, 91997), 189

[95] Z.Nagy and Z.Trócsányi, hep-ph/9708343

[96] Z.Nagy and Z.Trócsányi, Phys.Lett. B414, (1997), 187

[97] Z.Nagy and Z.Trócsányi, Phys.Rev.Lett 79, (1997), 3604

[98] Z.Nagy and Z.Trócsányi, Nucl.Phys.Proc.Suppl. 64, (1998), 63

[99] Z.Nagy and Z.Trócsányi, Phys.Rev. D57, (1998), 5793

[100] E.W.N.Glover, hep-ph/9805481

[101] D.R.T. Jones, Nucl.Phys. B75, (1974), 531

[102] W.E.Caswell, Phys.Rev.Lett. 33, (1974), 244

[103] O.V.Tarasov, A.A.Vladimirov and A.Y.Zharkov, Phys.Lett. 93 B, (1986), 429